

EVALUATION OF CORAL REEF SEASCAPE IN ‘ĀHIHI KĪNA‘U, MAUI WITH
PERSPECTIVES IN LANDSCAPE ECOLOGY

A THESIS SUBMITTED TO THE GRADUATE DIVISION OF THE
UNIVERSITY OF HAWAI‘I AT MĀNOA IN PARTIAL FULFILLMENT OF THE
REQUIREMENTS FOR THE DEGREE OF

MASTER OF ARTS

IN

GEOGRAPHY

DECEMBER 2012

By
Yuko Okano Stender

Thesis Committee:

Ross Sutherland, Chairperson
Paul L. Jokiel
Stacy Jørgensen

© 2012 Yuko Okano Stender

ACKNOWLEDGEMENTS

This study was funded by ‘Āhihi Kīna‘u Natural Area Reserve System (NARS), the State of Hawai‘i. I would like to acknowledge a former Project Manager Matt Ramsey for providing us logistical support and coordination, the opportunity to experience the inshore reef community, and his enthusiasm for preserving ‘Āhihi Kīna‘u NARS. My field work was made possible by the NARS rangers: Danielle Kornfeind who willingly provided field support, additional monitoring data, and local knowledge of fish and near-shore fisheries on Maui. Judy Edwards, Joe Fell-McDonald, and Kepa Mano diligently escorted us to the closed-areas, monitored our safety in isolated shorelines, and provided expertise in cultural and terrestrial resources. Donna Liddicote-Brown from Marine Option Program, Maui Community College provided us with the necessary field equipment and lodging on Maui.

I am grateful for members of my committee, Drs. Ross Sutherland, Paul Jokiel, and Stacy Jørgensen for their guidance, literary contribution, and lasting patience in the preparation of this thesis. My chairperson, Dr. Ross Sutherland provided me with strong support and encouragement for my overall work, literary, and academic matters. Dr. Stacy Jørgensen exposed me to perspectives of landscape ecology and helped me expand them, linking to the coral reef environment. Dr. Paul Jokiel’s mentorship and research expertise in coral reef ecology have been motivating and inspiring, and supported me during both field- and labwork.

I would like to express my appreciation to the team at the Coral Reef Ecology Lab, Hawai‘i Institute of Marine Biology, University of Hawai‘i. I am truly thankful to Dr. Ku‘ulei Rodgers for providing me with this research opportunity, logistical and technical

support, advice in field research design and analysis, and her endless encouragement to stay on the path. Megan Ross who is efficient, productive, and positive has been an essential part of the project. The laboratory support provided by Ann Farrell, Claire Lager, and Dan Lager was fundamental for processing numerous sediment samples and photographic data.

I am indebted to my mother and my late father, Sachiko and Takao Okano, for always being supportive and letting me pursue my interest away from Japan. Finally, the completion of this thesis would not have been possible without contributions in technical assistance, endless proof-reading, emotional support, and comfort of my husband, Keoki Kekua‘ana Stender to whom I am deeply indebted.

ABSTRACT

The primary focus of this study was to produce temporal and spatial information needed to assist in the management of ‘Āhihi Kīna‘u Natural Area Reserve System (NARS). The research goals included quantifying temporal changes in inshore biological communities resulting from shoreline access closure, and characterizing spatial patterns of coral and crustose coralline algae (CCA) using a spatial statistical approach. Resultant temporal change in a location known as the *Montipora* Pond showed decreased live coral and increased dead coral during this study. Spatial structure and local clustering of CCA cover existed, but it was negligible for coral. CCA cover was better estimated by a spatial correlation model. Coral cover exhibited no autocorrelation, but weak spatial dependence on covariates. The spatial statistical approach should be considered in future studies. New temporal and spatial information produced during this study comprises a valuable baseline that will support future preservation and management decisions.

TABLE OF CONTENTS

ACKNOWLEDGEMENTS	iii
ABSTRACT	v
LIST OF TABLES	viii
LIST OF FIGURES	x
ABBREVIATIONS	xv
CHAPTER 1: GENERAL INTRODUCTION	
Status and Issues of Coral Reef Seascape	1
Perspectives in Landscape Ecology	5
CHAPTER 2: ASSESSMENT OF INSHORE SEASCAPE FOLLOWING SHORELINE ACCESS CLOSURE	
Introduction.....	9
Background.....	9
Objectives.....	12
Materials and Methods.....	12
Study Sites	12
General Field Sampling Protocol.....	17
<i>Benthic Sampling</i>	18
<i>Fish Sampling</i>	20
<i>Topographic Relief (Rugosity) and Depth</i>	21
<i>Sediment Composition</i>	22
<i>Sediment Grain-size</i>	23
<i>Water Temperature Sampling</i>	24
Results.....	25
Biological Community.....	25
<i>Benthos</i>	25
<i>Fish</i>	33
Biological Community by Sites	36
<i>Kanahena Cove</i>	36
<i>Kalaeloa</i>	42
<i>Mokuhā</i>	49
<i>Montipora Pond</i>	56
Topographic Relief (Rugosity) and Depth.....	62
Sediment	62
<i>Composition</i>	62
<i>Grain-size</i>	65
Water Temperature	66
Discussion.....	72
Benthic Cover, Composition, and Conditions	72
Fish Abundance and Biomass	78
Topographic Relief (Rugosity) and Depth	85
Sediment	86
Water Temperature	91
Conclusions.....	94

CHAPTER 3: CHARACTERIZING SPATIAL PATTERNS OF CORAL REEF AT A BROAD SCALE, ‘ĀHIHI KĪNA‘U, MAUI	
Introduction.....	98
Spatial Patterns in Heterogeneous Landscape	98
Spatial Statistical Approach.....	100
Characterizing Spatial Patterns of Crustose Coralline Algae and Corals at ‘Āhihi Kīna‘u.....	103
Objectives	105
Materials and Methods.....	106
Study Area	106
Data.....	109
General Field Sampling Protocol.....	109
<i>Benthic Sampling</i>	110
<i>Topographic Relief (Rugosity) and Depth</i>	111
<i>Sediment Composition</i>	112
<i>Sediment Grain-size</i>	113
Data and Statistical Analysis	113
<i>Analysis of Spatial Structures</i>	114
<i>Model Selection and Comparison</i>	119
<i>Visual Representation of Predicted Values</i>	122
Results.....	123
Analysis of Spatial Structures	126
Model Selection and Comparison	133
<i>Non-spatial Models with Independent Errors</i>	133
<i>Spatial Models with the Correlation Functions</i>	135
Visual Representation of Predicted Values and Uncertainty	146
Discussion	158
Analysis of Spatial Structures	158
Model Selection and Comparison	159
<i>Non-spatial Models with Independent Errors</i>	159
<i>Spatial Models with the Correlation Functions</i>	162
Visual Representation of Predicted Values and Uncertainty	165
Conclusions.....	167
CHAPTER 4: SUMMARY AND CONCLUSION	169
REFERENCES	175

LIST OF TABLES

<u>Table</u>	<u>Page</u>
2.1 (a) Percentages of benthic cover types in 2008 and 2010, Kanahena Cove and Kalaeloa	27
2.1 (b) Percentages of benthic cover types in 2008 and 2010, Mokuhā and <i>Montipora</i> Pond	28
2.2 (a) Percent cover of live Scleractinian corals in 2008 and 2010, Kanahena Cove and Kalaeloa.....	30
2.2 (b) Percent cover of live Scleractinian corals in 2008 and 2010, Mokuhā and <i>Montipora</i> Pond	31
2.3 The most frequent fish species across sites in 2008 and 2010.....	33
2.4 Mean number of individual fish per hectare (x 1000) in 2008 and 2010	34
2.5 Mean fish biomass (metric tons ha ⁻¹) in 2008 and 2010.....	35
2.6 Top 5 species for total number of individuals (%), Kanahena Cove, 2008	39
2.7 Top 5 species for total number of individuals (%), Kanahena Cove, 2010	39
2.8 Top 5 species for total number of individuals (%), Kalaeloa, 2008	45
2.9 Top 5 species for total number of individuals (%), Kalaeloa, 2010	45
2.10 Top 5 species for total number of individuals (%), Mokuhā, 2008	52
2.11 Top 5 species for total number of individuals (%),Mokuhā, 2010	52
2.12 Top 5 species for total number of individuals (%), <i>Montipora</i> Pond, 2008	59
2.13 Top 5 species for total number of individuals (%), <i>Montipora</i> Pond, 2010	59
2.14 Proportion (%) of sediment composition in 2008 and 2010.....	63
2.15 Proportion (%) of sediment grain-size in 2008 and 2010.....	66
2.16 (a) Monthly average temperature (°C) in Mokuhā and <i>Montipora</i> Pond	68
2.16 (b) Monthly average temperature (°C) in Kanahena Cove and Kalaeloa	69
3.1 Descriptive statistics of crustose coralline algae and coral cover proportions	126

LIST OF TABLES (cont'd)

<u>Table</u>	<u>Page</u>
3.2 Results of randomization tests for mean coralline algae cover.....	127
3.3 Results of randomization tests for mean coral cover	127
3.4 OLS models for CCA and corals with 4, 5, and 6 parameters	134
3.5 Estimated parameters and their standard errors of explanatory variables for CCA abundance with the six parameter OLS model	135
3.6 Estimated parameters and their standard errors of explanatory variables for coral abundance with the six parameter OLS model	135
3.7 Summary of geostatistical models for coralline algae cover	140
3.8 Summary of geostatistical models for coral cover.....	143
3.9 Summary of cross-validation results for kriged coralline algae cover	149
3.10 Descriptive statistics for simulated coralline algae cover.....	150
3.11 Comparisons of Inverse Distance Weighting methods for coral cover	155

LIST OF FIGURES

<u>Figure</u>		<u>Page</u>
1.1	Map of ‘Āhihi Kīna‘u Natural Area Reserve System, Maui	8
2.1	Map of inshore survey sites at ‘Āhihi Kīna‘u NARS	14
2.2	(a) Study sites, Kanahena Cove	15
2.2	(b) Study sites, <i>Montipora</i> Pond	15
2.2	(c) Study sites, Kalaeloa	16
2.2	(d) Study sites, Mokuhā	16
2.3	(a) Underwater camera system for benthic surveys, front view	19
2.3	(b) Underwater camera system for benthic surveys, side view	19
2.4	<i>Montipora capitata</i> with lost tissue and algal growth, <i>Montipora</i> Pond	32
2.5	(a) Inshore benthic cover, sand-covered turf algae at Kanahena Cove.....	37
2.5	(b) Inshore benthic cover, pavement with encrusting coralline algae, live corals, sea urchins, and algae at Kanahena Cove.....	37
2.5	(c) Inshore benthic cover, colonies of live corals at Kanahena Cove.....	37
2.6	Absolute change in mean percent cover of benthic types at Kanahena Cove from 2008 to 2010	38
2.7	(a) Top 5 fish with the highest mean number of individuals per hectare (x 1000) at Kanahena Cove in 2008	40
2.7	(b) Top 5 fish with the highest mean number of individuals per hectare (x 1000) at Kanahena Cove in 2010	40
2.8	(a) Top 10 fishes (%) for total biomass at Kanahena Cove in 2008	41
2.8	(b) Top 10 fishes (%) for total biomass at Kanahena Cove in 2010.....	41
2.9	Encrusting coralline algae at Kalaeloa.....	43
2.10	Absolute change in mean percent cover of benthic types at Kalaeloa from 2008 to 2010	44

LIST OF FIGURES (cont'd)

<u>Figure</u>	<u>Page</u>
2.11 (a) Top 5 fish with the highest mean number of individuals per hectare (x 1000) at Kalaeloa in 2008	46
2.11 (b) Top 5 fish with the highest mean number of individuals per hectare (x 1000) at Kalaeloa in 2010	46
2.12 (a) Top 10 fishes (%) for total biomass at Kalaeloa in 2008	47
2.12 (b) Top 10 fishes (%) for total biomass at Kalaeloa in 2010	47
2.13 <i>Acanthurus triostegus</i> aggregating and grazing over inshore reef, Kalaeloa	48
2.14 (a) Basalt pavement covered with crustose coralline and turf algae at north end of Mokuhā	50
2.14 (b) Coralline-and turf-covered rock at seaward beach of Mokuhā	50
2.15 Absolute change in mean percent cover of benthic types at Mokuhā from 2008 to 2010	51
2.16 (a) Top 5 fish with the highest mean number of individuals per hectare (x 1000) at Mokuhā in 2008	53
2.16 (b) Top 5 fish with the highest mean number of individuals per hectare (x 1000) at Mokuhā in 2010	53
2.17 (a) Top 10 fishes (%) for total biomass at Mokuhā in 2008	54
2.17 (b) Top 10 fishes (%) for total biomass at Mokuhā in 2010	54
2.18 A group of <i>Scarus psittacus</i> common at Mokuhā.....	55
2.19 Absolute change in mean percent cover of benthic types at <i>Montipora</i> Pond from 2008 to 2010	57
2.20 Macroalgae occupying and outgrowing understory of live <i>M. capitata</i>	58
2.21 <i>Diplosoma similis</i> , phototrophic colonial tunicate.....	58
2.22 (a) Top 5 fish with the highest mean number of individuals per hectare (x 1000) at <i>Montipora</i> Pond in 2008	60

LIST OF FIGURES (cont'd)

<u>Figure</u>	<u>Page</u>
2.22 (b) Top 5 fish with the highest mean number of individuals per hectare (x 1000) at <i>Montipora</i> Pond in 2010	60
2.23 (a) Top 10 fishes (%) for total biomass at <i>Montipora</i> Pond in 2008	61
2.23 (b) Top 10 fishes (%) for total biomass at <i>Montipora</i> Pond in 2010	61
2.24 Mean proportion of sediment composition (%) in 2008 and 2010	63
2.25 Mean proportion of sediment grain-size (%) in 2008 and 2010	66
2.26 (a) Monthly average temperature observed in Mokuhā and <i>Montipora</i> Pond, 2008- 2009	70
2.26 (b) Monthly average temperature observed in Kanahena Cove, Kalaeloa, Mokuhā and <i>Montipora</i> Pond, 2009 – 2010	70
3.1 Map of survey sites, south Maui	107
3.2 A flowchart of data and statistical analysis.....	114
3.3 Theoretical functions for spatial correlation	117
3.4 Scatterplots of a) sampling sites in Y (N-S) and X (E-W) coordinates, b) coralline algae cover against Y coordinate, c) crustose coralline algae cover against X coordinate, d) histogram of transformed mean proportion of coralline algae	124
3.5 Scatterplots of a) sampling sites in Y (N-S) and X (E-W) coordinates, b) coral cover against Y coordinate, c) coral cover against X coordinate, d) histogram of transformed mean proportion of corals.....	125
3.6 Distribution of pairwise distances among 47 sampling sites	126
3.7 Significance map of similarity for coralline algae cover in proportion	128
3.8 Map of cluster types for crustose coralline algae cover in proportion.....	128
3.9 Significance map of similarity for coral cover in proportion	129
3.10 Map of cluster types for coral cover in proportion	130

LIST OF FIGURES (cont'd)

<u>Figure</u>	<u>Page</u>
3.11 Omnidirectional sample variograms for coralline algae cover in proportion, a) fitted with spherical model, and b) with wave model	131
3.12 Sample variogram of coralline algae cover in proportion in four directions	131
3.13 Omnidirectional sample variograms for coral cover in proportion, a) fitted with gaussian model, and b) with spherical model	132
3.14 Sample variogram of coral cover in proportion in four directions	133
3.15 Omni-directional sample variogram of the selected OLS residuals for coralline algae cover in proportion, fitted to the spherical model	136
3.16 Sample variogram of the selected OLS residuals for coralline algae cover in proportion in four directions	137
3.17 Omni-directional sample variogram of the selected OLS residuals for coral cover in proportion.....	138
3.18 Sample variogram of the selected OLS residuals for coral cover in proportion in four directions	138
3.19 Maps of predicted mean proportion of crustose coralline algae by a) simple kriging and b) simple co-kriging	147
3.19 Maps of prediction standard error of crustose coralline algae proportion by c) simple kriging, and d) simple co-kriging	148
3.20 Maps of mean proportion of crustose coralline algae cover generated, from a) five realizations, and b) 100 realizations by conditional simulations	151
3.20 Maps of mean proportion of crustose coralline algae cover, generated from c) 500 realizations, and d) 1000 realizations by conditional simulations	152
3.21 Maps of standard deviation for crustose coralline algae proportion, generated from a) five realizations, and b) 100 realizations by conditional simulations	153
3.21 Maps of standard deviation for crustose coralline algae proportion, generated from c) 500 realizations, and d) 1000 realizations by conditional simulations ...	154
3.22 Maps of predicted mean proportion of coral cover interpolated by IDW, determined by a) standard method, anisotropy, and optimized power of 1.09	156

LIST OF FIGURES (cont'd)

<u>Figure</u>	<u>Page</u>
3.22 Map of predicted mean proportion of coral cover interpolated by IDW, determined by b) standard method, isotropy, and optimized power of 3.56, and c) smoothing method, isotropy, and optimized power of 3.48.	157

ABBREVIATIONS

AIC	Akaike Information Criterion
AKSE	Average Kriging Standard Error
CASI	Compact Airborne Spectrographic Imager
CCA	Crustose Coralline Algae
COTS	Crown-of-Thorn Sea Star
CRAMP	Coral Reef Assessment and Monitoring Program
CV	Coefficient of Variation
DAR	Division of Aquatic Resources
GBR	Great Barrier Reef
IDW	Inverse Distance Weighting
KED	Kriging with External Drift
LIDAR	Light Detection and Ranging
LISA	Local Indicators of Spatial Association
LRT	Likelihood Ratio Test
MPE	Mean Prediction Error
MSPE	Mean Standardized Prediction Error
MWS	<i>Montipora</i> White Syndrome
NARS	Natural Area Reserve System
OLS	Ordinary Least Square Regression
RAT	Rapid Assessment Techniques
REML	Restricted Maximum Likelihood
RMSE	Root Mean Squared Error
RMSPE	Root Mean Squared Prediction Error

ABBREVIATIONS (cont'd)

RMSTDPE	Root Mean Standardized Prediction Error
SD	Standard Deviation of Mean
SE	Standard Error of Mean
SHOALS	Scanning Hydrographic Operational Airborne LIDAR Survey
SL	Standard Length
TL	Total Length
WAAS	Wide Area Augmentation System

CHAPTER 1

GENERAL INTRODUCTION

Status and Issues of Coral Reef Seascapes

Seascapes of coral reefs encompass high biodiversity (Connell 1978), complex geomorphic structures, and associated biotic and abiotic processes providing important ecosystem services and goods for many islands and nations (Costanza *et al.* 1997; Bryant *et al.* 1998; Moberg and Folke 1999). Coral reefs are one of the most ecologically- and socially-valued ecosystems in the world. Yet the integrity of coral reef ecosystems continues to be compromised by natural and anthropogenic impacts at both local- and global-scales (Wilkinson 1999, 2008; Pandolfi *et al.* 2003, 2005). According to ‘Status of Coral Reefs of the World’, 19% of total coral reef area in the world was ‘effectively lost’ (i.e. $\geq 90\%$ of the corals were lost and unlikely to recover soon), 15% was at ‘critical stage’ (50 to 90% loss of corals and likely to become lost in 10 to 20 years), and 20% was categorized as ‘threatened’ (20 to 50% loss of corals and likely to become lost in 20 to 40 years) (Wilkinson 2008). Acute and chronic disturbances, such as hurricanes and storms, earthquakes and volcanic activity, disease, predation, sedimentation, eutrophication, pollution, land and shoreline modification, ship groundings, over- or destructive fishing practices, coral mining, and recreational use (Grigg and Dollar 1990; Brown 1997; Rodgers and Cox 2003; Rodgers 2005; Jokiel 2008), are responsible for degradation and ecological change of coral reef seascapes. Degradation of coral reefs is potentially greater when these disturbances are compounded with changing climate and ocean chemistry (e.g., Gattuso *et al.* 1999; Hoegh-Guldberg 1999; Kleypas *et al.* 1999; Hughes *et al.* 2003; Orr *et al.* 2005; Hoegh-Guldberg *et al.* 2007; Jokiel *et al.* 2008).

Acute and chronic events impact coral reef ecosystems at multiple spatial and temporal scales, and impair the health and self-recovery of coral reefs (Connell *et al.* 1997; Hughes and Connell 1999; Nyström *et al.* 2000). Thus, marine resource and environmental managers are no longer limited to managing a single type of habitat, stressors, and/or species; they are challenged to discern and address multiple biological and environmental issues in time and space. While Hawai‘i’s reefs are considered to be in relatively good condition (Wilkinson 2008), a holistic evaluation of coral reefs and the surrounding environment will help identify the best management options for sustainable use in context of various stressors at multiple scales.

In Hawai‘i, coral reefs typically occur at the land-sea interface where they are strongly influenced by both terrestrial and marine processes. The land-sea interface is a critical transition zone that serves as a conduit of terrestrial and marine processes and interactions among abiotic and biotic elements (Ewel *et al.* 2001). It plays an important role in the flow of materials, energy, organisms, and human-caused processes such as shoreline modification and recreational use. In tropical and subtropical environments, coral reefs are found adjacent to the land-sea interface accounting for great biodiversity (Connell 1978) and providing valuable ecosystem services and goods (Moberg and Folke 1999). Throughout the Main Hawaiian Islands fringing reef is the dominant type of reef formation at the land-sea interface. Therefore its patterns and conditions are often directly affected by natural and anthropogenic stressors from both land and sea.

Hawai‘i’s coral reef seascapes are in need of better understanding for effects of natural and anthropogenic processes inherent to the land-sea interface. Hawai‘i’s natural ecosystems, including coral reefs, are unique due to its geographic isolation and

characteristics, thus these hold high significance for local and global conservation.

Although a low number of species are found in Hawai‘i’s marine fauna, the proportion of endemic species is high. For example, the endemism of shore fishes is 25%, the highest in the Indo-Pacific region (Randall 2007). A characteristic of the Hawaiian shore fish fauna is that many endemic species are strikingly common and abundant (Gosline and Brock 1960). These species are highly adapted to and dependent upon Hawai‘i’s reef environment. Local socio-economic activities rely on ecologically functioning, aesthetic, unique, and protective coral reef seascapes for their economic, cultural, and protective value. The Hawaiian Archipelago encompasses 85% of all U.S. coral reefs, with an estimated reef area of 2536 km² within the Main Hawaiian Islands, and 8521 km² within the Northwestern Hawaiian Islands (Cesar and Van Beukering 2004). Overall asset value of the reefs among the Main Hawaiian Islands was estimated at almost \$10 billion with an annual net benefit of \$360 million to the State’s economy (Cesar and Van Beukering 2004). Conservation and socio-economic values depend on the health of Hawai‘i’s coral reefs. The degradation, lack of resilience, and loss of coral reefs is a problem for Hawai‘i and the U.S. since coral reefs occupy relatively small areas of ocean, therefore are very limited resources.

Climate change and ocean acidification influences local dynamics and complexities of natural and anthropogenic processes on coral reefs at the land-sea interface. Fletcher (2010) stated that Hawai‘i’s rainfall intensity, offshore sea surface temperature, and ocean acidity had increased in recent decades. Topography of the Main Hawaiian Islands typically includes steep mountains with numerous small valleys that accumulate and rapidly discharge high volumes of rain water. High intensity rainfall may

result in severe flooding, accelerated erosion, and sediment transport into the nearshore zone. The introduction of sediment, nutrients, and excess fresh water is a particular concern for coral reefs within embayments where circulation is limited (Jokiel 2006; 2008). Jokiel *et al.* (2008) demonstrated that the growth of crustose coralline algae (CCA) was significantly inhibited in experimental outdoor microcosms treated with acidified seawater and partial pressures of CO₂ equivalent to atmospheric levels during the current century. Calcification and linear extension of coral was also reduced under the acidified environment. CCA is a dominant calcifying organism that plays a major role in cementing carbonates and providing a framework for coral reefs (Adey 1998). CCA is also a preferred settlement substrate and natural inducer for larval metamorphosis of marine invertebrates including corals (Morse *et al.* 1988; Heyward and Negri 1999). Such biological and geochemical processes will change with increasing acidity at the land-sea interface.

While the structure and patterns of Hawai'i's coral reef community is largely shaped by natural disturbances such as wave force, near-bed shear stress, and other oceanographic processes (Dollar 1982; Grigg 1983; Storlazzi *et al.* 2002), anthropogenic stressors are also important drivers affecting their condition and structure. Threats from anthropogenic processes include land-based pollution, such as sediment, sewage, nutrients, pesticide run-off, and thermal effluent discharge, as well as shoreline modification and dredging, ship grounding, anchor damage, fishing, recreational use, and trampling, (Grigg and Dollar 1990; Richmond 1993; Rodgers and Cox 2003; Rodgers 2005; Jokiel 2008) which vary spatially and temporally (Chabanet *et al.* 2005). Chronic anthropogenic impacts can disrupt the ability of corals to recover from acute natural

disturbances such as storms (Connel *et al.* 1997; Hughes and Connell 1999). Chronic anthropogenic stressors may be less obvious than acute stressors, but can be detrimental to the health and recovery of coral reefs with sufficient intensity and/or at large spatial scales.

Increasing human population in coastal areas is a major concern because associated activities likely amplify the intensity of anthropogenic processes. Hawai‘i’s resident population has grown to approximately 1.3 million in 2010. Population density was 11.5 persons per square kilometer in 1910, and increased to 81.8 persons/ km² by 2010 (DBEDT, 2010). A fair proportion of 1600 randomly surveyed households engage in marine activities such as ocean swimming (66%), recreational fishing (31%), surfing (29%), snorkeling (32%), and subsistence fishing (10%) on a regular basis (Hamnet *et al.* 2006). In 2009 approximately 6.5 million visitors arrived in Hawai‘i. About 72% of these visitors (4.7 million) participated in ocean recreation such as swimming and sunbathing (~80-90%), or snorkeling and scuba diving (~45-60%) (HTA 2009). The majority of residents and visitors reside in coastal lowlands since a large portion of the islands are uninhabitable mountains. Land modification and development continues to take place as the population expands. Careful use and management of coral reefs and adjacent lands are needed as Hawai‘i’s population and resource use increases.

Perspectives in Landscape Ecology

The conceptual framework of landscape ecology offers a holistic view and guidance for conservation efforts and effective management of the environment and resources. Landscape ecology is the study of how spatial compositions (amounts of

different entities) and configurations (their arrangements in space; the spatial relationship) affect ecological functions (Forman and Godron 1986), biotic and abiotic processes (Turner 1989), and abundance and distribution of organisms (Fahrig 2005). It is concerned with the interplay between heterogeneous patterns of landscape structures and flux of energy, materials, organisms, and human-modified processes at a multitude of scales and organizational levels (Turner 1989, 2005; Wiens 1989; O'Neill *et al.* 1991; Levin 1992; Pickett and Cadenasso 1995; Liu and Taylor 2002; Wu 2006). The underlying framework is interdisciplinary, integrating abiotic, biotic, and human factors and their interrelationships within physically-explicit spaces (Forman 1983; Turner 1989, 2005; Forman 1995; Pickett and Cadenasso 1995; Liu and Taylor 2002; Turner *et al.* 2002; Wu 2006; Lepczyk *et al.* 2008). Hierarchical organization and effects of scales (Wiens 1989; Wiens and Milne 1989; Levin 1992) are core to the concept, linking broad-scale environmental issues and fine-scale processes or mechanisms (Turner *et al.* 2001). Many landscape ecological studies focus on temporal differences in patterns and processes. The approach of landscape ecology was not applied in the United States until the 1980's (Liu and Taylor 2002; Turner 2005) despite its origins with Russian and European geographers in the early to mid 1900's. The fundamental concept of 'landscape ecology' was widely introduced by Troll, a German geographer in 1950. British ecologists Tansley and Watt also recognized the importance of spatial perspectives in patterns of organisms from the 1930's through the late 1940's. Later, the spatial aspect of regional geography and functional aspect of ecology were catalyzed and refined shaping the modern landscape ecology in North America (Forman 1983, Turner

et al. 2001). These frameworks and principles have now become a major environmental research approach.

Historically, there have been a number of landscape ecological studies focusing on the terrestrial environment (Forman and Gordon 1986; Turner 1989, 2005). These studies have been successfully applied to conservation and management of resources and land uses (Turner *et al.* 2002). Today, more and more marine and coastal scholars are exploring the approach to understand the interrelationship of patterns and processes of marine and coastal landscapes (e.g., Pittman *et al.* 2004; Harborne *et al.* 2006; Pittman *et al.* 2007; Grober-Dunsmore *et al.* 2008; Hinchey *et al.* 2008) and its relevance to effects of scale on observed phenomena (Mumby *et al.* 2004a; Chabanet *et al.* 2005) with the help of advancements in geographic information systems (GIS), remote sensing applications, spatial statistics and modeling (Liu and Taylor 2002; Turner *et al.* 2002).

Resource and environmental management must deal with the dynamic utility of a given physical landscape as it is impacted by organisms and humans. Thus decision-makers would benefit from spatially-explicit information that integrates ecological functions, abiotic, biotic, and human processes and their change over time. Application of this conceptual framework is appropriate to coastal and coral reef environments that are complex and highly stressed by both natural and anthropogenic processes at various scales.

The primary focus of this study is to produce temporal and spatial information needed to assist the management and conservation of ‘Āhihi Kīna‘u Natural Area Reserve System (NARS, Fig. 1.1). Seascapes of ‘Āhihi Kīna‘u NARS consist of mosaics of ecologically-important habitats, unique biotic and abiotic forms and structures, and

human use. This study aims to explore the conceptual framework of landscape ecology to further our understanding of relationships between the seascape pattern, local impacts, and distributions of marine resources within ‘Āhihi Kīna‘u NARS, thereby guiding future conservation and management decisions.

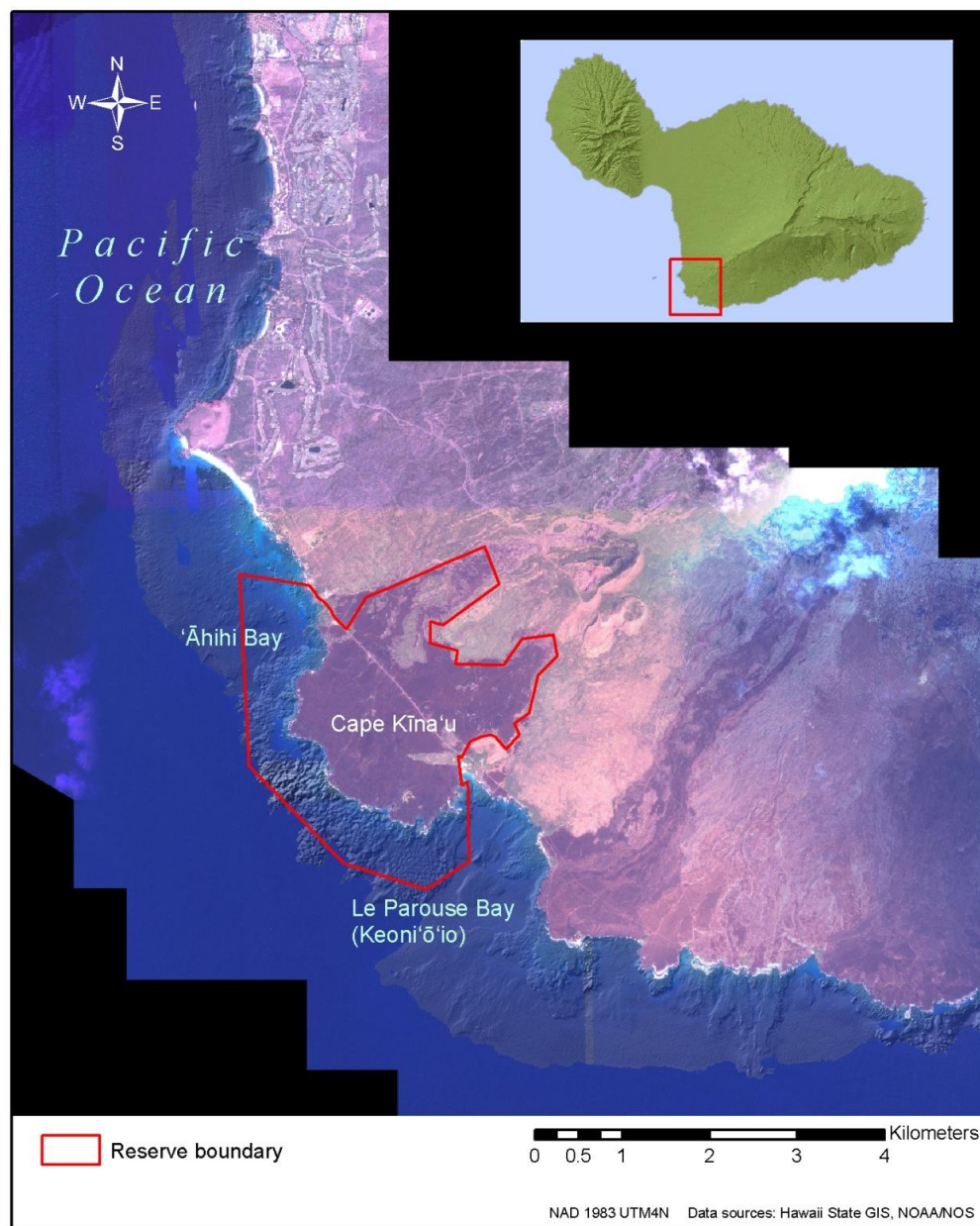


Fig. 1.1 ‘Āhihi Kīna‘u Natural Area Reserve System, Maui.

CHAPTER 2

ASSESSMENT OF INSHORE SEASCAPE FOLLOWING SHORELINE ACCESS CLOSURE

Introduction

Background

‘Āhihi Kīna‘u NARS, located on the southwestern tip of Mount Haleakalā, Maui, is a unique reserve system within the State of Hawaii (Figure 1.1). Since designation as the first NARS in 1973 (DOFAW 2008), it is the only NARS which combines marine (3.27 km^2) and terrestrial (6.55 km^2) areas within its jurisdictional boundary (Rodgers and Jokiel 2008; Rodgers *et al.* 2008). Thus ‘Āhihi Kīna‘u NARS aims to protect not only terrestrial landscape but also ecologically and socially valued seascape. Various landscape features such as aeolian, anchiline, coral reef, and low dryland systems exist within the NARS. The reserve includes a variety of biotic and abiotic components such as anchialine ponds, complex basalt rocks and lava structures shaped by weathering and wave action (Macdonald *et al.* 1990), protected small coves and tide pools, sandy bottoms, pavement of CCA, live corals, and associated diverse aquatic species. Anthropogenic components, such as a historic Hawaiian fish pond and archaeological sites, are also an integral part of the reserve. Extraction of marine resources has been generally prohibited within the reserve boundary for more than 30 years (DOFAW 2008). Observations indicate that the surrounding areas of the NARS receive limited anthropogenic modification, thus keeping its seascape far less impacted than other coastal and seascapes on Maui.

The unique and highly valued NARS seascape, however, faces potential degradation from increased visitation and non-consumptive human uses. As the NARS

became a popular ecotourism destination, increasing numbers of visitors and associated activities such as kayaking, wading, and snorkeling within the reserve have increased over the last decade (HTA 2003; DOFAW 2008; Rodgers and Jokiel 2008). Frequent human visitation and concomitant use facilitates direct and indirect alteration of biotic and abiotic components of land- and seascapes. For example, intense human-trampling have chronic impacts on soil-hydrologic conditions, biogeochemistry, habitat integrity, and an organism's physical and ecological states in natural land- and seascapes (Kay and Liddle 1989; Hawkins and Roberts 1993; Allison 1996; Sutherland *et al.* 2001; Rodgers and Cox 2003; Kerbiriou *et al.* 2008). On a reef, impacts of human-trampling include mechanical breakage, tissue damage, reduced growth rate, partial mortality of corals, and loss of aesthetic appeal (Liddle and Kay 1987; Kay and Liddle, 1989; Hawkins and Roberts 1993; Allison 1996; Rodgers and Cox 2003). Damaged areas may eventually lead to habitat change or loss for fishes and other marine organisms. Frequent human use may also cause conflict among other stakeholders. Careless visitors have altered archaeological and historic structures of ‘Āhihi Kīna‘u’s cultural land- and seascapes (pers. comm. Ramsey 2008). Potential negative impacts from non-extractive uses on the seashore and the need for regulatory measures have recently emerged.

There was strong public and government concern regarding impact from non-consumptive uses in ‘Āhihi Kīna‘u NARS. It eventually led to a ban on commercial kayaking within the reserve in 2003, reducing visitor use (HTA 2003; DOFAW 2008; Rodgers and Jokiel 2008). Visitors to the adjacent Keoni‘ō‘io or La Perouse Bay, a popular destination to the south, was estimated at almost 277,000 in 2006 while the estimate was near 273,000 in 2003 (Vann *et al.* 2006), therefore the estimated number of

visitors using the NARS in 2006 may likely surpass 2003 (Vann *et al.* 2006). Upon the NARS request, qualitative surveys were conducted by the Hawai‘i Coral Reef Assessment and Monitoring Program (CRAMP) of the Hawai‘i Institute of Marine Biology (HIMB), University of Hawai‘i, to assess areas exhibiting potential impacts associated with human-trampling on corals in late 2007 (Rodgers and Jokiel 2008). From the preliminary investigation, it was concluded that there was an additional need to collect quantitative ecological information on seascape attributes in ‘Āhihi Kīna‘u NARS. In August 2008, NARS management placed a two-year temporary restriction on terrestrial access within the reserve except Kanahena Cove (Figure 1.1) located near the western management boundary (DOFAW 2008). The management team also decided to conduct a quantitative evaluation of inshore marine resources and potential impacts by non-consumptive uses during this two-year period.

Inshore seascapes of ‘Āhihi Kīna‘u NARS consist of mosaics of coral reefs, other biotic and abiotic forms and structures, and human land-uses. Some habitat patches and mosaics may be small and less dominant yet hold high ecological and social value. Ironically, these same areas are where human-trampling is most frequent. Further concerns have been expressed about the potential for the surrounding landscapes of the ‘Āhihi Kīna‘u area to be transformed into human-dominated types (pers. comm. Fielding 2008). Disruption in contributing areas negatively affects patterns and processes within the reserve since natural systems are often connected and occur along gradients, regardless of arbitrary management boundaries. Thus, it is imperative that we gain a better understanding of the seascape characteristics within the reserve and in neighboring areas.

Objectives

The goal of this study was to assess the potential temporal change of subtidal benthos, fish, and sediment characteristics along gradients of human frequentation at a fine scale < 0.2 km. A specific research question was defined: do compositions of subtidal benthic, fish, and sediment characteristics change following the shoreline-access closure at a fine scale?

Materials and Methods

Quantitative inshore baseline surveys were conducted during September 20-21, 2008, January 2-9 and February 6, 2010 at ‘Āhihi Kīna‘u NARS, Maui. The purpose of these fine-scaled surveys was to quantify and document potential temporal changes to inshore fish and benthic characteristics resulting from shoreline access closure. Objectives also included quantifying abiotic environmental variables (i.e., rugosity, sediment composition and grain-size, and water temperature) that influence biotic factors. These variables may help discern potential impacts from natural and anthropogenic stressors. Further, these data will serve as an important inventory of resources and a baseline for the future. The survey was limited to the depth associated with recreational activities and relatively fine-scaled, spatially delineated areas.

Study Sites

Surveys were conducted in ‘Āhihi Kīna‘u NARS, and encompassed the area out to 0.8 km from the point at 0.2 km north of Kanahena Cove through ‘Āhihi Bay and around Cape Kīna‘u stretching to the western shoreline of Keoni‘ō‘io of south Maui (Fig.

1.1). It consists of relatively new lava (Stearns 1985; Macdonald *et al.* 1990) which forms dry, rough terrains and shoreline with very little vegetation at low altitude. In general, southern facing shorelines are relatively protected from high-energy northwest swells and prevailing northeast trade winds.

Within the NARS, four sites were chosen for field sampling based on visitor frequency and levels of snorkeling and wading activities before closure (Rogers and Jokiel 2008). Survey sites included a single open-access area and three closed areas: Kanahena Cove, *Montipora* Pond, Kalaeloa, and Mokuhā (Fig. 2.1). Kanahena Cove (Fig. 2.2a) is located near the western end of the reserve boundary and remains open to visitors for snorkeling, wading, and SCUBA diving. This is also one of the sites CRAMP established for state-wide long-term coral reef monitoring at depths of 1 m and 3 m. The *Montipora* Pond (Fig. 2.2b) is a small tidal pond located just within the eastern end of the reserve boundary adjacent to La Perouse Bay. Kalaeloa (Fig. 2.2c) is a protected cove located south of the *Montipora* Pond. It is larger and deeper than the other sites. Mokuhā (Fig. 2.2d) is the most remote site near the center of the reserve. The adjacent point west of the cove is called Kanahena Point, another CRAMP long-term monitoring site at 3 m and 10 m. The latter three sites have a history of frequent human visitation and recreational activities. These three sites have been closed to terrestrial public access since August 1, 2008.

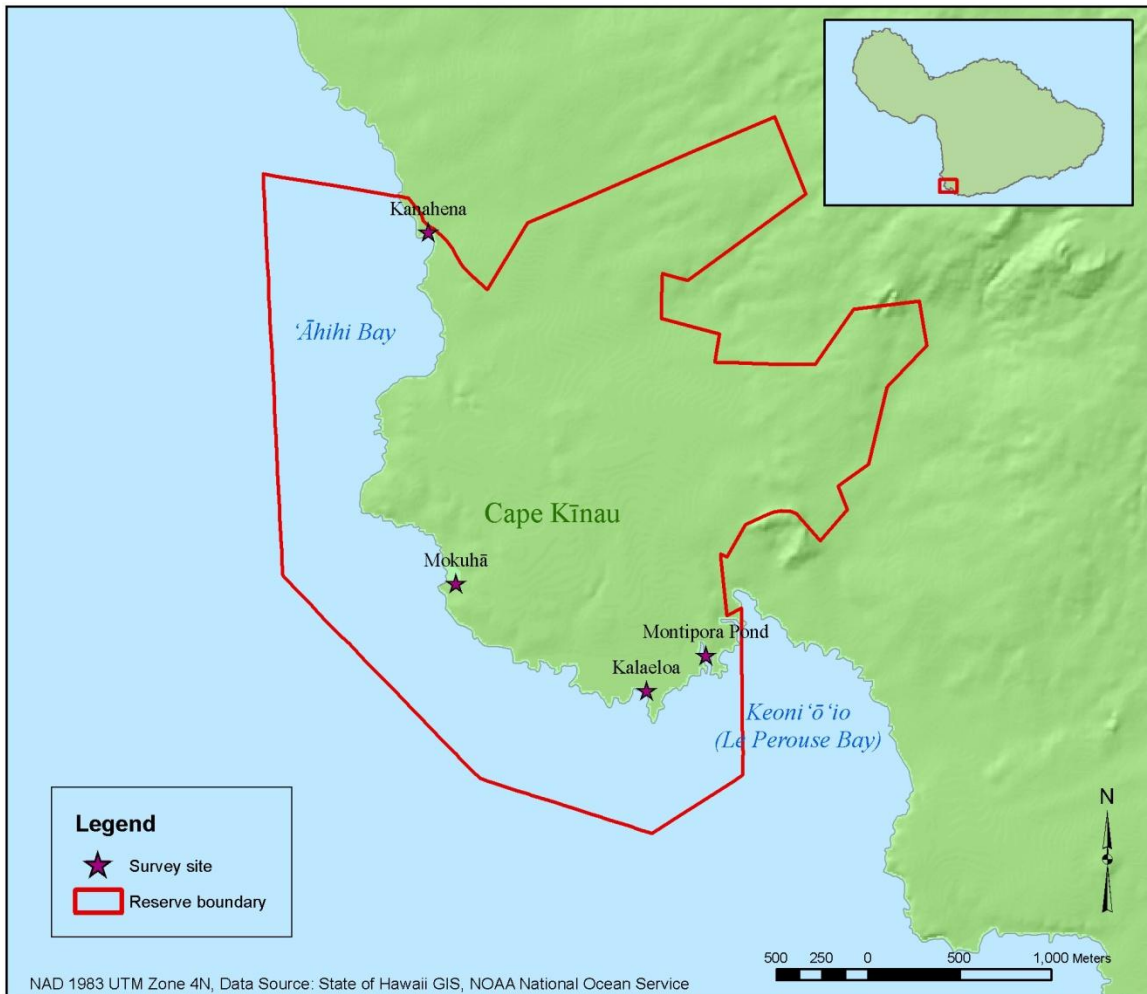


Fig. 2.1. Inshore survey sites, ‘Āhihi Kīna‘u Natural Area Reserve System, Maui.



Fig. 2.2. Study sites. (a) Kanahena Cove, and (b) *Montipora* Pond, indicated by the arrow.

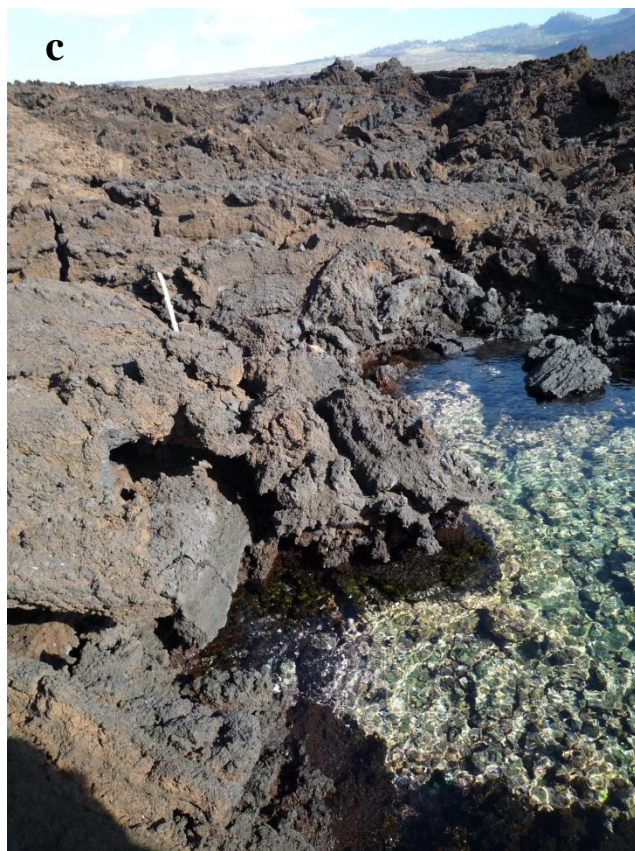


Fig. 2.2. Study sites. (c) surrounding terrain at Kalaeloa, and (d) Mokuhā.

General Field Sampling Protocol

Sampling was conducted in shallow inshore reefs at the land-sea interface at each of the four study sites previously identified. Field data was collected twice over a period of 16 months after closure of terrestrial access to the four study sites within the reserve. The first survey was carried out in September, 2008. The second survey was conducted in January, 2010 for Kalaeloa, Mokuhā, and *Montipora* pond; sampling in Kanahena Cove occurred in early February, 2010 due to rough seas.

Data included benthic cover, fish assemblage, sediment composition, grain-size, topographic relief (rugosity), and water temperature. Biological measurements were made by visual fish counts including estimates of total length along a belt transect, and benthic cover estimates by functional group and substrate using photoquadrats. Data were analyzed by site and survey years. Detailed field sampling methods for each data type is described in upcoming sections.

Generally, 25 m-long transect lines were deployed within areas subject to human-access and trampling. Sampling depth was recorded from transects. Sampling was typically carried out within depths of 0.5-1.5 m at each site, as much as topographic features allowed. Depths of less than 1.5 m, the zone of greatest impact by snorkelers and waders, were the focus of these transects. Transect starting positions were determined using a Garmin GPSMAP 76, providing \pm 3 m accuracy when Wide Area Augmentation System (WAAS) was enabled. In addition, physical features of transect points were qualitatively described and documented. Biological data collection was conducted by snorkeling, using the Rapid Assessment Techniques (RAT) designed by CRAMP (Jokiel *et al.* 2004; Rodgers 2005). Topographical relief (rugosity) was

measured along all transects at each site. Bulk sediment was sampled in 2008 and 2010 at each site. Temperature was continuously recorded starting from July 2008 to June 2009 at two sites and July/August 2009 to April/May 2010 at all sites. This data is comparable to an extensive database compiled for various locations within the Main Hawaiian Islands including 2007 and 2009 surveys conducted in the ‘Āhihi Kīna‘u NARS at depths ranging between 3 and 18 m.

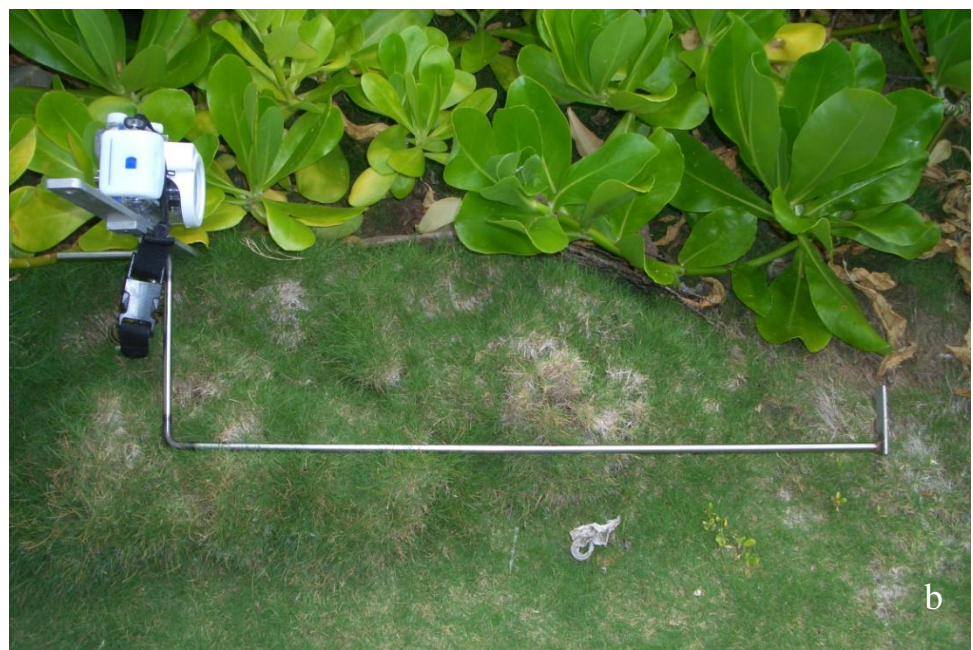
The following methods and protocols were adapted and slightly modified from RATs for non-invasive surveying in shallow inshore environments. It optimizes the ability to obtain data on ecological functional groups and abiotic characteristics of seascapes.

Benthic Sampling

Approximately 50 high resolution digital images were taken along a 25 m transect using a Panasonic FX35 zoom digital camera within a Panasonic MCFX35 underwater housing for assessing the characteristics of fine scale benthic seascapes structures. The camera was assembled with an aluminum monopod frame, 0.5 m from the substrate providing a 50 x 69 cm image (Fig. 2.3a and 2.3b). A 6 cm bar on the monopod base served as a measurement scale.



a



b

Fig. 2.3. Underwater camera system for benthic surveys. (a) front-view, and (b) side-view. Monopod is 0.7 m long.

The software program PhotoGrid (Bird 2001) was used for quantifying percent cover of biotic functional groups and abiotic substrate. Twenty non-overlapping images from each 25 m transect were randomly selected and imported into PhotoGrid where 50 randomly selected points were displayed onto each image. This processed data, exported in a comma separated values (CSV) file, was imported into Microsoft Excel 2007 for further descriptive statistical analysis. It was also be imported into Microsoft Access XP for database management.

Fish Sampling

Fish populations were assessed using the standard visual belt transect approach (Brock 1954; Brock 1982). Transect positions were randomly selected within each site depending on its extent and scope of survey. A diver swam along two to five 25 m x 5 m transects (125 m^2) at each site. Species, quantity, and total length of fishes were recorded. All fishes were identified to the lowest taxon possible. The same individual quantified fishes for all samples to eliminate observer variability.

Total length (TL) of fish was estimated to the nearest centimeter in the field. The estimated length was converted to biomass density estimates, metric tons per hectare (t ha^{-1}), with length-mass fitting parameters. This unit of measure was chosen to maintain consistency with most reef fish surveys and studies conducted within the past twenty years. Fitting parameters of the length-mass relationship were estimated by a linear regression model of $\log M$ vs. $\log L$. Length estimates were converted to mass using the function $M = aSL^b$ where M = mass in grams, SL = standard length in mm, a and b are estimated fitting parameters available from the Hawai‘i Cooperative Fishery Research

Unit (HCFRU). FishBase (www.fishbase.org) was used for obtaining fitting parameters when unavailable from HCFRU. If a specific fitting parameter is not available, a congener of similar shape within the genus was used. To estimate fish biomass from underwater length observations, recorded TL may be converted to other length types (e.g., standard length, SL) depending on available fitting parameters derived from length types indicated in the above database. Linear regression models and ratios from FishBase (www.fishbase.org) were used to convert TL to SL or other length types. Mean density (mean number of individuals $\text{ha}^{-1} \times 1000$) of fishes for each site were also estimated. Data were analyzed using the software programs Microsoft Excel 2007 and Minitab 15.1 (Minitab Inc. 2007).

Topographic Relief (Rugosity) and Depth

High rugosity and habitat complexity is important for fish and coral community structures (Friedlander and Parrish 1998; Friedlander *et al.* 2003; Jokiel *et al.* 2004). Habitat complexity and topographic relief can be altered by physical disturbances. Rugosity was measured to determine topographical relief and spatial complexity. A 15 m chain marked at 1 m intervals with 1.3 cm links was draped along the length of the transect (10 m) following the contours of the bottom relief. An index of rugosity, the ratio of the reef contour distance as measured by the chain length to the horizontal linear distance, was calculated for each transect (McCormick 1994). Approximate depth was estimated using the 0.5 m-monopod and a transect line for extremely shallow areas between 0.5 and 1.0 m. A hand-held electronic depth sounder was also used for

estimating depth at the occasional site deeper than 1.5 m. This was due to variable topographic relief.

Sediment Sampling

Sediment composition and grain-size help describe patterns of water circulation and input sources. Entrainment of fine sediment grains (silts and fine sands) and organic particles requires less velocity or shear stress than larger particles (Boggs 1995) so these are generally transported further downstream, frequently entering the ocean during storm floods.

Replicate sediment samples were collected at each of four sites in both 2008 and 2010. Three samples were collected at Kanahena Cove, and two samples were each collected at Kalaeloa, Mokuhā, and *Montipora* Pond annually. Each Fisher brand 9 x 18 cm sample bag was filled with approximately 500 cm³ of sediment. Composition and grain-size of sediment were determined following sedimentological methods described in Rodgers (2005). Samples were thoroughly mixed for subsequent processing and analysis. For each sample percentages of sediment composition and grain-size were calculated using Microsoft Excel. Results were summarized by descriptive statistics.

Sediment Composition

Inorganic and organic carbon were partitioned from marine sediments by incinerating them at different temperatures (Dean 1974; Parker 1983; Bengtsson and Enell 1986; Craft *et al.* 1991; Sutherland 1998; Heiri *et al.* 2001). Approximately 10 g of sediment was finely ground using a mortar and pestle, prior to the determination of the

inorganic-organic carbon fractions. Two subsamples of 10 g were taken from each replicate to reduce variability. These were dried in crucibles to remove moisture for 10 h at 100°C then placed in a desiccator and weighed. Samples were then incinerated in a muffle furnace for 12 h at 500°C to remove organic matter. Following incineration, samples were placed in a desiccator and weighed. For removal of the carbonate material, samples were again placed in a muffle furnace for 2 h at 1000°C. These were cooled in a desiccator and weighed. The percent loss on ignition (LOI) was calculated based on mass changes at each step. LOI₅₀₀ was used as an index of organic matter and LOI₁₀₀₀ was primarily an index of the calcium carbonate (CaCO₃).

Sediment Grain-size

Subsamples were taken from each of two or three replicates collected from each site. These were wet-sieved (McManus 1988) using standard brass sieves. Mesh-size of sieves included 2.8 mm, 500 µm, 250 µm, and 63 µm (USA Standard Testing Sieve: A.S.T.M.E.-11 specifications). A brass catch pan collected the silt/clay sized fraction (<63 µm). Five size fractions were determined: granule (> 2.8 mm), very coarse and coarse sand (500 µm-2.8 mm), medium sand (250-500 µm), fine and very fine sand (63-250 µm), and silt/clay (<63 µm) in accordance with the Wentworth scale (Folk 1974). Each size fraction was filtered through pre-weighed Whatman 114 wet strength filters and air-dried. These were then weighed on three separate days to determine the proportion of each size fraction. Extremely large pebbles or cobbles were removed before sieving to minimize variability and skewed weights.

Water Temperature Sampling

Water temperature affects geochemical processes, biological activity, and distributions of most marine organisms, thus it is an important measure particularly during times of potential climate change. Ambient temperature was measured with a portable aquatic temperature data logger, HOBO U22 Water Temp Pro v2 manufactured by Onset Computer Corporation. The unit's small size of 11.4 cm allowed it to be easily hidden. According to manufacturer specifications, measurement and recording accuracy was $\pm 0.2^{\circ}\text{C}$ and ± 1 min per month between 0° and 50°C . Each unit was calibrated and tested for accuracy at zero and 34°C in the lab before deployment in the field. The logging interval was set for every 15 min referenced on Greenwich Mean Time -10:00 hours for Hawai‘i.

The first data loggers, one per site, were deployed at Kanahena Cove, Mokuhā, and *Montipora* Pond in July 2008. A logger was deployed at Kalaeloa in August 2009. Loggers were mounted and secured with cable ties on a representative section of reef near coral colonies approximately 1 m deep. Data collection cycles were one year before downloading data. The second deployment occurred upon retrieval of the first logger for continuous measurement between July 2009 and around April/May 2010.

HOBOware software was used for downloading data and analysis. HOBOware along with an optical USB interface from the manufacturer was required to complete the process. Analysis was also assisted by Microsoft Excel for descriptive statistics.

Results

Surveys were conducted during September 20-21, 2008, January 2-9 and February 6, 2010. For benthic coverage 12 transects were surveyed in 2008, and 15 transects in 2010. For fish 10 transects were surveyed in 2008, and 15 transects were surveyed in 2010. Data and results for each site are summarized in the following subsections. Small sample size and high variability limited statistical interpretation and confidence in detecting change in biological community at each site over the 17 months. However, the results will provide useful baseline values and are valuable describing the various habitats and environmental conditions.

Biological Community

Benthos

Benthic cover composition and percentage of observed cover classes varied among sites (Table 2.1a and 2.1b). Rarely was continuous abiotic surface left unoccupied by benthic organisms across sites. Common benthic cover types in inshore environments included encrusting coralline algae and turf algae. Observed CCA included *Hydrolithon*, *Neogoniolithon*, and *Lithophyllum*, commonly found throughout the Hawaiian Archipelago (pers. comm. Squair 2010). Unconsolidated sand and/or silt deposits loosely covering turf algae on volcanic rock and/or pavement was also a common cover type. In this survey, such heterogeneous mixed cover types were referred to as ‘substrate’. Subtle distinction was made classifying either turf algae or ‘substrate’ on relative portions of sand and/or silt deposits on turf algae. Large percentages of turf algae and small percentages of encrusting macroalgae occupied shady, small pits and slits of rugose

basalt surfaces at Kalaeloa and Mokuhā. Turf algae was generally very short which is probably the result of grazing. Relatively few sea urchins were recorded from Kanahena, Kalaeloa, and Mokuhā samples in both years.

Table 2.1a. Percentages of benthic cover types (%) in 2008 and 2010. Sample statistics are mean \pm standard deviation with number of transects in parentheses.

Benthic cover type	Kanahena Cove 2008	Kanahena Cove 2010	Kalaeloa 2008	Kalaeloa 2010
Coral	11.6 \pm 12.9 (3)	9.2 \pm 4.6 (5)	3.7 \pm 4.4 (4)	3.9 \pm 4.6 (5)
Dead coral	0.1 \pm 0.1 (3)	0.1 \pm 0.1 (5)	0.3 \pm 0.4 (4)	0.1 \pm 0.2 (5)
Zoanthid	0.0 \pm 0.0 (3)	0.0 \pm 0.0 (5)	0.1 \pm 0.1 (4)	0.0 \pm 0.0 (5)
<i>Echinometra mathaei</i>	0.6 \pm 0.6 (3)	0.7 \pm 0.3 (5)	0.5 \pm 0.3 (4)	0.2 \pm 0.2 (5)
<i>Echinothrix calamaris</i>	0.0 \pm 0.0 (3)	0.0 \pm 0.0 (5)	0.0 \pm 0.0 (4)	0.1 \pm 0.2 (5)
Tunicate	0.0 \pm 0.0 (3)	0.0 \pm 0.0 (5)	0.0 \pm 0.0 (4)	0.0 \pm 0.0 (5)
Mollusk	0.0 \pm 0.0 (3)	0.0 \pm 0.0 (5)	0.1 \pm 0.1 (4)	0.1 \pm 0.1 (5)
Coralline algae	2.0 \pm 1.6 (3)	5.0 \pm 3.3 (5)	30.4 \pm 10.0 (4)	29.4 \pm 6.5 (5)
Macroalgae	0.3 \pm 0.4 (3)	0.1 \pm 0.3 (5)	1.7 \pm 2.0 (4)	0.4 \pm 0.3 (5)
Turf algae	3.8 \pm 0.9 (3)	33.9 \pm 21.8 (5)	49.4 \pm 11.5 (4)	49.0 \pm 8.6 (5)
Substrate	75.4 \pm 12.5 (3)	45.5 \pm 26.9 (5)	10.3 \pm 4.7 (4)	11.6 \pm 8.6 (5)
Bare rock	0.0 \pm 0.0 (3)	0.0 \pm 0.1 (5)	0.1 \pm 0.2 (4)	0.0 \pm 0.0 (5)
Sand	3.7 \pm 2.6 (3)	4.2 \pm 5.2 (5)	0.0 \pm 0.0 (4)	0.0 \pm 0.0 (5)
Silt	0.0 \pm 0.0 (3)	0.0 \pm 0.1 (5)	0.0 \pm 0.0 (4)	0.3 \pm 0.4 (5)
*Other	2.5 \pm 0.3 (3)	1.3 \pm 0.9 (5)	3.6 \pm 1.8 (4)	5.0 \pm 2.3 (5)

*This category represents shadows and survey gear in photographic data, and not actual benthic and substrate types.

Table 2.1b. Percentages of benthic cover types (%) in 2008 and 2010. Sample statistics are mean \pm standard deviation with number of transects in parentheses.

Benthic cover type	Mokuhā		<i>Montipora</i> Pond	
	2008	2010	2008	2010
Coral	0.0 \pm 0.1 (3)	0.0 \pm 0.1 (3)	48.5 \pm 20.9 (2)	30.2 \pm 6.2 (2)
Dead coral	0.1 \pm 0.1 (3)	0.0 \pm 0.0 (3)	2.9 \pm 2.1 (2)	5.8 \pm 2.3 (2)
Zoanthid	1.2 \pm 1.2 (3)	0.4 \pm 0.5 (3)	0.0 \pm 0.0 (2)	0.0 \pm 0.0 (2)
<i>Echinometra mathaei</i>	0.1 \pm 0.1 (3)	0.1 \pm 0.1 (3)	0.0 \pm 0.0 (2)	0.0 \pm 0.0 (2)
<i>Echinothrix calamaris</i>	0.0 \pm 0.0 (3)	0.0 \pm 0.0 (3)	0.0 \pm 0.0 (2)	0.0 \pm 0.0 (2)
Tunicate	0.0 \pm 0.0 (3)	0.0 \pm 0.0 (3)	0.1 \pm 0.1 (2)	1.2 \pm 1.6 (2)
Mollusk	0.0 \pm 0.1 (3)	0.0 \pm 0.0 (3)	0.0 \pm 0.0 (2)	0.0 \pm 0.0 (2)
Coralline algae	41.5 \pm 15.1 (3)	36.2 \pm 11.9 (3)	2.3 \pm 3.2 (2)	1.5 \pm 2.1 (2)
Macroalgae	0.0 \pm 0.1 (3)	0.1 \pm 0.1 (3)	8.1 \pm 9.5 (2)	10.4 \pm 12.0 (2)
Turf algae	17.6 \pm 6.0 (3)	19.2 \pm 12.1 (3)	23.8 \pm 11.3 (2)	30.5 \pm 10.5 (2)
Substrate	28.3 \pm 12.8 (3)	29.2 \pm 12.6 (3)	5.4 \pm 2.6 (2)	10.5 \pm 1.6 (2)
Bare rock	0.0 \pm 0.0 (3)	0.0 \pm 0.0 (3)	0.0 \pm 0.0 (2)	0.0 \pm 0.0 (2)
Sand	9.1 \pm 14.7 (3)	8.8 \pm 14.3 (3)	2.1 \pm 2.8 (2)	5.0 \pm 1.2 (2)
Silt	0.1 \pm 0.2 (3)	0.1 \pm 0.2 (3)	0.2 \pm 0.1 (2)	0.7 \pm 0.7 (2)
*Other	1.9 \pm 0.9 (3)	6.0 \pm 1.8 (3)	6.9 \pm 1.1 (2)	4.4 \pm 1.4 (2)

*This category represents shadows and survey gear in photographic data, and not actual benthic and substrate types.

A total of 13 coral species were observed within the four sites between 2008 and 2010 (Table 2.2a and 2.2b). The highest richness (9 species) was observed at Kanahena Cove for both years. Seven species in 2008 and 8 species in 2010 were recorded at Kalaeloa. A single species was observed at Mokuhā and *Montipora* pond. Percent cover of live hard corals ranged from less than 1% to 48.5% in 2008, and from less than 1% to 30.2% in 2010. Mean coral cover was the highest at *Montipora* Pond, followed by Kanahena Cove, Kalaeloa, and least at Mokuhā for both years.

During surveys in 2008 and 2010 coral disease was documented at *Montipora* Pond (Fig. 2.4) although it was not formally included in the scope of the survey. *Montipora* White Syndrome (MWS) was observed on colonies of Rice coral, *Montipora capitata*, in this small confined habitat during the preliminary visit in July 2008. MWS is a coral disease known to result in tissue loss and occurs throughout the Hawaiian Archipelago (Aeby *et al.* 2010). It has been known to be especially prevalent in Kāne‘ohe Bay, Oahu, yet much of its pathology, etiology, and ecology is unclear (Aeby 2006; Aeby *et al.* 2010). The estimated prevalence of MWS in 2010 was similar to 2008 at *Montipora* Pond, roughly 8% and 9% (pers. comm. Ross 2010, unpub. data). This small area exhibited the highest reported percentage of MWS compared to Northwestern Hawaiian Islands or Main Hawaiian Islands (Friedlander *et al.* 2005; Aeby 2006; Aeby *et al.* 2010).

Table 2.2a. Percent cover of live Scleractinian corals (%) in 2008 and 2010. Sample statistics are mean \pm standard deviation with number of transects in parentheses.

Species	Kanahena Cove		Kalaeloa	
	2008	2010	2008	2010
<i>Cyphastrea ocellina</i>	0.0 \pm 0.0 (3)	0.0 \pm 0.0 (5)	0.2 \pm 0.1 (4)	0.0 \pm 0.0 (5)
<i>Montipora capitata</i>	1.4 \pm 2.5 (3)	1.5 \pm 1.5 (5)	0.2 \pm 0.3 (4)	0.04 \pm 0.1 (5)
<i>Montipora patula</i>	0.0 \pm 0.0 (3)	1.2 \pm 1.6 (5)	0.0 \pm 0.0 (4)	0.6 \pm 0.7 (5)
<i>Montipora studeri</i>	0.1 \pm 0.1 (3)	0.0 \pm 0.0 (5)	0.0 \pm 0.0 (4)	0.0 \pm 0.0 (5)
<i>Pavona duerdeni</i>	0.1 \pm 0.2 (3)	0.0 \pm 0.0 (5)	0.2 \pm 0.3 (4)	0.3 \pm 0.7 (5)
<i>Pavona varians</i>	0.1 \pm 0.2 (3)	0.1 \pm 0.1 (5)	0.3 \pm 0.3 (4)	0.4 \pm 0.5 (5)
<i>Pocillopora damicornis</i>	0.1 \pm 0.1 (3)	0.04 \pm 0.1 (5)	0.0 \pm 0.0 (4)	0.1 \pm 0.1 (5)
<i>Pocillopora meandrina</i>	0.2 \pm 0.2 (3)	0.2 \pm 0.3 (5)	0.5 \pm 0.5 (4)	0.2 \pm 0.2 (5)
<i>Porites brighamii</i>	0.1 \pm 0.1 (3)	0.2 \pm 0.3 (5)	0.0 \pm 0.0 (4)	0.0 \pm 0.0 (5)
<i>Porites evermanni</i>	1.1 \pm 2.0 (3)	0.5 \pm 0.4 (5)	0.0 \pm 0.0 (4)	0.0 \pm 0.0 (5)
<i>Porites lobata</i>	8.4 \pm 8.3 (3)	5.4 \pm 3.8 (5)	2.3 \pm 4.0 (4)	1.8 \pm 3.5 (5)
<i>Psammocora nierstraszi</i>	0.0 \pm 0.0 (3)	0.0 \pm 0.0 (5)	0.1 \pm 0.1 (4)	0.2 \pm 0.2 (5)
<i>Psammocora stellata</i>	0.0 \pm 0.0 (3)	0.04 \pm 0.1 (5)	0.0 \pm 0.0 (4)	0.0 \pm 0.0 (5)
Total mean cover	11.6	9.2	3.7	3.6

Table 2.2b. Percent cover of live Scleractinian corals (%) in 2008 and 2010. Sample statistics are mean \pm standard deviation with number of transects in parentheses.

Species	Mokuhā		Montipora Pond	
	2008	2010	2008	2010
<i>Cyphastrea ocellina</i>	0.0 \pm 0.0 (3)	0.0 \pm 0.0 (3)	0.0 \pm 0.0 (2)	0.0 \pm 0.0 (2)
<i>Montipora capitata</i>	0.0 \pm 0.0 (3)	0.0 \pm 0.0 (3)	48.5 \pm 20.9 (2)	30.2 \pm 6.2 (2)
<i>Montipora patula</i>	0.0 \pm 0.0 (3)	0.0 \pm 0.0 (3)	0.0 \pm 0.0 (2)	0.0 \pm 0.0 (2)
<i>Montipora studeri</i>	0.0 \pm 0.0 (3)	0.0 \pm 0.0 (3)	0.0 \pm 0.0 (2)	0.0 \pm 0.0 (2)
<i>Pavona duerdeni</i>	0.0 \pm 0.0 (3)	0.0 \pm 0.0 (3)	0.0 \pm 0.0 (2)	0.0 \pm 0.0 (2)
<i>Pavona varians</i>	0.0 \pm 0.0 (3)	0.0 \pm 0.0 (3)	0.0 \pm 0.0 (2)	0.0 \pm 0.0 (2)
<i>Pocillopora damicornis</i>	0.0 \pm 0.06 (3)	0.0 \pm 0.06 (3)	0.0 \pm 0.0 (2)	0.0 \pm 0.0 (2)
<i>Pocillopora meandrina</i>	0.0 \pm 0.0 (3)	0.0 \pm 0.0 (3)	0.0 \pm 0.0 (2)	0.0 \pm 0.0 (2)
<i>Porites brighamii</i>	0.0 \pm 0.0 (3)	0.0 \pm 0.0 (3)	0.0 \pm 0.0 (2)	0.0 \pm 0.0 (2)
<i>Porites evermanni</i>	0.0 \pm 0.0 (3)	0.0 \pm 0.0 (3)	0.0 \pm 0.0 (2)	0.0 \pm 0.0 (2)
<i>Porites lobata</i>	0.0 \pm 0.0 (3)	0.0 \pm 0.0 (3)	0.0 \pm 0.0 (2)	0.0 \pm 0.0 (2)
<i>Psammocora nierstraszi</i>	0.0 \pm 0.0 (3)	0.0 \pm 0.0 (3)	0.0 \pm 0.0 (2)	0.0 \pm 0.0 (2)
<i>Psammocora stellata</i>	0.0 \pm 0.0 (3)	0.0 \pm 0.0 (3)	0.0 \pm 0.0 (2)	0.0 \pm 0.0 (2)
Total mean cover	0.03	0.03	48.5	30.2



Fig. 2.4. *Montipora capitata* with lost tissue and algal growth on a fresh skeleton at *Montipora* Pond.

Fish

Table 2.3 is a list of the 10 most frequently counted fish species (60 -100% of all transects) across all sites in 2008 and 2010.

Table 2.3. The most frequent fish species across sites in 2008 and 2010 in a descending taxonomic order. Fish names follow terminology of Hoover (2007) and Randall (2007).

Taxonomic Names	Common Names	Hawaiian Names
<i>Abudefduf sordidus</i>	Blackspot Sergeant	kūpīpī
<i>Stethojulis balteata</i>	Belted Wrasse	‘omaka
<i>Gomphosus varius</i>	Bird Wrasse	hīnālea ‘i‘iwi
<i>Thalassoma duperreyi</i>	Saddle Wrasse	hīnālea lauwili
<i>Scarus psittacus</i>	Palenose Parrotfish	uhu
<i>Chlorurus spilurus</i>	Bullethead Parrotfish	uhu
<i>Acanthurus triostegus</i>	Convict Tang	manini
<i>A. nigrofasciatus</i>	Brown Surgeonfish	māikoiko
<i>Zebrasoma flavescens</i>	Yellow Tang	lau‘ipala
<i>Canthigaster jactator</i>	Hawaiian Whitespotted Toby	

The highest total number of species observed (richness) at a given site was 50 while the lowest was 19 in 2008, and from 26 and 46 species in 2010. Average species richness by transect ranged from 8 to 16 species across sites in 2008, and between 8 to 15 species per transect in 2010. The total number of species remained similar at Kalaeloa and Mokuhā between 2008 and 2010. At the *Montipora* Pond and Kanahena Cove, the total number of species observed was higher during 2010 than 2008.

Estimated mean number of individual fish per hectare (x 1000) ranged from approximately 9.7 to 45.1 in 2008 between sites, and between 14.0 and 41.9 in 2010 (Table 2.4). In general, a higher number of fish per area were found in Kalaeloa, Mokuhā, and *Montipora* Pond compared to Kanahena Cove. In 2010, the mean increased at *Montipora* Pond and Kanahena Cove while values decreased at Mokuhā by 24% with a

34% decrease in Kalaeloa. Despite a 44% increase in fish numbers at Kanahena Cove in 2010, the three other sites have significantly higher numbers, between 41 and 67% higher.

Table 2.4. Mean number of individual fish per hectare (x 1000) in 2008 and 2010. Sample statistics are overall mean \pm standard deviation with number of transects in parentheses from each site.

Site	Shoreline access	2008	2010	% change
Kanahena Cove	Open	9.7 ± 3.3 (3)	14.0 ± 4.3 (5)	44.3
Kalaeloa	Closed	36.4 ± 20.9 (3)	23.9 ± 13.2 (5)	-34.3
Mokuhā	Closed	45.1 ± 11.8 (2)	34.5 ± 13.2 (3)	-23.5
<i>Montipora</i> Pond	Closed	19.3 ± 6.4 (2)	41.9 ± 17.0 (2)	117.1

Temporal variation in mean biomass showed trends similar to mean number of individuals at each site (Table 2.5). Biomass increases were observed at Kanahena Cove and *Montipora* Pond while mean biomass decreased in Kalaeloa and Mokuhā. During 2010, mean biomass doubled at Kanahena Cove, and increased by 2.6-fold at *Montipora* Pond compared to 2008. Fish biomass at Mokuhā and Kalaeloa in 2010 were 33% and 47% below their respective estimates in 2008. Mean biomass ranged from 0.128 to 5.004 t ha⁻¹ in 2008. The range narrowed from 0.339 to 3.365 t ha⁻¹ in 2010. Overall, the estimated mean biomass was highest at Mokuhā during both years while the least biomass was found in *Montipora* Pond, the smallest area of study.

Table 2.5. Mean biomass (metric tons ha^{-1}) in 2008 and 2010. Sample statistics are mean \pm standard deviation with number of transects in parentheses for each site.

Site	Shoreline access	2008	2010	% change
Kanahena Cove	Open	0.923 ± 0.696 (3)	1.869 ± 1.388 (5)	102.4
Kalaeloa	Closed	3.702 ± 2.518 (3)	1.945 ± 0.958 (5)	-47.4
Mokuhā	Closed	5.004 ± 1.949 (2)	3.365 ± 0.911 (3)	-32.8
<i>Montipora</i> Pond	Closed	0.128 ± 0.040 (2)	0.339 ± 0.069 (2)	164.8

Aggregations of fish were observed in both closed and open areas during the two survey periods. A substantial proportion of the total individual counts (56-71%) and biomass (23-25%) consisted of juvenile *Scarus* spp. at *Montipora* Pond for both years. A total of approximately 80 *M. flavolineatus* were counted at Kanahena Cove in each of the two years. Large aggregations of *Kuhlia* spp. (Flagtails, or āholehole) and *Neomyxus leuciscus* (Sharpnose Mullet, or uouoa), estimated at between 50 and 400 individuals, were present on transects during surveys in 2008 at Mokuhā and Kalaeloa. Fairly large aggregations of *Kuhlia* spp. were also observed in 2010 while fewer *N. leuciscus* were observed at Mokuhā and Kalaeloa. Approximately 200 *A. triostegus* were observed on transects at Kalaeloa in 2008. The minimum of 1000 individual *Atherinomorus insularum* (Hawaiian Silverside or ‘iao) were estimated within a school in 2008 at Mokuhā. These were excluded from the overall mean number of individuals and mean biomass by site and year. This was due to the unavailability of a constant value from HCFRU and FishBase for the length-mass conversion necessary in calculating biomass. There was no congener of similar shape within the genus that might be used for the length-mass conversion and fitting parameters.

Biological Community by Site

Kanahena Cove

The dominant benthic cover type was turf-covered rocks and pavements with sand and/or silt deposits over turf algae (Fig. 2.5a). Nearly 80% of the total cover was turf algae and substrate. Coralline algae (Fig. 2.5b) (2.0-5.0 %) had relatively low cover. The highest percent cover of the Rock-boring urchin (0.6-0.7%), *Echinometra mathaei*, was found at Kanahena. Lower percent cover of substrate (turf algae loosely covered with fine sand and/or silt deposits) was recorded in 2010 and turf algae appeared to have less loose sediment deposits (Fig. 2.6). A total of 9 coral species were recorded in 2008 and 2010. The lobe coral, *Porites lobata*, one of the most common corals in Hawai'i was dominant at Kanahena at depths less than 1.5 m (Fig. 2.5c). Overall coral cover was 11.6 ± 12.9% while the percent cover of dead coral was low (0.1%) in both years. A few live *P. lobata* colonies were observed with small dead areas. The estimated live coral cover was slightly lower in 2010 (9.2 ± 4.5 %). However the decrease may not be statistically significant as the given variability was high and sample size was small. Overall live coral cover and species composition appeared similar between years and (Table 2.2a) with the exception of an increase in *Montipora patula* and a decrease in *P. lobata* across years.

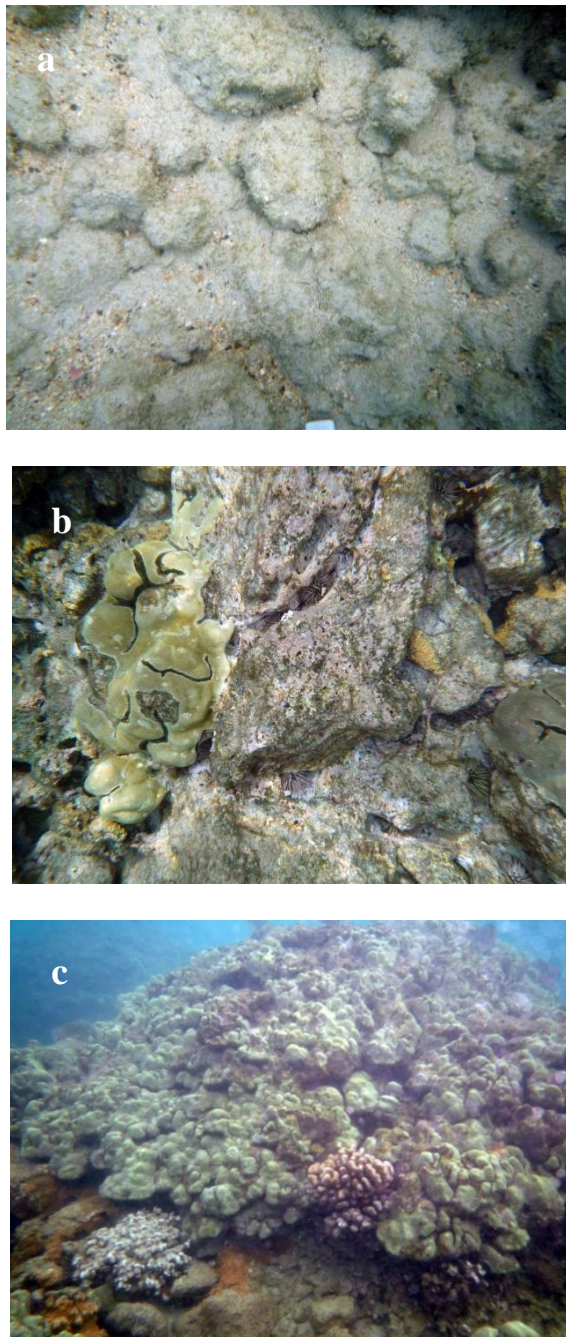


Fig. 2.5. Examples of inshore benthic seascapes of transect sites at a fine scale at Kanahena Cove. (a) sand-covered turf algae, (b) pavement with encrusting coralline algae, live corals, sea urchins, and algae, and (c) colonies of live corals (*Porites lobata*, *Pocillopora meandrina*, and *Montipora patula*).

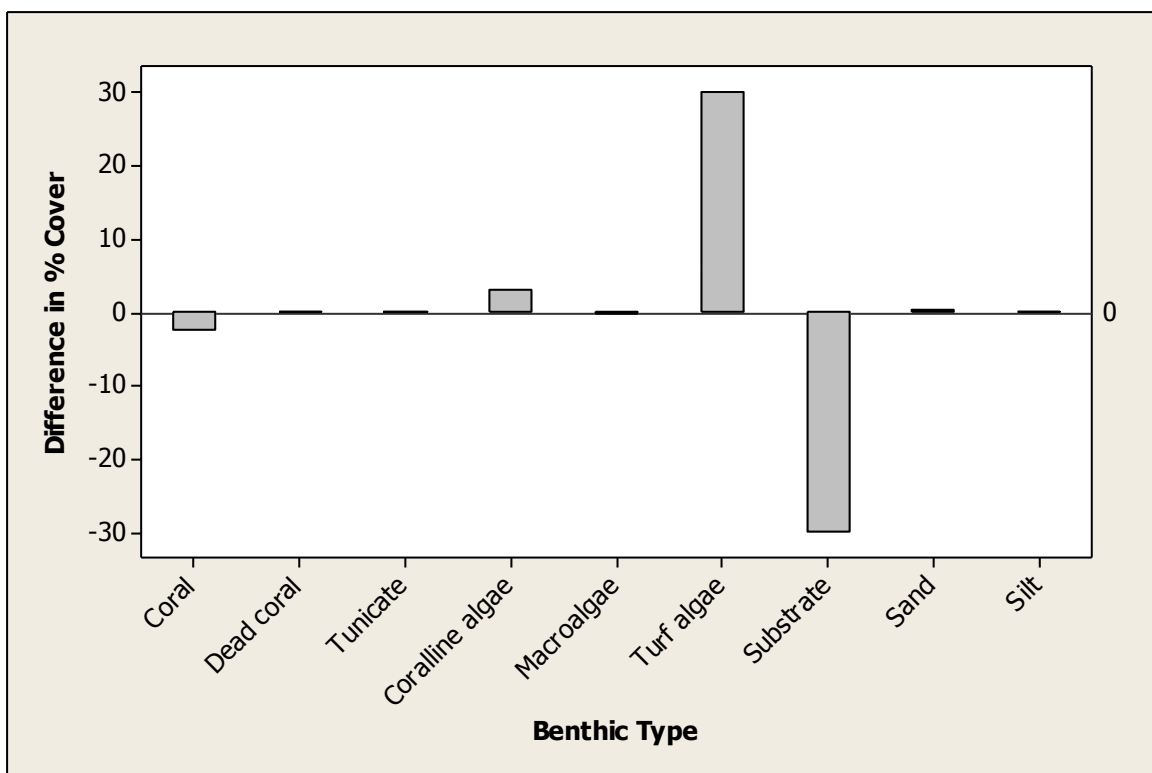


Fig. 2.6. Absolute change in mean percent cover of benthic types at Kanahena Cove from 2008 to 2010.

A total of 33 fish species were observed on three transects in 2008 and 42 species on five transects in 2010 at Kanahena Cove. A lower mean number of individuals were estimated in 2008 (9.7) than in 2010 (14.0). The top five species comprised approximately 52% of the total number of individuals in 2008. These were *Mulloidichthys flavolineatus*, *Acanthurus leucopareius*, *Abudefduf sordidus*, *Acanthurus triostegus*, and *Zebrasoma flavescens* (Table 2.6 and Fig. 2.7a). *Thalassoma duperrey*, *A. triostegus*, *M. flavolineatus*, *Plectroglyphidodon imparipennis*, and *Stethojulis balteata* comprised 63% of the total number of individuals in 2010 (Table 2.7 and Fig. 2.7b). The species with the highest biomass (Fig. 2.8a and 2.8b) included *M. flavolineatus*, *A. leucopareius*, and *Scarus rubroviolaceus* in 2008 (70%). A substantial portion of the total biomass (52%) was represented by *Caranx melampygus*, *M. flavolineatus*, *A. leucopareius*, *S. rubroviolaceus*, and *A. triostegus* in 2010.

Table 2.6. Top 5 species for total number of individuals (%), Kanahena Cove, 2008.

Taxonomic Names	Common Names	Hawaiian Names	% of total individuals
<i>Mulloidichthys flavolineatus</i>	Yellowstripe Goatfish	weke‘ā	21.9
<i>Acanthurus leucopareius</i>	Whitebar Surgeonfish	māikoiko	18.1
<i>Abudefduf sordidus</i>	Blackspot Sergeant	kūpīpī	4.7
<i>Acanthurus triostegus</i>	Convict Tang	manini	4.7
<i>Zebrasoma flavescens</i>	Yellow Tang	lau‘īpala	3.0

Table 2.7. Top 5 species for total number of individuals (%), Kanahena Cove, 2010.

Taxonomic Names	Common Names	Hawaiian Names	% of total individuals
<i>Thalassoma duperrey</i>	Saddle Wrasse	hīnālea lauwili	17.8
<i>Acanthurus triostegus</i>	Convict Tang	manini	16.7
<i>Mulloidichthys flavolineatus</i>	Yellowstripe Goatfish	weke‘ā	11.1
<i>Plectroglyphidodon imparipennis</i>	Bright-eye Damselfish		9.0
<i>Stethojulis balteata</i>	Belted Wrasse	‘omaka	8.0

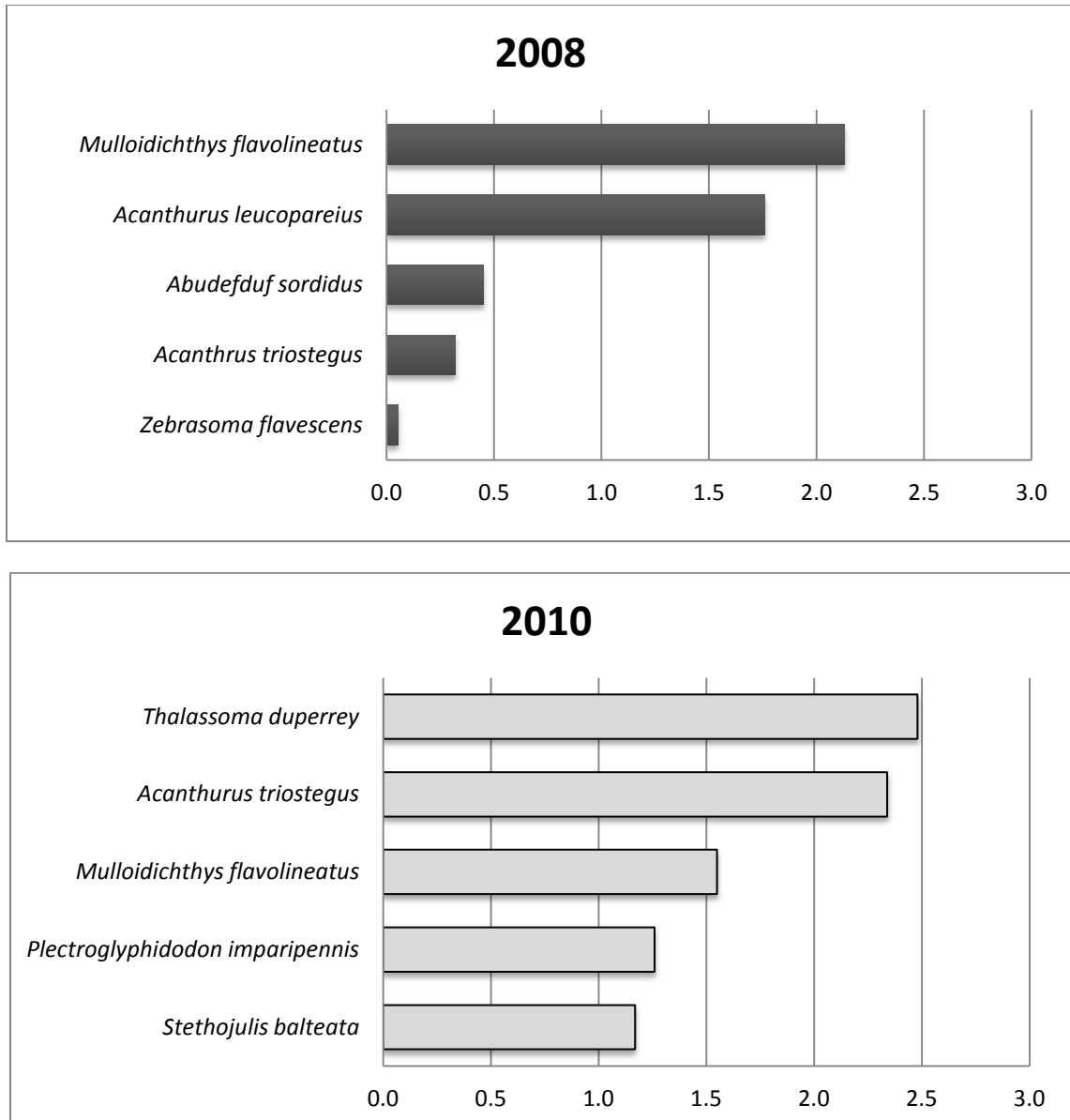


Fig. 2.7a and 2.7b. Top 5 fish with the highest mean number of individuals per hectare (x 1000) at Kanahena Cove, 2008 and 2010.

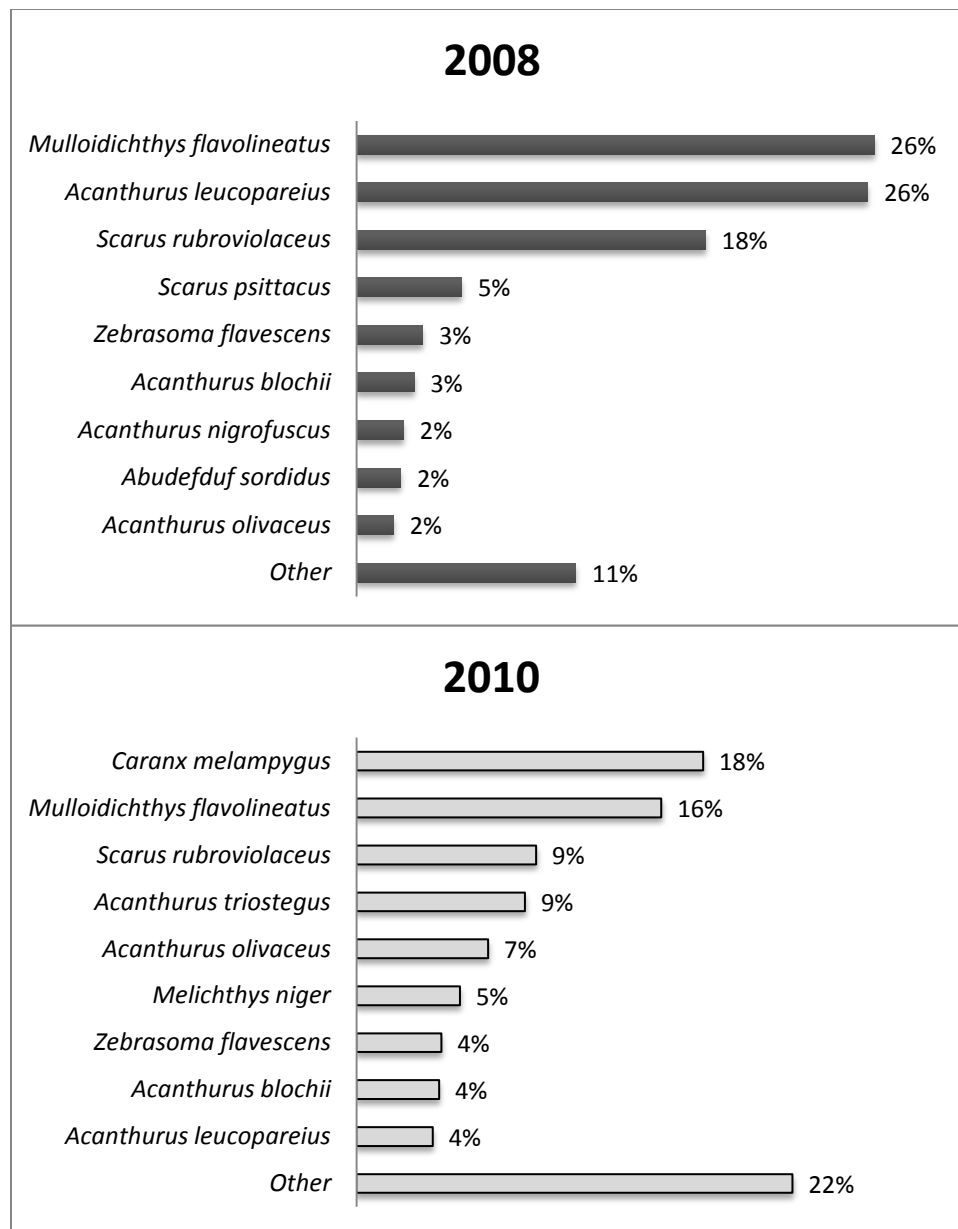


Fig. 2.8a and 2.8b. Top 10 fish with the greatest proportion of total biomass at Kanahena Cove, 2008 and 2010.

Kalaeloa

The dominant benthic type was turf and CCA covering basalt pavements and rocks (Fig. 2.9). Nearly 80% of the total cover was comprised of turf and encrusting coralline algae. Almost no sand or silt was recorded. A relatively low coverage of macroalgae (0.4-1.7 %) was observed, and these were primarily encrusting and fleshy red algae. Low coverage of the Rock-boring urchin (0.2-0.5%), and occasionally, a small fraction of mollusks (0.1%) were recorded. Total of 7 and 8 coral species (Table 2.2b) were recorded here in 2008 and 2010, respectively. *P. lobata* was dominant at Kalaeloa. Total coral cover was $3.7 \pm 4.4\%$ in 2008 and $3.9 \pm 4.6\%$ in 2010, respectively. Percent cover of dead coral was slightly higher in 2008 ($0.3 \pm 0.4\%$) than in 2010 ($0.1 \pm 0.2\%$) (Fig. 2.10). Observed dead coral were algae-covered, older skeletons of *Pocillopora meandrina* (Cauliflower coral). Total live coral cover was similar between years while species composition was slightly different. Low coverage of *Montipora patula* (Ringed Rice coral, 0.6%) was recorded in 2010 while none was recorded in 2008. This is probably the result of increasing the number of transects surveyed in 2010. Overall, benthic cover and coral composition values remained relatively similar between years falling within the range of acceptable error. While coral cover was not the dominant substrate on transects, 11 species were observed at deeper depths from 2-6 m, primarily at the seaward end.

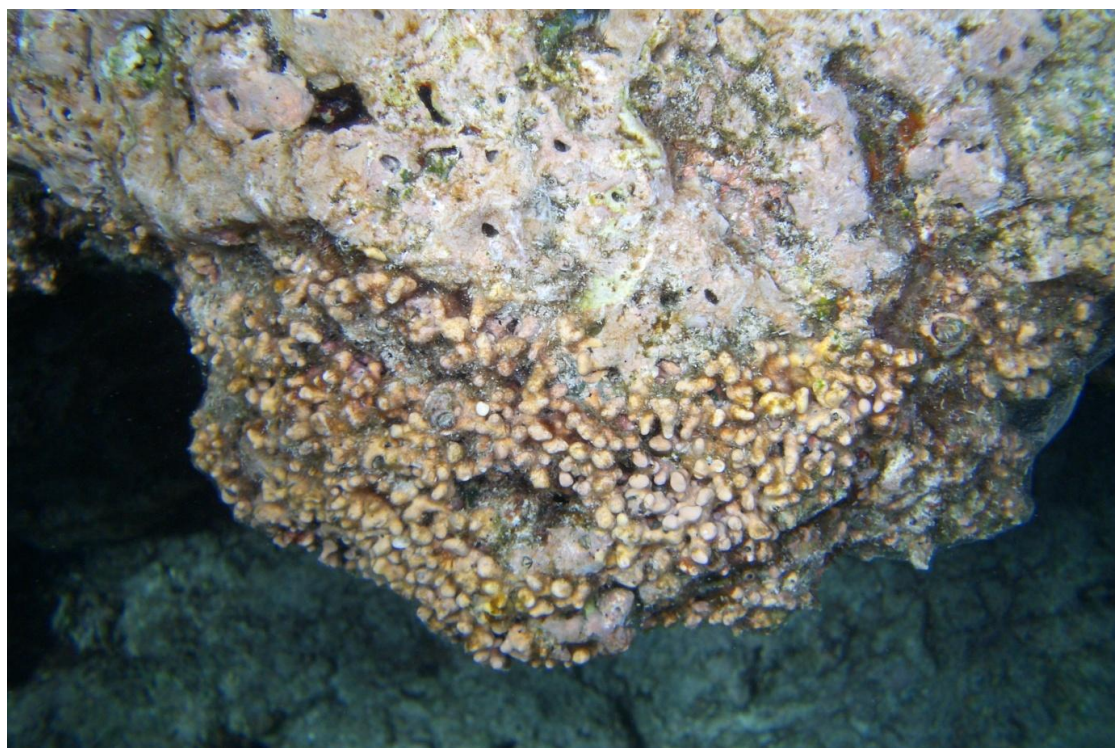


Fig. 2.9. Encrusting coralline algae and well-cropped turf algae occupying basalt substrate leaving no bare space (Kalaeloa).

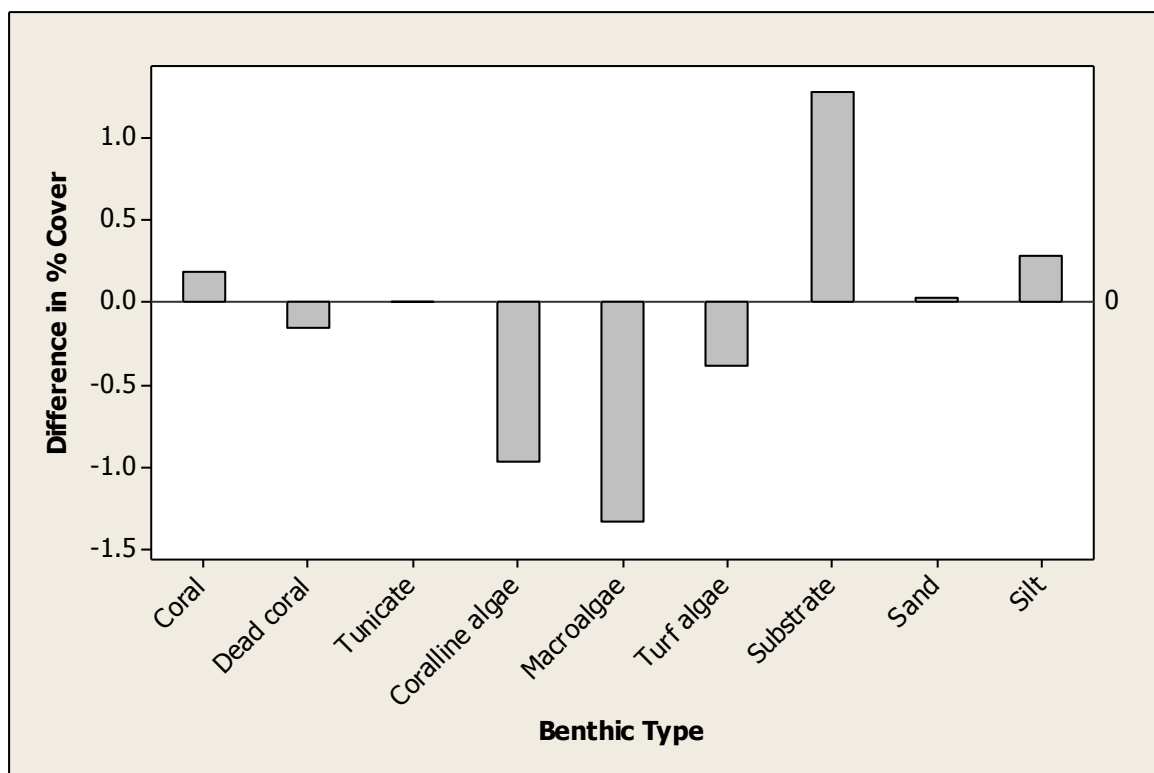


Fig. 2.10. Absolute change in mean percent cover of benthic types at Kalaeloa from 2008 to 2010.

A total of 50 fish species were observed among three transects in 2008 and 46 species were observed among five transects in 2010 at Kalaeloa. The top five species comprised 73% of the total number of individuals in 2008 and approximately 52 % in 2010 (Table 2.8 and 2.9). *Kuhlia* spp. accounted for the largest proportion of the total biomass (Fig. 2.11a and 2.11b; 2.12a and 2.12b) and the total number of individuals in both years. *A. triostegus* (Fig. 2.13) and *Acanthurus nigrofasciatus* also ranked high. *Neomyxus leuciscus* had the highest numerical abundance and biomass in 2008 (Fig. 2.11a and 2.12a); however, it was not one of the top species in 2010 (Fig. 2.11b and 2.12b). There were 34% less individuals and 47% lower biomass in 2010 as compared to 2008.

Table 2.8. Top 5 species for total number of individuals (%), Kalaeloa, 2008.

Taxonomic Names	Common Names	Hawaiian Names	% of total individuals
<i>Kuhlia</i> spp.	Flagtails	āholehole	36.0
<i>Acanthurus triostegus</i>	Convict Tang	manini	15.5
<i>Neomyxus leuciscus</i>	Sharptooth Mullet	uouoa	10.5
<i>Thalassoma duperrey</i>	Saddle Wrasse	hīnālea lauwili	5.6
<i>Acanthurus nigrofasciatus</i>	Brown Surgeonfish	mā‘i‘i‘i	5.4

Table 2.9. Top 5 species for total number of individuals (%), Kalaeloa, 2010.

Taxonomic Names	Common Names	Hawaiian Names	% of total individuals
<i>Kuhlia</i> spp.	Flagtails	āholehole	14.4
<i>Acanthurus nigrofasciatus</i>	Brown Surgeonfish	mā‘i‘i‘i	13.4
<i>Thalassoma duperrey</i>	Saddle Wrasse	hīnālea lauwili	8.6
<i>Ctenochaetus strigosus</i>	Goldring Surgeonfish	kole	8.6
<i>Platybelone argalus</i>	Keeltail Needlefish	‘aha	7

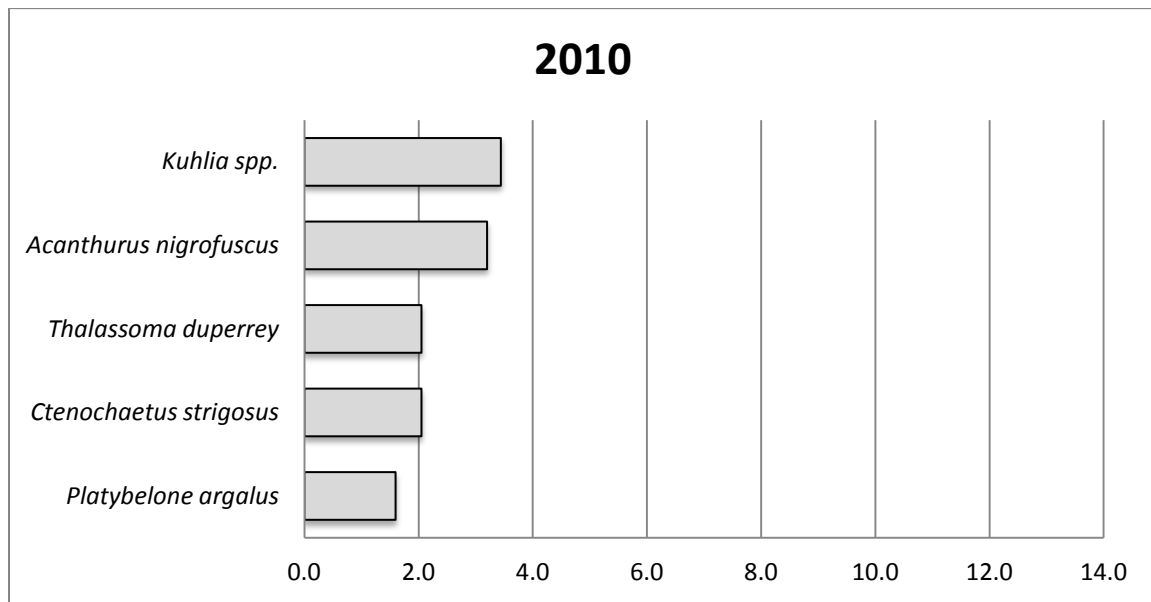
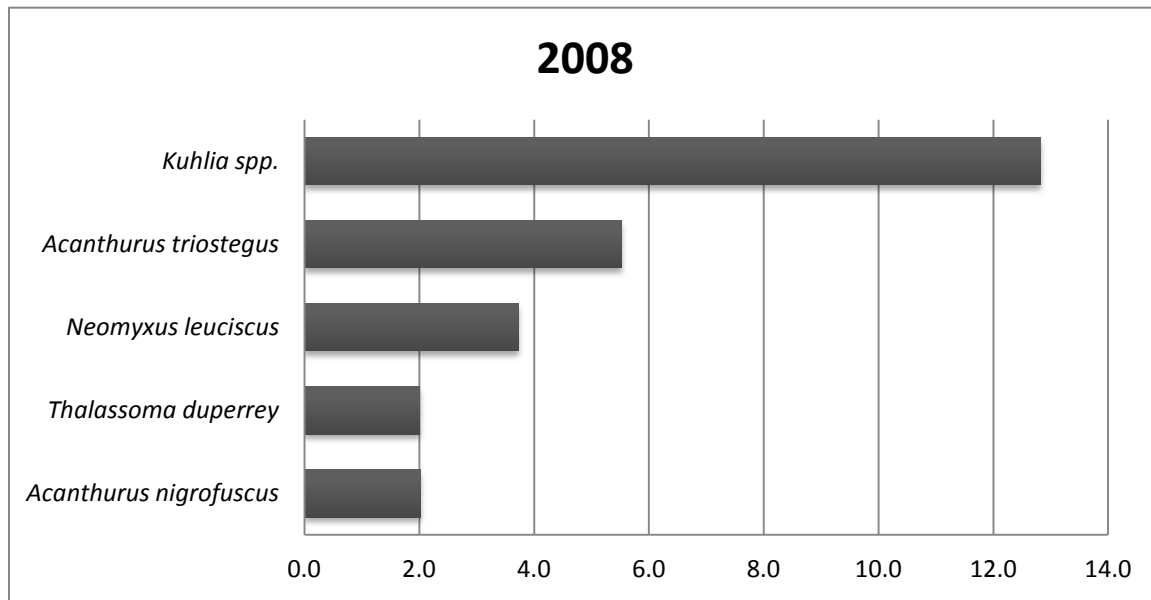


Fig. 2.11a and 2.11b. Top 5 fish with the highest mean number of individuals per hectare (x 1000) at Kalaeloa, 2008 and 2010.

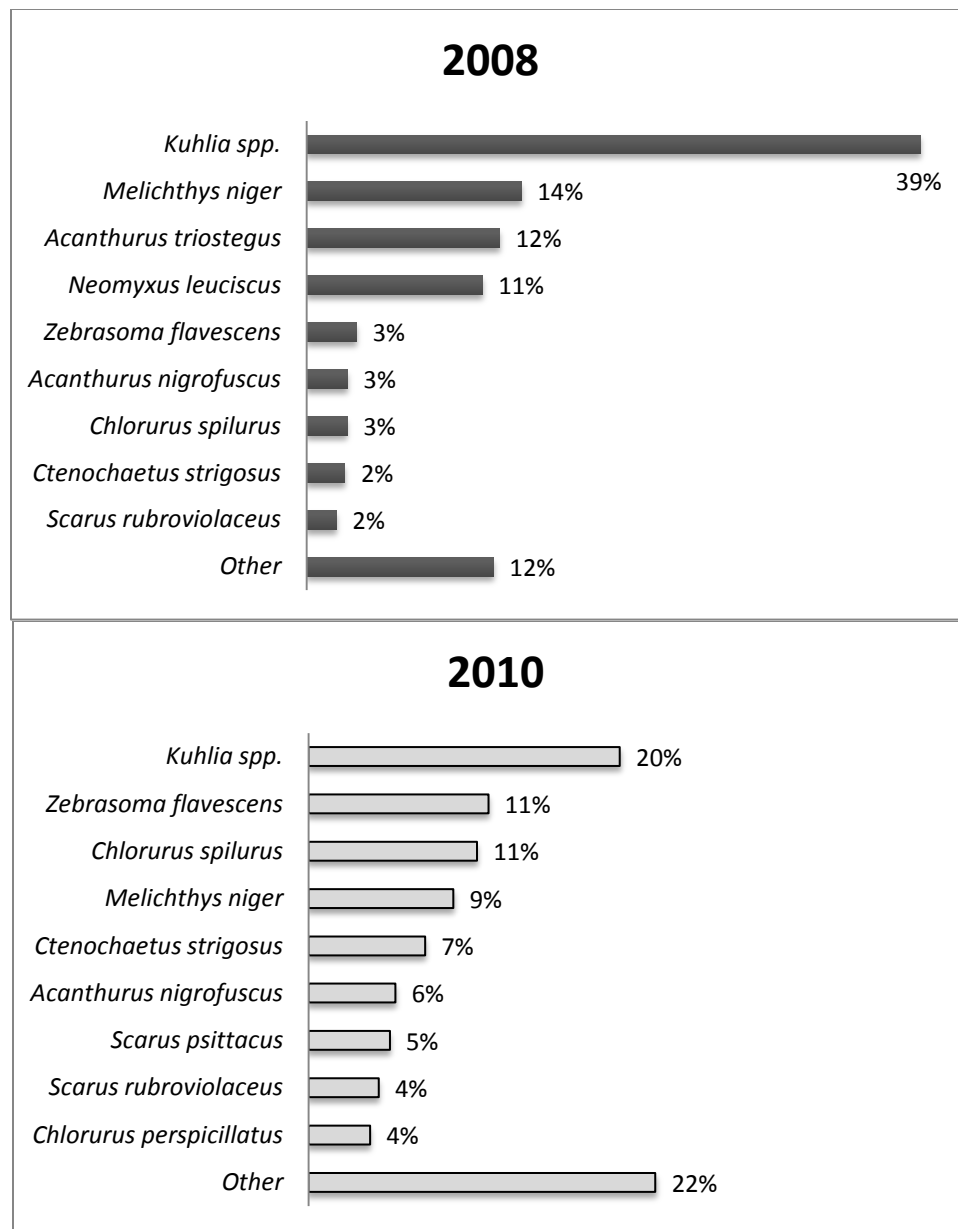


Fig. 2.12a and 2.12b. Top 10 fish with the greatest proportion of total biomass at Kalaeloa, 2008 and 2010.



Fig. 2.13. *Acanthurus triostegus*, aggregating and grazing over inshore reef, is a major contributor to the high number of individuals and biomass at Kalaeloa.

Mokuhā

Crustose coralline and turf algae covering basalt rocks and pavements (Fig. 2.14a and 2.14b) dominated benthic cover type at Mokuhā. Coralline algae had the highest cover here (42%, 2008 and 36%, 2010) (Table 2.1b). Substrate (turf algae loosely covered with fine sand and/or silt deposits) ranked second (28-29%) to Kanahena in 2008 and 2010. The highest sand cover (~ 9%) was observed at working depths for both years. Coverage of macroalgae was very low (< 0.1%). These were primarily encrusting and some fleshy red algae. Low coverage of the Rock-boring urchin (0.1%), and occasionally, a small fraction of mollusks (0.1%) were recorded. The only coral species recorded was *Pocillopora damicornis*, Lace coral (Table 2.1b). Total coral cover was less than 0.1%. Overall, benthic cover and composition were similar from 2008 to 2010 (Fig. 2.15).



a



b

Fig. 2.14. (a) Basalt pavement covered with crustose coralline and turf algae at cove's north end, and (b) coralline-and turf-covered rock at seaward beach of Mokuhā.

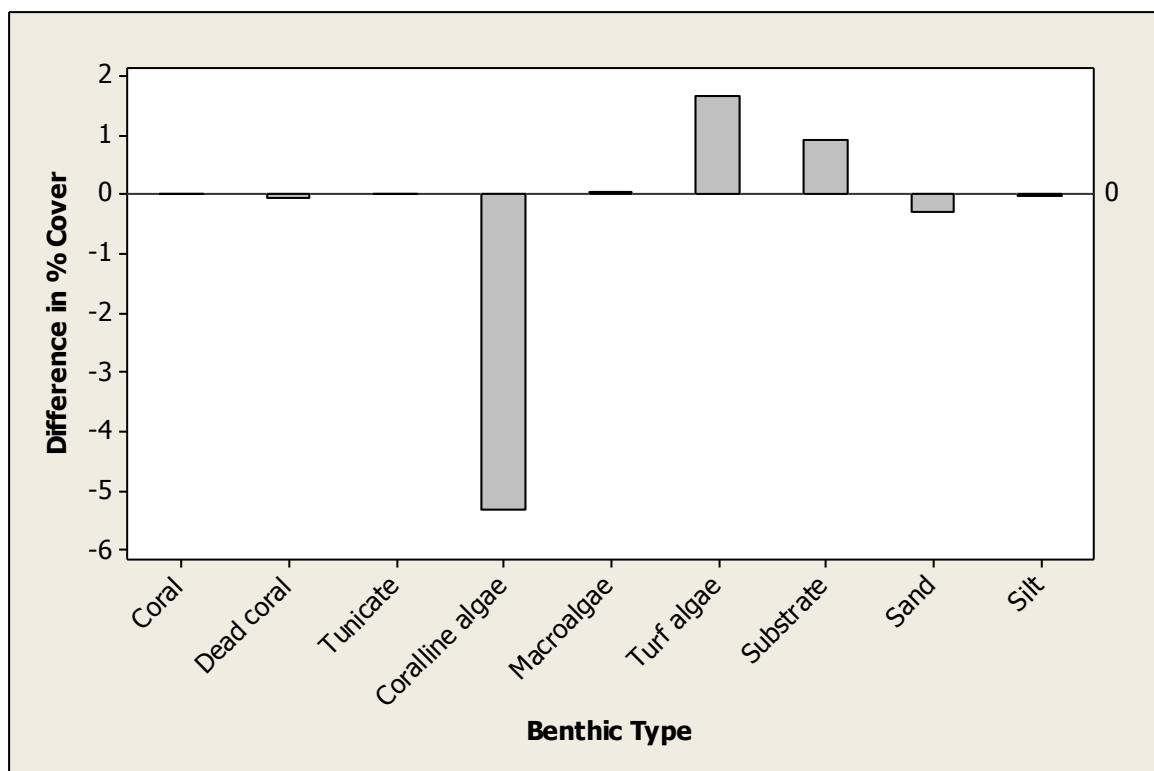


Fig. 2.15. Absolute change in mean percent cover of benthic types at Mokuhā from 2008 to 2010.

A total of 35 species of fishes were recorded on two transects in 2008 and 36 species on three transects in 2010. Numerical abundance was 24% lower and mean biomass was 33% lower in 2010 as compared to 2008 (Table 2.3 and 2.5). The top five species comprised 41% of individuals in 2008 and approximately 70% in 2010 (Table 2.10 and 2.11). Species composition was similar between the two survey years while numerical abundance was different (Fig. 2.16a and 2.16b). *Kuhlia* spp. ranked in the second highest for the total number of individuals at Mokuhā in 2008 and the highest in 2010 (Fig. 2.16a and 2.16b; 2.17a and 2.17b). It also accounted for the largest proportion of overall mean and total biomass for both years. *N. leuciscus* in numerical abundance and biomass in 2008; but was not included as one of the top species in 2010. Its total biomass was nearly as high (32%) as *Kuhlia* spp. in 2008. A moderate number of *Scarus psittacus* (Palenose parrotfish, Fig. 2.18) was observed in both years.

Table 2.10. Top 5 species for total number of individuals (%), Mokuhā, 2008.

Taxonomic Names	Common Names	Hawaiian Names	% of total individuals
<i>Neomyxus leuciscus</i>	Sharpnose Mullet	uouoa	15.5
<i>Kuhlia</i> spp.	Flagtails	āholehole	14.1
<i>Scarus psittacus</i>	Palenose Parrotfish	uhu	4.7
<i>Acanthurus triostegus</i>	Convict Tang	manini	3.7
<i>Thalassoma duperrey</i>	Saddle Wrasse	hīnālea lauwili	2.9

Table 2.11. Top 5 species for total number of individuals (%), Mokuhā, 2010.

Taxonomic Names	Common Names	Hawaiian Names	% of total individuals
<i>Kuhlia</i> spp.	Flagtails	āholehole	28.6%
<i>Acanthurus triostegus</i>	Convict Tang	manini	14.3%
<i>Scarus psittacus</i>	Palenose Parrotfish	uhu	11.2%
<i>Acanthurus nigrofasciatus</i>	Brown Surgeonfish	mā'i'i'i	7.7%
<i>Thalassoma duperrey</i>	Saddle Wrasse	hīnālea lauwili	7.7%

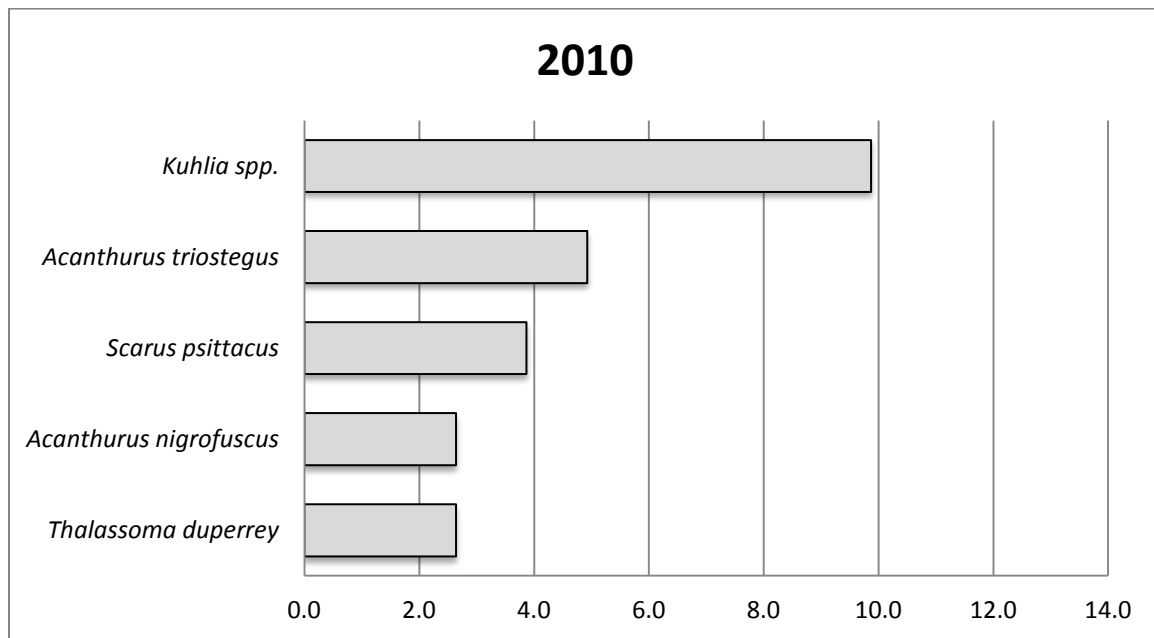
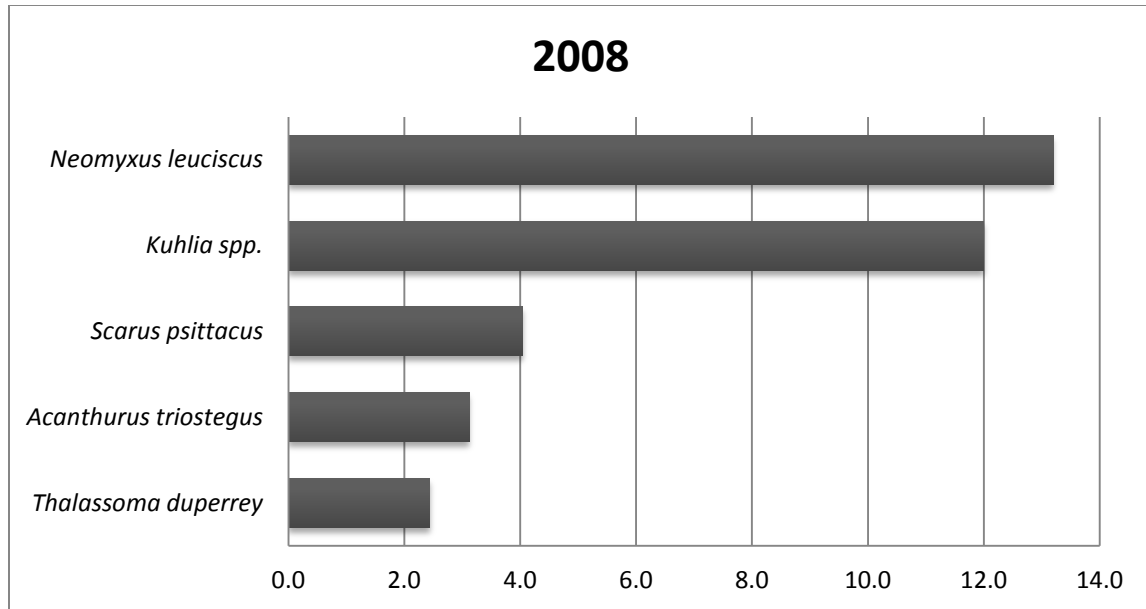


Fig. 2.16a and 2.16b. Top 5 fish with the highest mean number of individuals per hectare (x 1000) at Mokuhā, 2008 and 2010.

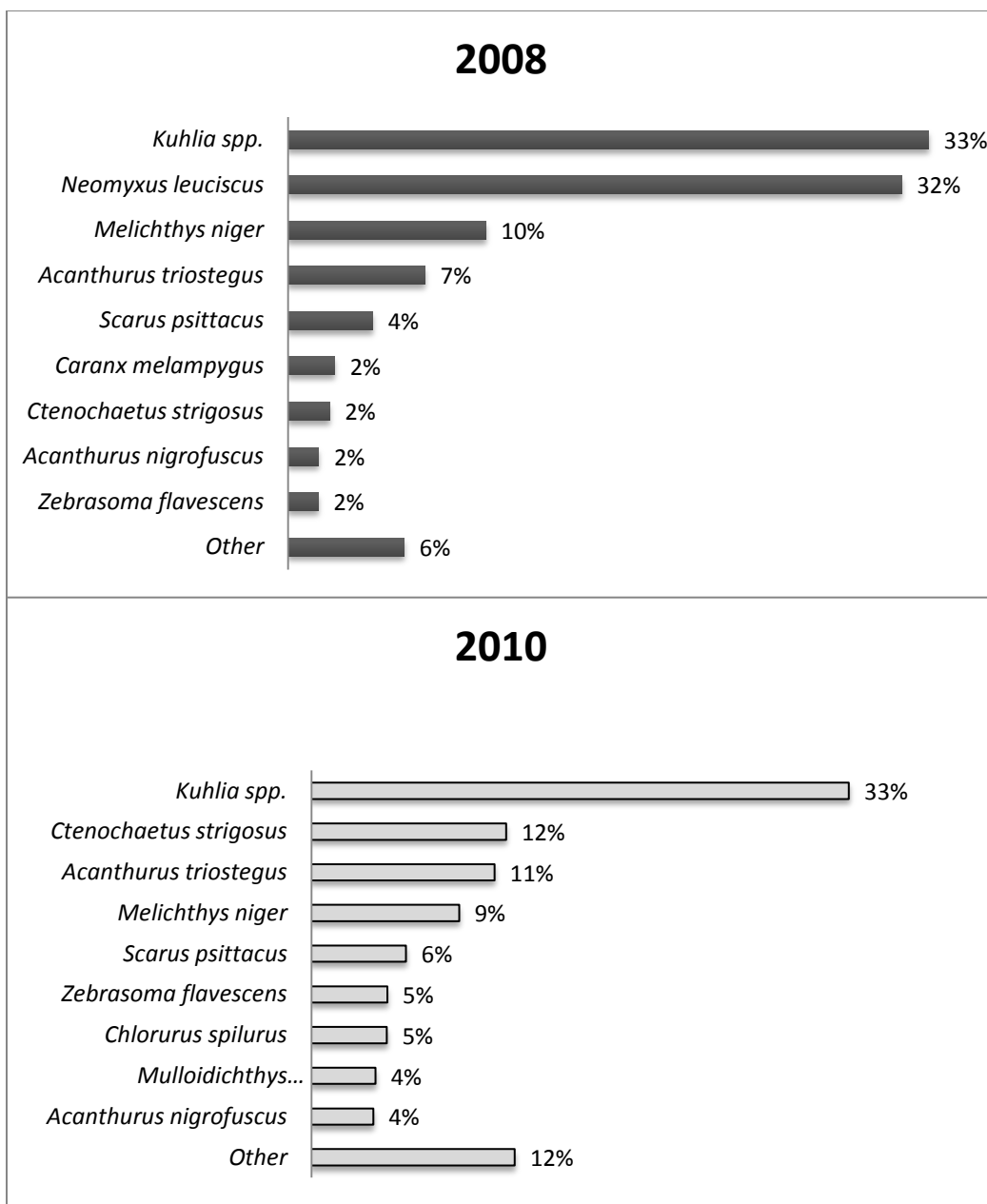


Fig. 2.17a and 2.17b. Top 10 fish with the greatest proportion of total biomass at Mokuhā, 2008 and 2010.



Fig. 2.18. A group of *Scarus psittacus* common at Mokuhā.

***Montipora* Pond**

Mean percent cover and composition of benthic cover were different between 2008 and 2010 (Fig. 2.19). *Montipora capitata*, represented the greatest proportion of overall benthic cover (~ 49% in 2008) (Table 2.1b) followed by turf algae and macroalgae. Percent cover of live *M. capitata* in 2010 ($30.2 \pm 6.2\%$) decreased by 37% as compared to mean cover in 2008 ($48.5 \pm 20.9\%$).

In contrast, dead coral and turf algae noticeably increased between 2008 and 2010 (Fig. 2.19). Mean dead coral cover in 2008 was $2.9 \pm 2.1\%$, and in 2010 was $5.8 \pm 2.3\%$. Mean turf algae cover was $23.8 \pm 11.3\%$ in 2008 while it increased to $30.5 \pm 10.5\%$ in 2010.

Mean cover of macroalgae showed a slight increase from $8.1 \pm 9.2\%$ to $10.4 \pm 12.0\%$ with large variability. While densely growing macroalgae were observed along the southeast side of the pond, there were no visible macroalgae occupying or outgrowing the understory of live corals along the northwest side during a 2008 survey, however outgrowth of macroalgae was obvious in 2010 (Fig. 2.20). Coverage of turf algae, macroalgae, and dead coral in both years was greater than values from other sites (Table 2.1a and 2.1b).

The Didemnid tunicate (*Diplosoma similis*, Fig. 2.21) not observed in 2008, became apparent from the 2010 data on the inshore transect. This Indo-Pacific species of colonial tunicate is common and native to Hawai‘i and known to be invasive in American Sāmoa (Vargas-Ángel *et al.* 2008; pers. comm. Godwin 2010).

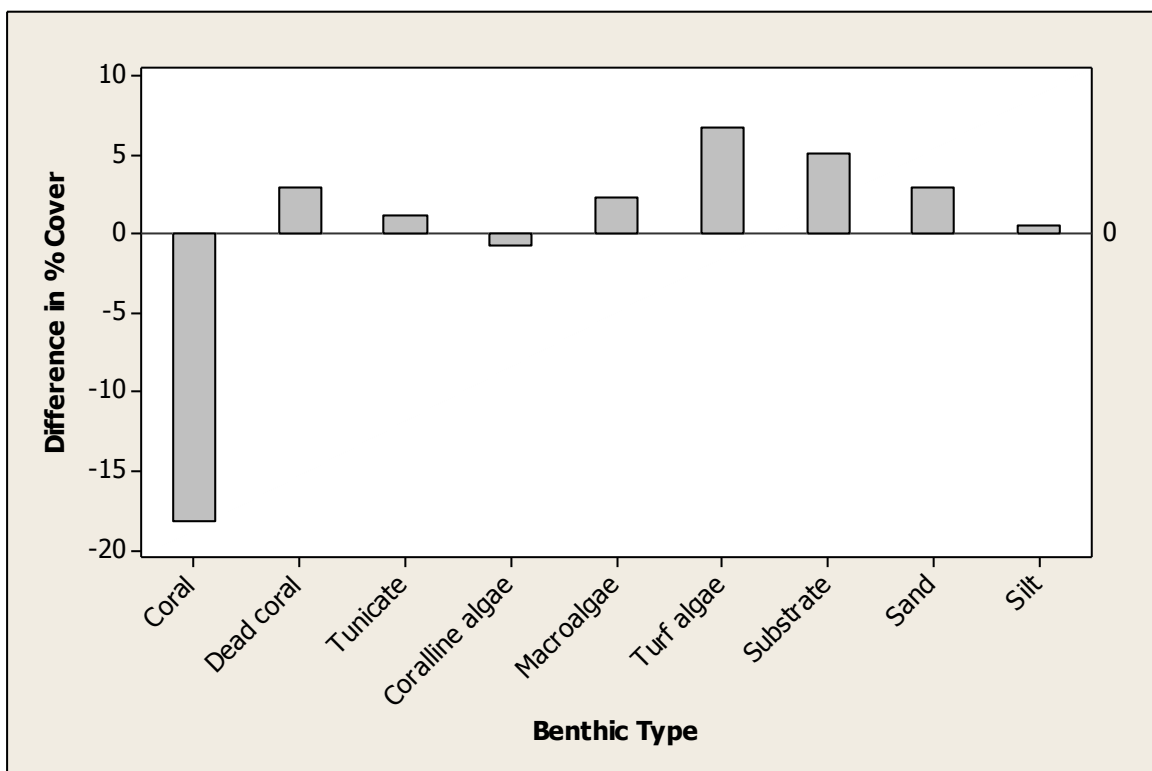


Fig. 2.19. Absolute change in mean percent cover of benthic types at *Montipora* Pond from 2008 to 2010.



Fig. 2.20. Calcified macroalgae occupying and outgrowing understory of live *M. capitata* while the dead surface is covered by turf algae at *Montipora* Pond.



Fig. 2.21. *Diplosoma similis*, phototrophic colonial tunicate encrusting dead *Montipora capitata* at *Montipora* Pond.

A total of 19 species of fish in 2008 and 26 species in 2010 were observed on two transects. Species composition and ranking in percent of the total number of individuals were slightly different between years (Table 2.12 and 2.13). The top five species comprised 89% of the total number of individuals in 2008 and approximately 88% in 2010. Several species of juvenile uhu, *Scarus* spp., dominated the counts (56%, 2008; 71%, 2010). Overall mean number of individuals increased twofold in 2010 from 2008 (Fig. 2.22a and 2.22b). Abundance of juvenile Scarids was 10.9 ($\text{ha}^{-1} \times 1000$) in 2008 and 32.0 ($\text{ha}^{-1} \times 1000$) in 2010.

Overall mean biomass was higher in 2010 (0.339 t ha^{-1}) than in 2008 (0.128 t ha^{-1}). Family contributions to total biomass at this site varied between years. Approximately 60% of the estimated total biomass was accounted for by three families (Scaridae, Pomacentridae, Mugilidae) in 2008 while a single family, Scaridae (~53%), had the largest contribution to total biomass at *Montipora* Pond (Fig. 2.23a and 2.23b).

Table 2.12. Top 5 species for total number of individuals (%), *Montipora* Pond, 2008

Taxonomic Names	Common Names	Hawaiian Names	% of total individuals
<i>Scarus</i> spp. (juv.)	Parrotfish	uhu	56.0
<i>Abudefduf abdominalis</i>	Hawaiian Sergeant	mamo	19.3
<i>Gobiidae</i> spp.	Gobies		7.3
<i>Thalassoma duperrey</i>	Saddle Wrasse	hīnālea lauwili	4.4
<i>Acanthurus triostegus</i>	Convict Tang	manini	2.5

Table 2.13. Top 5 species for total number of individuals (%), *Montipora* Pond, 2010

Taxonomic Names	Common Names	Hawaiian Names	% of total individuals
<i>Scarus</i> spp. (juv.)	Parrotfish	uhu	71.2
<i>Chlorurus spilurus</i>	Bullethead Parrotfish	uhu	5.0
<i>Scarus psittacus</i>	Palenose Parrotfish	uhu	4.2
<i>Thalassoma duperrey</i>	Saddle Wrasse	hīnālea lauwili	4.2
<i>Acanthurus triostegus</i>	Convict Tang	manini	3.2

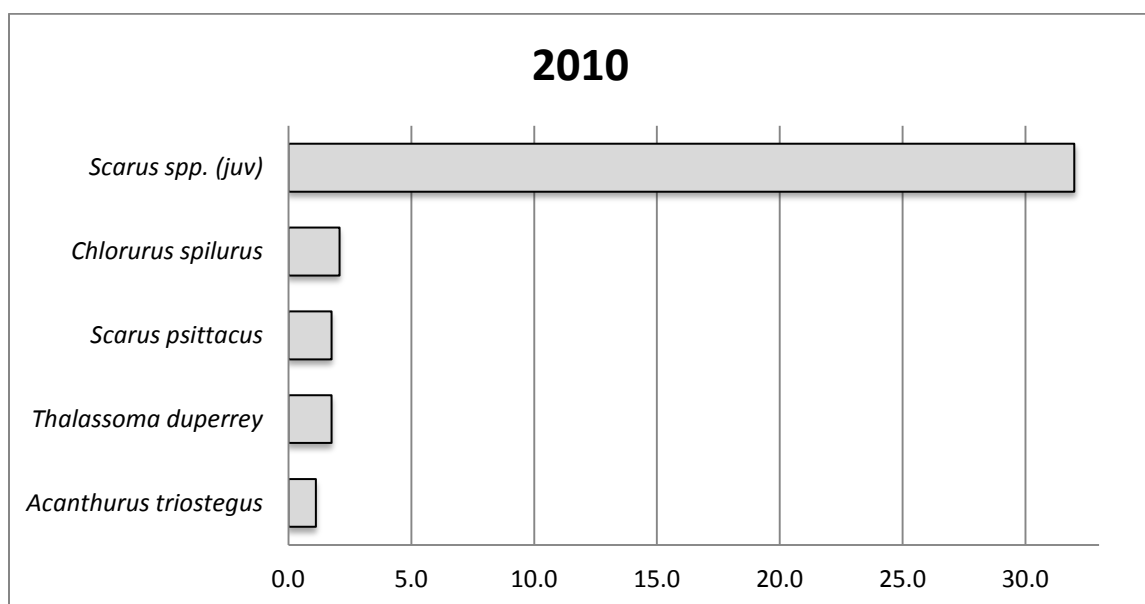
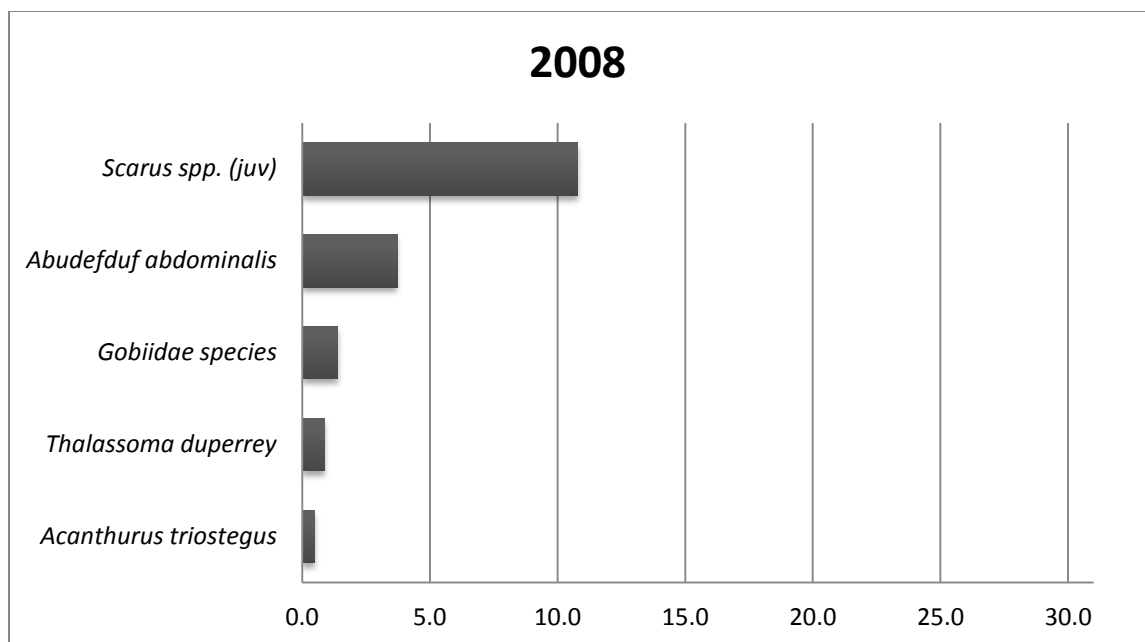


Fig. 2.22a and 2.22b. Top 5 fish with the highest mean number of individuals per hectare (x 1000) at Montipora Pond, 2008 and 2010

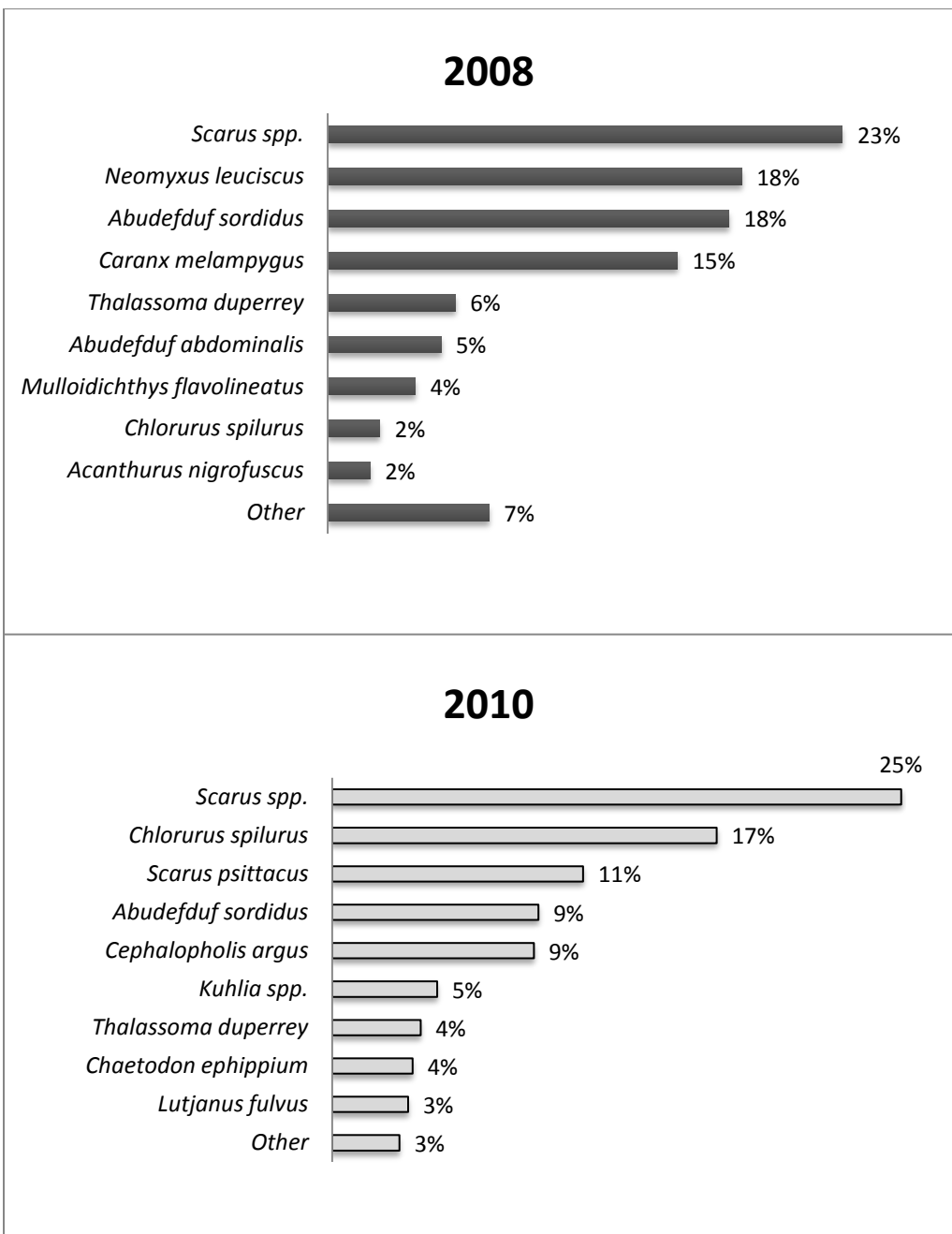


Fig. 2.23a and 2.23b. Top 10 fish with the greatest proportion of total biomass at *Montipora* Pond, 2008 and 2010.

Topographic Relief (Rugosity) and Depth

The average rugosity was relatively consistent between survey periods at each site. It ranged from approximately 1.20 to 1.50. Overall mean index was 1.31 ± 0.23 ($n = 11$) in 2008, and 1.39 ± 0.17 ($n = 15$) in 2010. At Kanahena Cove the average rugosity index was 1.17 ± 0.15 ($n = 3$) in 2008 and 1.22 ± 0.13 ($n = 5$) in 2010. The average rugosity index was 1.30 ± 0.06 ($n = 3$) in 2008 and 1.27 ± 0.24 ($n = 3$) in 2010 at Mokuhā. Values were similar at Kalaeloa (1.46 ± 0.40 , $n = 3$, 2008 and 1.42 ± 0.16 , $n = 5$, 2010) while the average value of 2010 was slightly higher than 2008 at *Montipora* Pond (1.32 ± 0.03 , $n = 2$, 2008 and 1.50 ± 0.01 , $n = 2$, 2010). Although seasonal and diurnal tidal fluctuations occurred, a depth of 0.5-1.5 m was maintained as much as possible during measurements.

The index value of <1.10 is typically associated with very smooth bottom (e.g., carbonate pavement) with a few encrusting or lobe coral colonies and/or rocks. Values >2.00 indicate high rugosity, commonly associated with very high cover of branching, lobe, and plate-like corals. Topographic relief at Kanahena Cove and Mokuhā had relatively smooth underlying geomorphic structures with some biological cover (e.g., lobe corals and coralline algae) as values indicate. The relief at Kalaeloa and *Montipora* Pond was slightly more complex than Kanahena and Mokuhā.

Sediment

Sediment Composition

Temporal and spatial variations in sediment composition are shown in Table 2.14 and Fig. 2.24. Calcium carbonate was dominant across all sites and years, ranging from

52.6 to 90.9%. The highest mean proportion of carbonate was found at Kalaeloa followed by *Montipora* Pond, Kanahena Cove, and Mokuhā for both years. Terrigenous material ranged from 3.6 to 44.1% among sites in 2008 and 2010. For both survey

Table 2.14. Proportion (%) of organic, calcium carbonate, and terrigenous materials in 2008 and 2010. Sample statistics are overall mean \pm standard deviation with number of samples in parentheses.

	Organic	Carbonate	Terrigenous
2008 Kanahena Cove (3)	3.0 ± 0.8	67.1 ± 18.7	29.9 ± 19.5
2010 Kanahena Cove (3)	4.0 ± 0.2	86.2 ± 3.0	9.9 ± 2.8
2008 Kalaeloa (2)	5.0 ± 0.3	86.5 ± 1.0	8.5 ± 0.6
2010 Kalaeloa (2)	5.5 ± 0.2	90.9 ± 0.3	3.6 ± 0.4
2008 Mokuhā (2)	3.3 ± 1.9	52.6 ± 34.1	44.1 ± 36.0
2010 Mokuhā (2)	4.5 ± 0.4	76.9 ± 5.1	18.5 ± 5.4
2008 <i>Montipora</i> Pond (2)	4.5 ± 0.1	85.5 ± 0.6	10.0 ± 0.5
2010 <i>Montipora</i> Pond (2)	4.2 ± 0.1	89.2 ± 1.0	6.6 ± 0.1

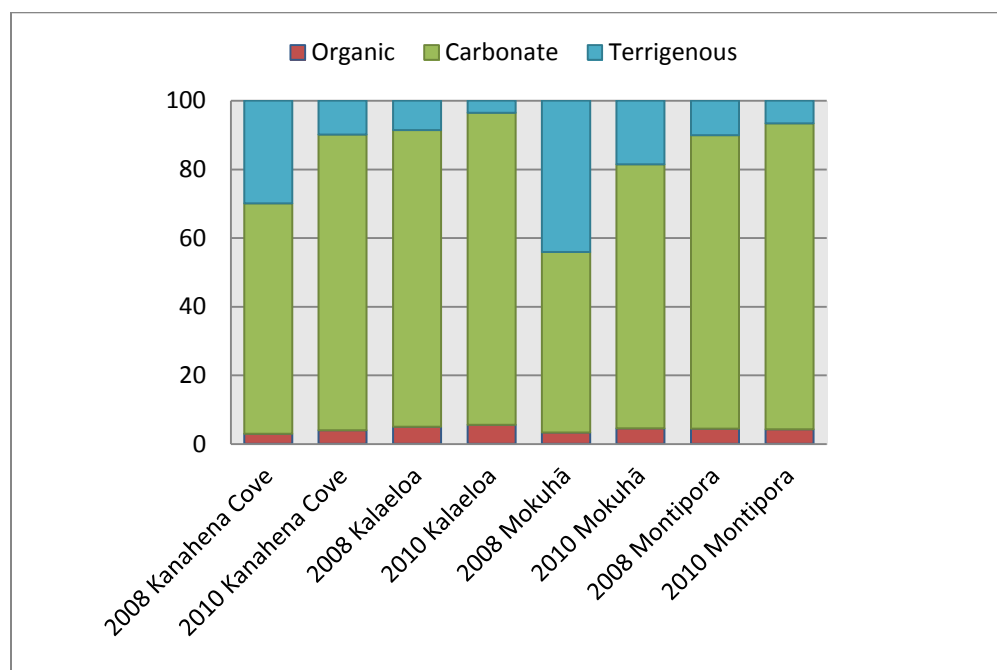


Fig. 2.24. Mean proportion of sediment composition (%) from Kanahena Cove, Kalaeloa, Mokuhā, and *Montipora* pond, 2008 and 2010.

periods the highest proportion of terrigenous material was found at Mokuhā, followed by Kanahena Cove, *Montipora* Pond, and Kalaeloa. The mean proportion of organic matter from all sites was low, ranging from 3.0% at Kanahena to 5.5% at Kalaeloa. The values in 2008 and 2010 were similar to a reported mean proportion of organic matter in 2001 ($2.77 \pm 0.19\%$, CRAMP) at Kanahena Cove.

The mean proportions of carbonate and terrigenous material were slightly different between years at each site. The observed mean proportion of carbonate was greater in 2010 than in 2008 while the mean proportion of terrigenous material decreased in 2010 from those in 2008 (Fig. 2.24). This temporal variation was consistent across sites. The mean proportion of organic material varied a little, and its temporal variation was not consistent across sites.

There was substantial variability between 2008 and 2010 at Mokuhā and Kanahena Cove. The coefficient of variation (CV) was relatively large among samples from Mokuhā (65% carbonate, 82% terrigenous, and 58% organic) and Kanahena Cove (28% carbonate, 65% terrigenous, and 27% organic) in 2008. The CV was low and relatively consistent for samples from Kalaeloa (1% carbonate, 7% terrigenous, and 6% organic) and *Montipora* Pond (1% carbonate, 5% terrigenous, and 2% organic) in 2008. Variability was substantially less at Mokuhā (7% carbonate and 9% organic) and Kanahena Cove (4% carbonate and 5% organic) in 2010. Despite a two- to three-fold decrease of CV in terrigenous material at Mokuhā (29%) and Kanahena Cove (28%) in 2010, these sites were still significantly greater than Kalaeloa (11%) and *Montipora* Pond (2%).

Sediment Grain-size

Grain-size analyses for 2008 and 2010 from all sites are shown on Table 2.15 and Fig. 2.25. While there were some minor variations in mean proportion of grain-size among sites, the dominant grain-size fractions were very coarse and coarse sand at Kanahena Cove, Kalaeloa, and Mokuhā. About 86% of sediment particles were very coarse and coarse sand at Kanahena, which had the highest proportion among all sites. Very little fine sand (0.8-1.7%) and silt/clay (0.3-0.4%) was found at Kanahena Cove. At Mokuhā, 61.1-84.0% of the sediment was very coarse and coarse sand. While the proportion of medium sand (10.4-24.5%) was similar to Kanahena Cove (12.3-12.9%), fine sand (4.5-13.1%) and silt/clay (1.1-1.2%) were slightly greater. About 50% of the total was very coarse and coarse sand at Kalaeloa while the other 50% consisted of relatively even proportions of medium (18.7-27.2%) and fine sand (22.0-23.4%), and 2.2-6.8% silt/clay. At *Montipora* Pond, 65 to 85 % of the total consisted of medium sand (19.4-34.9%) and fine sand (45.3-47.7%). Silt/clay was substantial at *Montipora* Pond (11.0-11.9%) relative to other sites.

Mokuhā and *Montipora* Pond showed noticeable changes in mean grain-size proportion between 2008 and 2010. Very coarse/coarse and medium sand fractions shifted substantially at these sites. Very coarse/coarse sand decreased at Mokuhā in 2010; medium and fine sand fractions increased more than two-fold since 2008. Silt/clay remained relatively consistent at these sites between 2008 and 2010. Less silt/clay was observed at Kalaeloa in 2010 than in 2008. Kanahena Cove demonstrated the least amount of variability over the study period.

Table 2.15. Proportion (%) of sediment grain-size for Kanahena, Kalaeloa, Mokuhā, and *Montipora* pond, 2008 and 2010. Sample statistics are overall mean \pm standard deviation with number of samples in parentheses.

	very coarse/coarse sand	medium sand	fine sand	silt/clay
2008 Kanahena Cove (3)	86.0 \pm 11.3	12.9 \pm 3.2	0.8 \pm 0.3	0.3 \pm 0.1
2010 Kanahena Cove (3)	85.6 \pm 5.2	12.3 \pm 2.7	1.7 \pm 0.4	0.4 \pm 0.1
2008 Kalaeloa (2)	51.2 \pm 9.6	18.7 \pm 1.8	23.4 \pm 6.5	6.8 \pm 1.5
2010 Kalaeloa (2)	48.6 \pm 2.0	27.2 \pm 3.2	22.0 \pm 4.2	2.2 \pm 0.3
2008 Mokuhā (2)	84.0 \pm 6.7	10.4 \pm 4.1	4.5 \pm 2.1	1.1 \pm 0.1
2010 Mokuhā (2)	61.1 \pm 5.6	24.5 \pm 5.3	13.1 \pm 2.9	1.2 \pm 0.2
2008 <i>Montipora</i> Pond (2)	7.9 \pm 3.3	34.9 \pm 2.7	45.3 \pm 7.3	11.9 \pm 6.1
2010 <i>Montipora</i> Pond (2)	21.9 \pm 0.8	19.4 \pm 1.5	47.7 \pm 1.4	11.0 \pm 1.3

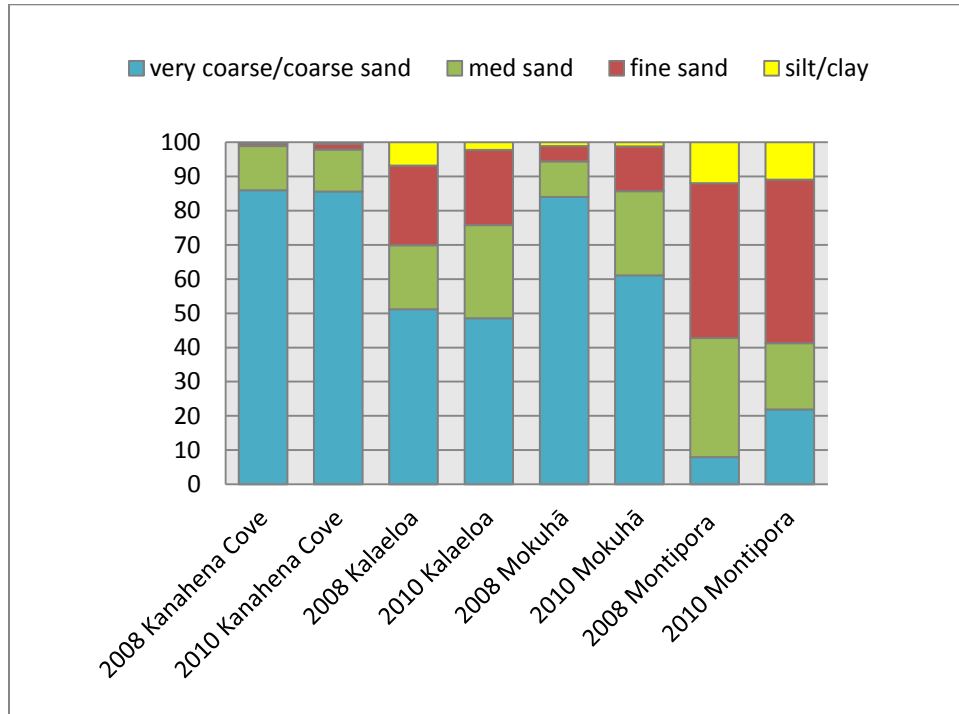


Fig. 2.25. Mean proportion of sediment grain-size for Kanahena Cove, Kalaeloa, Mokuhā, and *Montipora* Pond, 2008 and 2010.

Water Temperature

Data loggers were placed at approximately 1 m depth at all sites. The first data logger deployed on July 19, 2008 in Kanahena Cove could not be located in July 2009. A replacement was mounted at the same reef structure in Kanahena Cove on July 14, 2009. Loggers deployed in 2008 at Mokuhā and *Montipora* Pond were retrieved and replaced with fresh units in July 2009. The final set of loggers was retrieved from all sites during May 2010. The following are data collection periods: July 14, 2009 – May 19, 2010 in Kanahena Cove; August 28, 2009 - May 20; 2010 in Kalaeloa; July 20, 2008 - April 11, 2010 in Mokuhā; July 20, 2008 - April 11, 2010.

The annual mean temperature in 2009-2010 ranged from 25.0°C at *Montipora* Pond to 25.5°C at Kanahena Cove (Table 2.16a and 2.16b). Inter-annual means at Mokuhā and *Montipora* Pond were similar to each other (Table 2.16a).

Shifts in monthly mean temperature were similar for 2008-2009 and 2009-2010 across sites (Fig. 2.26a and 2.26b). The highest monthly mean temperature was observed between July and October in 2008 and 2009. In July-October 2008, the observed highest monthly mean temperature ranged from 25.6 and 26.0°C in Mokuhā. The range was between 25.8 and 26.7°C in *Montipora* Pond. In 2009, the highest monthly mean temperature ranged from 25.8 and 26.2°C in Mokuhā, 25.9 and 26.6°C in *Montipora* pond, and 26.5 and 26.9°C in Kanahena Cove. The highest monthly means (26.3-26.5°C) were also observed in August, September, and October in Kalaeloa during 2009. The lowest monthly means were typically observed in March and April at all sites. The lowest means ranged from 22.6 to 23.2°C in *Montipora* pond in 2008 while these were

Table 2.16a. Monthly average temperature (°C) in Mokuhā and *Montipora* Pond, July 2008-April 2010.

CV = coefficient of variation; Max = the maximum temperature recorded for the month;
Min = the minimum temperature recorded for the month.

Month/Year	Mokuhā				Montipora Pond			
	Mean (°C)	CV * (%)	Max (°C)	Min (°C)	Mean (°C)	CV* (%)	Max (°C)	Min (°C)
July 2008	26.0	0.2	27.2	24.7	26.0	0.3	27.9	24.7
Aug 2008	25.7	0.2	27.3	24.7	26.7	0.2	27.2	24.6
Sept 2008	25.7	0.2	27.4	24.7	26.0	0.2	27.9	24.8
Oct 2008	25.6	0.2	27.2	24.7	25.8	0.2	27.6	24.4
Nov 2008	25.3	0.2	26.9	24.2	25.1	0.3	27.4	23.3
Dec 2008	24.7	0.1	25.8	23.6	24.3	0.3	26.4	22.6
Jan 2009	24.3	0.2	25.9	23.0	23.6	0.4	26.4	21.2
Feb 2009	23.9	0.2	25.4	22.1	23.4	0.2	25.0	21.2
Mar 2009	23.3	0.2	24.8	21.6	22.6	0.3	25.2	20.9
April 2009	23.6	0.2	25.6	22.3	23.2	0.4	26.4	21.2
May 2009	24.9	0.3	27.4	23.5	25.6	0.5	28.6	23.2
June 2009	25.3	0.2	27.5	24.3	25.6	0.2	27.3	24.1
July 2009	25.8	0.2	27.0	24.0	25.9	0.2	27.1	24.5
Aug 2009	26.1	0.2	27.8	24.8	26.3	0.3	28.4	24.5
Sept 2009	26.2	0.2	27.5	25.1	26.3	0.2	27.7	25.0
Oct 2009	26.2	0.2	27.8	24.5	26.6	0.2	28.6	24.9
Nov 2009	25.5	0.2	27.0	23.6	25.3	0.2	27.1	24.0
Dec 2009	24.9	0.1	26.3	23.4	24.8	0.2	26.4	23.2
Jan 2010	24.8	0.1	26.1	22.9	24.6	0.3	26.2	22.2
Feb 2010	24.4	0.2	25.6	22.7	23.6	0.3	25.6	21.5
Mar 2010	24.0	0.1	25.5	22.7	23.4	0.2	25.3	21.9
April 2010	24.0	0.1	24.9	23.0	23.8	0.2	25.4	21.8
2008-2009	24.9	0.2	26.5	23.6	24.8	0.3	26.9	23.0
2009-2010	25.2	0.2	26.5	23.7	25.0	0.2	26.8	23.0

*Coefficient of variation was calculated from mean temperature on an absolute temperature scale (i.e., the Kelvin scale).

Table 2.16b. Monthly average temperature (°C) in Kanahena Cove and Kalaeloa, July 2009-May 2010.
 CV = coefficient of variation; Max = the maximum temperature recorded for the month; Min = the minimum temperature recorded for the month.

Month/Year	Kanahena Cove				Kalaeloa			
	Mean (°C)	CV* (%)	Max (°C)	Min (°C)	Mean (°C)	CV* (%)	Max (°C)	Min (°C)
July 2009	26.5	0.2	28.5	25.3				
Aug 2009	26.7	0.2	28.2	25.3	26.3	0.1	26.8	26.1
Sept 2009	26.7	0.2	28.3	25.5	26.4	0.1	27.2	25.8
Oct 2009	26.9	0.2	28.9	25.5	26.5	0.1	27.9	25.8
Nov 2009	26.0	0.2	27.8	24.5	25.7	0.1	26.9	25.0
Dec 2009	25.2	0.2	26.7	23.9	25.1	0.1	26.0	24.3
Jan 2010	24.8	0.2	26.3	23.4	24.8	0.1	25.8	23.9
Feb 2010	24.5	0.2	26.0	23.0	24.5	0.1	25.3	23.5
Mar 2010	24.1	0.2	26.0	22.7	23.8	0.1	25.2	22.9
April 2010	24.1	0.2	26.3	22.4	23.8	0.1	24.9	22.8
May 2010	24.8	0.2	26.2	23.9	24.5	0.1	25.3	23.9
2009-2010	25.5	0.2	27.2	24.1	25.1	0.1	26.1	24.4

*Coefficient of variation was calculated from mean temperature on an absolute temperature scale (i.e., the Kelvin scale).

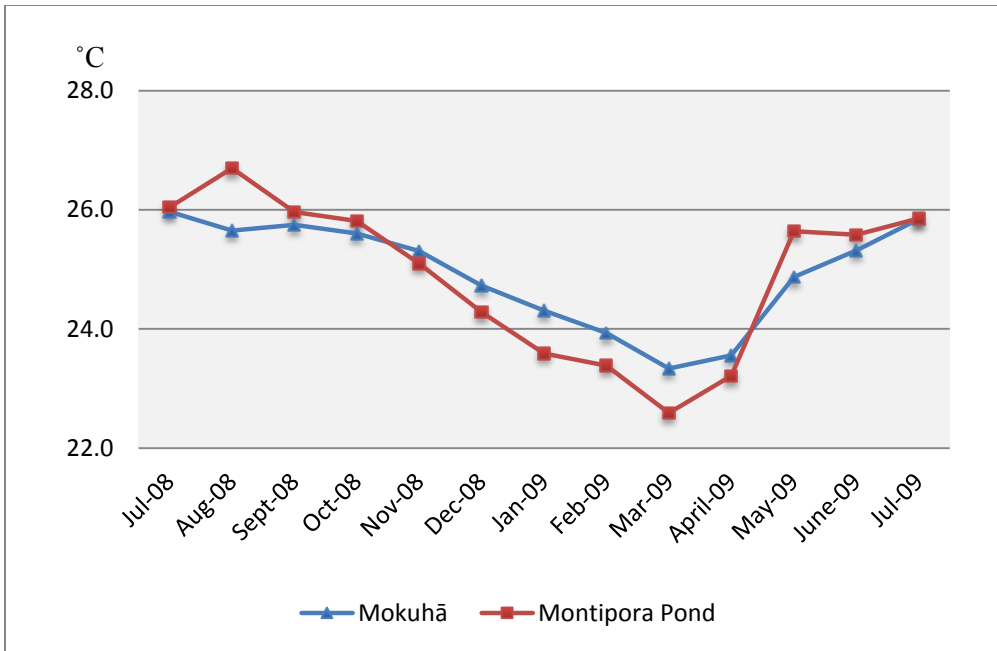


Fig. 2.26a. Monthly average temperature observed in Mokuhā and *Montipora* Pond, July 2008 – July 2009.

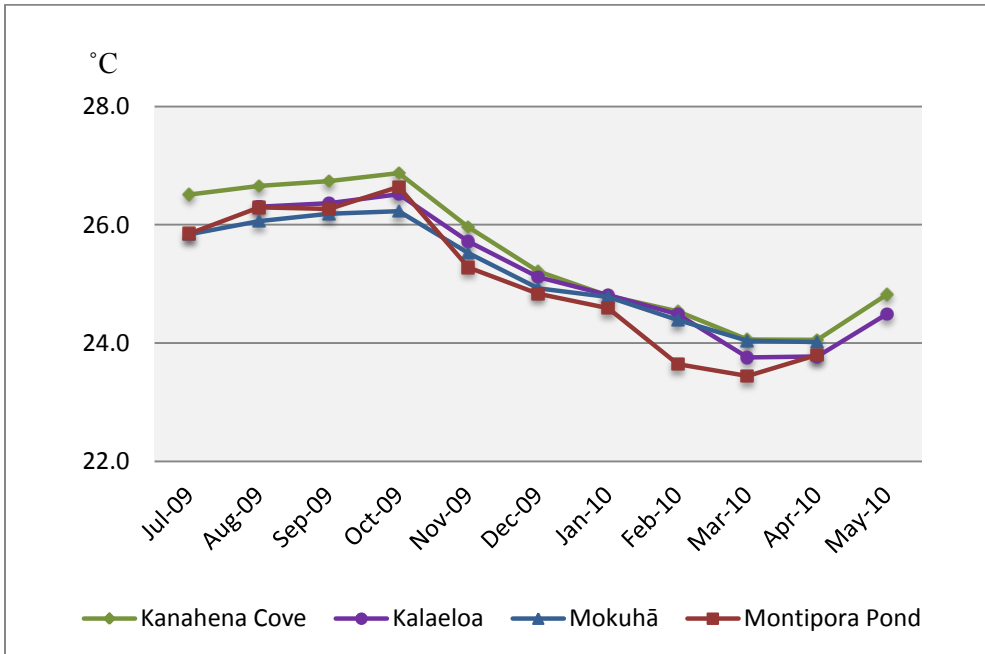


Fig. 2.26b. Monthly average temperature observed in Kanahena Cove, Kalaeloa, Mokuhā and *Montipora* Pond, July 2009 – July 2010.

23.4 and 23.6°C in 2009. The lowest means of 23.3 and 23.6°C were recorded in 2008 at Mokuhā while the mean was 24.0°C in March and April 2009. The lowest monthly means were 24.1°C at Kanahena Cove and 23.8°C at Kalaeloa in March and April 2009 respectively. Although quantitative measurements were not taken, water temperature was noticeably cooler near shorelines at the mountain side of Kalaeloa and Mokuhā. This was likely due to subsurface freshwater (ground water) input seeping through porous basalt rock.

In 2009, the highest maximum temperatures, exceeding 28.0°C, were recorded in Kanahena Cove between July and October generally in the afternoon through evening. The highest record (28.9°C) was measured on October 8 and 9, peaking around 14:45-15:45. A temperature above 28.0°C was also recorded on four consecutive days in May (28.1-28.6°C), two days in August (28.3-28.4°C), and five days in October (28.2-28.6°C) 2009 for *Montipora* pond. Each event lasted less than 24 h. The longest event lasted about 15 h, peaking between 21:45 and 22:30 on October 9 at *Montipora* pond. The mean maximum temperature, between July 2009 and May 2010, was the highest for Kanahena (27.2°C), followed by *Montipora* Pond (26.8°C), Mokuhā (26.5°C), and Kalaeloa (26.1°C).

Some of the lowest temperatures were recorded between January and April 2009 for *Montipora* Pond (20.9-21.2°C). The lowest recorded minimum temperature (21.5-21.9°C) was also found in *Montipora* pond in 2010. *Montipora* Pond also showed the most daily and seasonally fluctuating temperatures among all sites. A recorded temperature decreased from about 26.0°C to 21.3°C occurred within 40 hours in January 2009.

Discussion

Benthic Cover, Composition, and Conditions

Results of the data analysis suggest that there were no obvious differences in relative abundance of live corals at Kanahena Cove, Kalaeloa, and Mokuhā between 2008 and 2010, however, several considerations should be made regarding the lack of obvious differences at these sites. First, it is difficult to detect the change especially when coral cover is very low. At Mokuhā, the relative abundance of corals was less than 0.1% cover for both years. At both Kanahena Cove and Kalaeloa, the magnitude of difference in mean coral cover was small when compared to the range of variability. The estimated dispersion from the mean was greater than the difference in % mean between the two years. Coral cover is generally less at the shoreward reef bench than at the seaward reef bench and reef slope due to natural wave stress (Dollar 1982). The small magnitude of differences in cover is to be expected under such natural conditions and difficult to capture with the technique used. Second, the time scale of the surveys may not match the time scale for the response of *Porites lobata* or Lobe coral, the most abundant species at Kanahena and Kalaeloa, to impacts of trampling and/or other human activities. Rodgers *et al.* (2003) reported that the average linear extension rate of *P. lobata* was 7.4 mm per year while *P. compressa* (Finger coral) was 16.7 mm, and 24.3 mm for *Montipora capitata* (Rice coral) over an 11-month experimental growth period at a depth of 1 m for a control group (i.e., no trampling). This slow linear extension rate of *P. lobata* makes it difficult to detect changes in cover over a relatively short period. While the difference in live coral cover did not appear substantial at Kanahena Cove during this survey, there was a noticeable difference when 2008-2010 results are compared to historic data

collected by Hawai‘i Division of Aquatic Resources (DAR) in partnership with CRAMP by using their long-term monitoring method. The CRAMP RAT protocol includes fewer benthic transects per site than the CRAMP long-term monitoring protocol, yet it employs comparable and consistent variables of interest and survey techniques (Jokiel *et al.* 2004). According to a summary of the 1999-2008 CRAMP and DAR results for Kanahena Cove, coral cover increased over the ten year period. Reported coverage in 1999-2002 was approximately 11-13% (SE ±2-3%) and increased to 16-21% (SE ±2-4%) in 2003-2008. Mean cover obtained from RATs in 2008-2010 was similar (9-12%, SE±3-7%) to the 1999-2002 data. Noticeable cover change appeared to occur after 3-5 years. This may suggest that two years may not be long enough to detect measurable increase in *P. lobata* cover. Third, the differences in coral cover may be attributed to temporal scales of data and coral exposure to both natural and anthropogenic forces over a decade. The differences may be also attributed to spatial scales of data and heterogeneous distributions or patchiness in coral cover. Fourth, additional measurements such as extent and rate of tissue abrasion may be desirable to better understand effects of trampling, particularly at Kanahena Cove and Kalaeloa where massive corals are dominant. Frequency of tissue abrasion to massive corals is higher where SCUBA diving is intense (Hawkins *et al.* 1999; Zakai and Chadwick-Furman 2002), and tissue damage may increase coral’s susceptibility to infectious diseases that might eventually lead to mortality (Hawkins *et al.* 1999). Recovery rates may be different between species at various sizes but it is known that the recovery rate of *Porites lutea*, a massive coral species similar to *P. lobata*, is slow (Liddle and Kay 1987). While *P. lobata* is more tolerant to mechanical damage than branching corals (Rodgers *et al.* 2003), it may be

impacted by direct and sub-lethal trampling stress. Although skeletal damage on *P. lobata* is not as obvious as on branching corals, it could suffer from tissue abrasion caused by trampling.

In contrast, the benthic cover and conditions changed substantially at the *Montipora* Pond over a 16 month period. *M. capitata* was the single species observed at this site. Its mean cover decreased substantially from 48.5% in 2008 to 30.2% in 2010, during the access-closure period. Mean dead coral cover doubled from 2.9 to 5.8% during the same period. Partial mortality on single and multiple colonies were observed *in-situ* and in photographic data. The conditions of the skeletons varied from recent to mature. Some recent skeletons were white and uncolonized by visible organisms. Others were lightly covered by turf algae with visible calices while others were fully settled by turf algae. Such conditions suggest continuous mortality of *M. capitata* throughout the period of study at this site.

Partial mortality of corals can result from predation by other marine organisms. The percent cover of dead coral in 2010 at *Montipora* Pond was similar to reported dead coral cover throughout ‘Āhihi Kīna‘u NARS by CRAMP in 2007 (Rodgers *et al.* 2009). Mean dead coral cover at depths between 3 and 10m was estimated as 6.1%. The primary species with high mortality within this depth range was *Pocillopora meandrina* indicating possible predation by *Acanthaster planci*, the Crown-of-thorns Starfish (COTS) (Rodgers and Jokiel 2008). Feeding preference of COTS also includes *Montipora* spp. and to a lesser extent *Porites* spp. (Rodgers and Jokiel 2008). However COTS and its feeding characteristics on skeletons were not detected at *Montipora* Pond. Therefore, increased partial mortality was not due to predation.

Synergic effects from both natural and anthropogenic stresses are suspected for changes to benthic cover and conditions manifesting during the closure period. Rodgers and Jokiel (2008) reported that abrasions and mobile coralliths were evident from trampling near the entry point at *Montipora* Pond. Mobile coralliths are spherical, unattached rock-like corals that are initially fragmented from sessile colonies by physical disturbances, and composed of CCA (Glynn 1974; Rodgers 2001). Unlike *P. lobata*, *M. capitata* is much less tolerant to mechanical damage (Rodgers *et al.* 2003). High intensity trampling causes significant damage, altering the benthic composition (Kay and Liddle 1989), resulting in fewer, smaller colonies (Hawkins and Roberts 1993), thereby reducing percent cover of live corals (Rodgers 2001). Hawkins *et al.* (1999) discussed the probable relationship between tissue abrasion by divers and coral disease in the Caribbean. Guzner *et al.* (2010) also concluded that frequent mechanical damage by divers enhanced susceptibility to predation and disease in the Red Sea. Therefore the occurrence of MWS at *Montipora* Pond may be the indirect result of trampling. Past and present states of the natural environment may facilitate the prevalence of coral disease and partial mortality in a place such as *Montipora* Pond. The magnitude of these effects is considered greater and more immediate in such a small (38 m-long), confined habitat where host density is particularly high. *Montipora* Pond appears to provide the optimum biotic and abiotic conditions for the prevalence of MWS. Partial mortality of *M. capitata* may be attributed to direct mechanical injury, tissue abrasions, and tissue loss from MWS.

It is interesting to note the prevalence of MWS during 2008 and 2010 surveys (pers. comm. Ross 2010, unpub. data) and the observed phenomena of a high density of juvenile *Scarus* or parrotfish at *Montipora* Pond. Williams *et al.* (2010) demonstrated

that juvenile Scarids and chlorophyll- α concentration were the two strongest predictors for MWS modeled with field data from Kāne‘ohe Bay, O‘ahu. Two dominant juvenile *Scarus* spp. observed here were *Scarus psittacus* (Palenose Parrotfish) and *Chlorurus spilurus* (Bullethead Parrotfish). No evidence of coral feeding by juvenile Palenose and Bullethead Parrotfish in Hawai‘i was reported in the literature review by Longenecker and Langston (2008). Grazing scars are commonly seen on *Porites* spp., however such scars were not apparent on live *Montipora* colonies during this survey. While juvenile *Scarus* may have a direct or indirect association with MWS (Williams *et al.* 2010), their potential roles are still unclear.

Dead and diseased coral contribute to shifting the present ecological state from coral-dominated to algal-dominated reefs. Tissue loss and broken surfaces provide open space for other sessile organisms through competitive interaction and succession. Damaged corals may not be able to repair and recover fast enough to compete against other sessile organisms, especially if environmental conditions (e.g., temperature, available light and nutrients) are optimal for such competitors. Mean percent cover of turf algae, calcified red algae, (e.g., *Galaxaura* and *Dichotomaria* spp.), and didemnid tunicate *Diplosoma similis* increased at *Montipora* Pond, between 2008 to 2010, from 23.8 to 30.5%, 8.1 to 10.4%, and 2.9 to 5.8%, respectively. *Diplosoma similis* is a common native species in Hawai‘i. It has shown its invasive nature by overgrowing live coral at a much broader scale on the remote reefs of Swains Island, American Sāmoa. The observed relative abundance was as high as 35.0 and 76.5% at the center of occurrence (Vargas-Ángel *et al.*, 2008). The rapid colonization of *Diplosoma* was apparently a secondary effect of storm damage in 2004, reducing live coral cover by

nearly 50% (Vargas-Ángel *et al.*, 2008). There appears to be a four-year lag between the observed *Diplosoma* invasion and storm damage. Therefore a rapid colonization of *Diplosoma* may occur at *Montipora* Pond as a secondary effect of trampling. It is suspected that the time-lag for *Diplosoma* invasion at *Montipora* Pond may be less due to its small confined nature. The relative abundance of non-coral functional groups might continue to change at *Montipora* Pond.

High algal cover is generally associated with high nutrient concentrations. While no water quality was measured during this survey, in the future it would be helpful to monitor nutrient concentrations at *Montipora* Pond. This site is relatively close (~ 90-100 m) to an anchialine pond where higher nutrient concentrations naturally prevail. Anchialine ponds were used as lavatories before closure since the nearest facilities were located at Le Perouse Bay and Maunakalā, better known as Dumps (pers. comm. Ramsey 2008). As anchialine ponds were being degraded by human waste and trash, increasing numbers of rats were also evident. Such conditions might have increased nutrient loading from human and animal waste entering the ponds. Subterranean flow of seawater and groundwater through porous basalt might influence nutrient loading at *Montipora* Pond. Algal cover in this tidal pond may be affected by changes in nutrient concentration at the anchialine pond.

No substantial difference in percent cover and composition of other cover types was observed between 2008 and 2010 in Kalaeloa and Mokuhā. Turf algae (49%) accounted for a greater proportion than coralline algae (29-30%) at Kalaeloa. Coralline algae (36.2-41.5%) accounted for a greater proportion than turf algae in Mokuhā. While the ratio of mean percent cover for each cover type to total mean cover varied between

sites, the ratio and composition of benthic cover was consistent during the two survey periods at each site.

The ratio of turf and sediment-covered turf algae changed considerably between 2008 and 2010 at Kanahena Cove . Sediment-covered turf algae accounted for 75.4 % and turf algae accounted only for 3.8% in 2008. In 2010, the relative abundance of turf algae increased to 33.9% while sediment-covered turf algae decreased to 45.5%. The difference could be attributed to sediment transport by wave action exposing the turf algae beneath. Uncolonized substrate may also be exposed to new colonization of turf algae. It was apparent that an existing sand patch during 2008 survey was no longer extant at one of the transects.

The impact from trampling alone is difficult to separate out from other confounding factors that may also contribute to coral decline. For example, coral cover may be altered due to sand movement by physical forces. Long-term observations with different frequencies would help capture a time scale for coral response to impacts from natural factors, trampling, and other human activities.

Fish Abundance and Biomass

Distributions of fish abundance and biomass were highly variable in both 2008 and 2010. While direct effects of the shoreline-closure were not obvious on the fish assemblage, the effects of a long history of legal protection for inshore habitats from fishing and relatively isolated shoreline are evident. Numeric abundance of fish was considerably higher ($9.7\text{-}45.1 \text{ ha}^{-1} \times 1000$) at inshore sites when compared to sites 3 to 10 m deep in ‘Āhihi Kīna‘u NARS. The mean abundance of inshore fish was $26.7 (\text{ha}^{-1} \times$

1000) in 2008, and 25.1 ($\text{ha}^{-1} \times 1000$) in 2010. Density ranged from 3.8 to 21.6 ($\text{ha}^{-1} \times 1000$) among 25 transects at sites 3 to 10 m deep with an average of 11.0 ($\text{ha}^{-1} \times 1000$). The five highest taxa, such as *Kuhlia* spp. (Flagtail) and *Neomyxus leuciscus* (Sharpnose Mullet) are highly-prized for inshore fisheries and were observed at two of four sites. The highest abundance was observed at Mokuhā for both years. High abundance was also observed at *Montipora* Pond and Kalaeloa while Kanahena had the lowest abundance of fishes.

The species with the highest biomass was the same as the species with the highest abundance in 2008 and 2010 at each site. This did not hold true for the remaining species where biomass varied between years at sites. As can be expected, the presence of one or a few larger species and aggregations affected differences in biomass by year and site. Overall, herbivores (e.g. Acanthuridae and Scaridae), comprised the greatest contribution to biomass (~36-63%) in both years. While *Zebrasoma flavescens* (Yellow Tang, Acanthuridae) did not rank as the highest, this species maintained fairly substantial biomass (2-11%) and high frequency (~27-36%) in both years at all sites except for *Montipora* Pond.

Overall numeric abundance increased in Kanahena from 2008 to 2010. This increase was attributed to wrasses, such as *Thalassoma duperrey* (Saddle Wrasse) and *Stethojulis balteata* (Belted Wrasse). *Acanthurus triostegus* (Convict Tang) ranked second in mean density increasing from less than 0.5 ($\text{ha}^{-1} \times 1000$) in 2008 to greater than 2.0 ($\text{ha}^{-1} \times 1000$) in 2010. The most abundant species in 2008, *Mulloidichthys flavolineatus* (2.1 $\text{ha}^{-1} \times 1000$), was also well-represented in 2010 (1.6 $\text{ha}^{-1} \times 1000$) ranking third in mean number of individuals. Benthic composition and cover changes

(e.g., shifting sand and an increase in turf-covered rock) may affect availability of habitat for different guilds. Such cover change may induce a shift in fish composition and abundance. For example, increases in the abundance of Saddle Wrasses could be attributed to increased cover of turf-covered rock because this species often forages over hard bottom, turning rocks and rubble to find prey.

Fish composition and the proportion to total biomass varied at the species level at Kanahena Cove between years. In 2008, *M. flavolineatus* (Yellowfin Goatfish), *Acanthurus leucopareius* (Whitebar Surgeonfish), *Scarus rubroviolaceus* (Redlip Parrotfish), *S. psittacus* (Palenose Parrotfish), and *Z. flavescens* were the five species highest in biomass. While *A. leucopareius* accounted for 26% of the biomass in 2008, it decreased substantially to 4% in 2010. Instead, *A. triostegus* and *Acanthurus olivaceus* (Orangeband Surgeonfish) had higher proportions and ranked in the top five for 2010. *S. rubroviolaceus* and *M. flavolineatus* had high proportions for both years; nearly 50% and 38% less mean biomass for 2010. A few large-sized *Caranx melampygus* (Bluefin Trevally) recorded for 2010 made up a large proportion of the biomass. Piscivores, such as *C. melampygus* and invertebrate-feeders together comprised at least 26% (2008) and 34% (2010) of the biomass. While herbivores comprised the majority of the biomass, unlike other sites, piscivores and invertebrate-feeders were well-represented at this site. Numeric abundance of fishes was generally high at Kalaeloa and Mokuhā, yet it varied between 2008 and 2010. Overall the mean number of individuals was less in 2010 than in 2008 at each site. The difference was due to the presence or absence of aggregating species at each site. Aggregating species, *Kuhlia* spp. and *N. leuciscus*, were both present at Kalaeloa and Mokuhā. These largely accounted for the inflated numbers of fishes and

biomass at both sites in 2008. The large aggregation of *N. leuciscus* was not recorded at either site in 2010. Mean density of *Kuhlia* spp. ($9.9 \times \text{ha}^{-1} \times 1000$) in 2010 at Mokuhā was similar to 2008. They were less abundant at Kalaeloa by more than 60% in 2010. Other high ranking species were consistent in abundance and presence between years at these sites.

Large zooplanktivores such as *Kuhlia* spp. (20-39%) and *Melichthys niger* (Black Triggerfish, 9-14%), which also feed on drift and coralline algae, ranked high in biomass at Kalaeloa and Mokuhā in both 2008 and 2010. A substantial part of the biomass was also comprised of adult and subadult Scarids (Parrotfish, 4-5% in 2008, 11-24% in 2010) and Acanthurids (Surgeonfish, 13-20% in 2008, 20-24% in 2010) at both sites. While the overall biomass was less in 2010 than in 2008, the biomass of these herbivorous fishes increased in 2010. Such an increase may be attributed to natural fluctuations in habitat utilization and population dynamics. *A. triostegus* typically form large aggregations, often overwhelming other territorial fishes upon grazing (Randall 2007). Such aggregations and behavior were observed at Kalaeloa and Mokuhā. *S. psittacus* and *Chlorurus spilurus* (Bullethead Parrotfish), also common at these sites, often mixed to form small aggregations, grazing shallow rocky reefs. Acanthurids and Scarids may be strong competitors against others such as *N. leuciscus* for habitat utilization.

A single family of fish accounted for the high values at *Montipora* Pond. Juvenile *Scarus* spp. were extremely abundant in both years. Abundance of juvenile Scarids were three-fold higher in 2010 ($32.0 \times \text{ha}^{-1} \times 1000$) compared to 2008 ($10.9 \times \text{ha}^{-1} \times 1000$). The area appears to function as a nursery for juvenile fish, particularly on the pond's west side. Scarids are an important inshore fishery species (DeMello 2004; HCFRU 2008;

DeMartini *et al.* 2010), and large individuals are ecologically important as ecosystem engineers for their production and distribution of carbonate sand and creation of freshly-denuded substrate through grazing (e.g., Kiene 1988; Bellwood 1995; Bruggemann *et al.* 1996; Ong and Hollad 2010). Recruits prefer rugose substrata, especially corals with tuberculate, digitate, and branched forms (DeMartini *et al.* 2010). The abundance of young Scarids might decrease if degradation of live corals and habitat loss occurs at *Montipora* Pond. Loss of suitable habitat has possible implications for fisheries management and conservation. Other abundant species were also much smaller in size at *Montipora* Pond than at other sites. Ranking for abundance changed between 2008 and 2010. There were substantially less *Abudefduf abdominalis* (Hawaiian Sergeant) in 2010, no longer ranking among the abundant species. Gobies (e.g. *Asterropteryx semipunctatus*) were also no longer ranked as one of the top five taxa. Differences in numeric abundance and species composition potentially relate to differences in benthic cover and condition and/or temporal fluctuation in recruitment. The absence of intense human activities in the pond might act as a refuge for juvenile resource fishes from larger predators.

Greater overall biomass appeared to be due to a high number of Scarids and differences in size distribution. Larger individuals were observed in 2010 (7-15 cm) compared to 2008 (6-8 cm) although the predominant size class was juveniles (2-5 cm) for both years. Abundance of both small and large Scarids were approximately three times higher in 2010 than in 2008. Biomass of all species of Scarids increased from 23% in 2008 to 53% in 2010. In addition to Scarids, several large individuals (e.g. *Lutjanus fulvus*, *Neoniphon sammara*, *Chaetodon ephippium*, *Chaetodon auriga*) were recorded in

2010 while fewer large individuals (*C. melampygus* and *N. leuciscus*) were observed in 2008. *Abudefduf sordidus* (Blackspot Sergeant) had relatively high biomass in both years. *Cephalopholis argus* (Peacock Grouper) was recorded as one of the highest ranking species in 2010 while it was not ranked within the top five in 2008 at *Montipora* Pond. However, high biomass of this introduced species was represented by a single large individual.

It should be noted that sample sizes for fish data were small, and high variability in mean number of individuals and biomass can be expected. Variability was high in both years at Kanahena Cove, Kalaeloa, and Mokuhā making it difficult to generalize patterns of difference and changes in fish parameters.

The estimated mean density of individuals and biomass of fish in shallow micro-habitats within the NARS appeared to be different from the estimated values in habitats deeper than 3 m, where SCUBA surveys are normally conducted. Values from these inshore sites (Kanahena Cove, *Montipora* Pond, Kalaeloa, and Mokuhā) are relatively high when compared to deeper sites surveyed within and outside the NARS. The presence of large schools would significantly influence and increase the estimated mean biomass at these sites. For example, *Kuhlia* spp. and *N. leuciscus* appeared to favor the particular habitat type at both Kalaeloa and Mokuhā. These fishes are often observed in shallow rocky inshore areas where groundwater seeps occur. While no electrical conductivity measurements were taken, a visible plume, created by mixing of water columns with extremely different densities, along with cooler temperatures indicated input of freshwater at some transect locations. Thus higher frequency of large aggregations of *Kuhlia* spp. and *N. leuciscus* would be expected in such shallow rocky

inshore habitat. However, surveys conducted in the shallow transition zone between 0.5 and 3 m is typically underrepresented in the archival record. Increasing the number of temporal observations and surveys within this transition zone would provide a better estimate of fish abundance and frequency of habitat use at these sites. Such observations can be replicated over short- and long-term temporal scales.

Large charismatic species such as sharks and jacks are generally skittish. These tend to be less frequent where snorkeling and swimming activities are intense. Many are crepuscular and may not be as active when surveys are being conducted, therefore these species may not be well-represented within transects. Brock (1982) suggested limiting use of visual transects to comparison of diurnally-exposed species because of the underestimation of cryptic and common fish species. His suggestion could also be applied to species with a large home range as such individuals are highly transient, sensitive to human impact (e.g., fishing), and may be affected behaviorally in the presence of divers. For example, a small gray reef shark, approximately 70 cm in total length, was observed at Mokuhā outside a transect in the late afternoon during the 2010 survey. No young sharks were observed at other times or at other sites. While two surveys provided a reference point for characteristics of diurnally-exposed inshore fish assemblages, they did not reasonably represent the frequency of large transient species in this unique habitat, therefore different survey designs and techniques (e.g., species-time sampling, Thompson and Schmidt 1977) should be utilized.

Topographic Relief (Rugosity) and Depth

Rugosity remained relatively unchanged at all sites between 2008 (1.31 ± 0.23 , n = 11) and 2010 (1.39 ± 0.17 , n = 15) overall, with means ranging between 1.20 and 1.50. It was not as high as the deeper sites (1.69 ± 0.31 , n = 48) of ‘Āhihi Kīna‘u reefs. This was expected since heavy wave activity in the inshore shapes the community structure and limits growth forms of reef building corals to forms that are highly resistant to mechanical damage. However, at Kalaeloa and Mokuhā, the less rugose inshore reef flat immediately connects to highly complex and textured topography within a distance of 5–20 m. The cove at Kalaeloa is bowl-shaped and its depth quickly increases to about 8 m at its center. At the seaward edge there is a shallow sill at 4m dropping rapidly offshore to greater depths. The shallow subtidal reef at Mokuhā also connects to deeper, more complex topography with live corals over a short distance (Kanahena Point). Such connectivity between protected reef flats within the cove and the rugose outer reef appears to be well-suited for fishes that utilize multiple habitats. Seascapes here were consistently occupied by fishes such as large adult (12-20 cm) *Z. flavescens* (Yellow Tang). Subadult *Z. flavescens* is the most popular species in Hawai‘i’s marine aquarium trade (Walsh *et al.* 2004). This species is known for ontogenetic shifts in habitat use (Ortiz and Tissot 2008; Claisse *et al.* 2009). Adults are found in shallow turf-covered boulders and pavement with high topographic complexity while recruits and juveniles are found in deeper, coral-rich areas and *Porites compressa* (Finger coral) reefs (Ortiz and Tissot 2008; Claisse *et al.* 2009; Williams *et al.* 2009). Habitat protection for broodstock is an important management measure for fishery sustainability. The inshore topography of Kalaeloa and Mokuhā, well within the NARS boundary, provides ideal habitat for Yellow

Tang broodstock with potential for a spillover effect (Williams *et al.* 2009) and stock enhancement.

Sediment

Reef-building or scleractinian corals are the primary organisms of concern since they can be severely impacted by sediment from terrestrial sources. Rogers (1990) noted that increased sedimentation rates ($>10 \text{ mg cm}^{-2} \text{ day}^{-1}$) and suspended solid concentrations ($>10 \text{ mg l}^{-1}$) would adversely affect individual corals, coral reef communities, and ecosystems. Sedimentation and suspended solids limit growth, vertical distribution, physiological responses, photosynthetic productivity, and survival of adult corals by smothering and limiting available light (see reviews by Rogers 1990; Richmond 1993; Fabricius 2005). Weber *et al.* (2006) demonstrated that coral fragments of *Montipora peltiformis*, a species similar to *M. patula* in Hawai‘i, suffered significantly when treated with silt/clay ($<63 \mu\text{m}$) grain-sizes. Photosynthetic efficiency was significantly reduced after 36 h exposure to the treatment while efficiency remained similar to the control when treated with medium (250-500 μm) and fine/very fine sand (63-250 μm). Recovery was incomplete 48-96 h after silt/clay was removed (Weber *et al.* 2006). Photosynthetic yields were lowest when treated with terrestrial silts, followed by marine silts, while yields were similar to the control when treated with aragonite dust. Their results indicated that photosynthetic yields were significantly related to sediment grain size and type associated with organic and nutrient-related parameters. In Hawai‘i terrigenous sediment reduced photosynthetic activity of *M. capitata* (reported as *M. verrucosa*) twice as much as carbonate silt (Te 2001). Suspended sediment also impedes

the larval settlement, survival, and fertilization of reef building corals (Gilmour 1999). Nutrient-rich sediment can result in tissue damage in the presence of bacteria (Hodgson 1990). High particulate organic matter and abundant phytoplankton can support growth and survival of corallivorous *Acanthaster planci* or Crown-of-Thorns seastar larvae, enhancing outbreaks and predation (Birkeland 1982). While the predation by *A. planci* is an indirect effect of sediment and/or terrestrial run-off, it has resulted in substantial loss of scleractinian corals throughout the Pacific. Sedimentation is also negatively related to cover of CCA. Reduced presence of CCA would inhibit the larval settlement of corals (Fabricius 2005). Prolonged impacts may enhance decreased cover, community-shift, and habitat change.

Sediment composition generally resembled the 2007 survey sample data for deeper stations inside and outside the NARS. Inshore sediment composition was characterized by relatively high carbonate content (52.6-90.9%) with moderate, but variable proportions of terrigenous material (3.6-44.1%). This characteristic is reasonable for the inshore environment at ‘Āhihi Kīna‘u where the seascape is dominated by biogenic marine carbonates such as coralline algae and corals, and terrigenous basalt. Processes of bio-erosion by animal agents and physical erosion by wind and waves are expected to be major contributors in this area. Grain sizes were predominantly very coarse/coarse to medium sand among most samples.

Variation among sites appeared to be slight; the difference in sediment composition was most evident at Mokuhā. Terrigenous material was more than three times greater at Mokuhā than Kalaeloa. Such variation may be influenced by the orientation of the shoreline to angles of wave and the exposure to high wave energy.

Long-period south or west swells and Kona Storm waves result in high surf conditions along southwest-facing shores. These large waves would have significant influence on geomorphic processes near Mokuhā. Direct exposure to high wave energy causes hydraulic action, abrasion, weathering, and ultimately erosion of low cliffs and shorelines (Stearns 1985; Macdonald *et al.* 1990). In fact, basalt boulders, cobbles, and gravels are common on the southwest-facing shoreline between Kanahena Point and Ka Lae Mamane through Nukulele Point. Gravels, cobbles, and boulders are also found at Mokuhā. Large, smooth round boulders were observed along basalt cliffs at Nukulele Point during a shoreline hike in 2009. Nukulele Point is the most exposed point facing southwest on Cape Kīnau. Movement of boulders by strong wave action was evident along southwest facing shorelines. Physical abrasion between these components especially during high surf events probably contributes to an influx of new terrigenous sediment. In contrast, higher carbonate compositions were observed at Kalaeloa and the well-protected *Montipora* Pond, both of which face southeast.

Compositions changed between 2008 and 2010 within each site. Overall, fractions of terrigenous material were greater in 2008 than 2010 at all sites. Two considerations were made regarding these temporal differences. First, overall temporal differences in terrigenous fractions might be influenced by seasonal patterns of tides, longshore currents, and waves generated by strong northeast tradewinds funneled through the Alenuihaha Channel around the south flank of Haleakalā past Kanaio and Keoni‘ō‘io (Le Parouse Bay). Patterns of sediment transport and deposition are controlled by grain size and flow velocity which vary significantly with wave, current, tidal dynamics, and bottom complexity (Leeder 1982; Eversole and Fletcher 2003; Storlazzi *et al.* 2004; Storlazzi *et*

al. 2009). The frequency of tradewinds fluctuates seasonally, occurring more than 90% of the time during summer and 40-60% during winter (Haraguchi 1979). Therefore seasonal patterns of wind waves and associated longshore currents might interact with tidal currents to affect sediment transport and deposition at ‘Āhihi Kīna‘u. Second, higher terrigenous content in 2008 might be associated with terrestrial storm-related runoff. A strong Kona storm produced heavy rainfall, strong southwesterly winds and waves statewide from December 4 to 11, 2007. On December 5, intense rainfall (101 mm in 24 h) and flooding occurred at Keokea, upland of ‘Āhihi Kīna‘u (National Weather Service Honolulu, NOAA), with a 5-day storm total of 211 mm. According to spatial data from the Hawaii Statewide GIS program, there are no perennial or intermittent stream channels in the ‘Āhihi Kīna‘u or Kanaio watersheds. While the likelihood of terrigenous input via obvious channel networks is minimal, terrigenous material might have been introduced from flooded uplands through a channel at Wailea, located northwest of ‘Āhihi Kīna‘u during the storm. General surface transport during heavy rainfall near the coast would also deliver silt-laden water into the ocean. High surf was also generated along the west-facing shores of Moloka‘i (3.7-5.5 m) and Hawai‘i (1.8-3.0 m) between December 1 and 6. Similar surf conditions probably also occurred along the west-facing shores of Maui influencing transport and deposition of introduced terrigenous material to ‘Āhihi Kīna‘u. The relatively young basalt terrain is porous and permeable in both horizontal and vertical aspects (Peterson 1972) potentially resulting in subsurface flow near study sites. It should be noted that sampling was conducted once each year, during the summer of 2008 and winter of 2010.

While composition change between years was relatively consistent across sites, the magnitude of change between years was different among sites. Differences in magnitude might be influenced by sporadic temporal events such as the number, direction, size, and duration of large swells and storms each year. The greatest magnitudes of composition change were observed in Mokuhā samples followed by Kanahena Cove. The openings of Mokuhā and Kanahena Cove face the south and southwest. Since the majority of southern hemisphere swells come from the south or southwest, with the island of Hawai‘i effectively blocking long-period energy from the southeast, these sites would be more directly affected by high-energy waves than Kalaeloa and *Montipora* Pond.

Compositions at Mokuhā and Kanahena Cove showed high variation between replicate samples within each site. Results suggest that inshore sediment composition varies substantially at a fine scale depending on relative sampling position, variation in wave intensity and exposure, and each site’s topography and its effect on waves and currents, thus affecting the movement of sediment. Representative samples were collected where ample sediment could be found at depths within the scope of this study. Samples were collected within relatively close proximity, yet there were noticeable differences between samples collected seaward and landward.

Proportions of organic matter appeared to be relatively consistent among sites and between years. Results of inshore organics were similar to the statewide trend of 3-5% among 95 sites (Rodgers *et al.* 2009). There were no substantial differences between open and closed sites. In addition to the influx of land-based organics, the level of organic matter is affected by aquatic biochemical processes such as decay and/or excretion by organisms in the marine environment (Kördel *et al.* 1997). The latter

processes are likely to be primary contributors at inshore sites at ‘Āhihi Kīna‘u. Being a very arid environment with little vegetation, minimal fluvial and wind-blown introduction of land-based organic matter would be expected.

In general, proportions of grain-size fractions seemed to be distinct among sites. The *Montipora* Pond showed very distinct grain-size characteristics with fine sand and silt/clay comprising 60% of the total. Fine sand and silt/clay would be expected here since the environment is well-protected from high surf and strong wave energy, while very coarse/coarse sand would predominate at sites exposed to high surf and strong wave energy. Such sites may include southwestern facing Mokuhā and Kanahena Cove. Fine sand and silt/clay fractions were of secondary importance at southeast-facing Kalaeloa.

In summary, there was no strong signal of anthropogenic impacts on sediment types, grain-size, and distributions. Geographic characteristics and associated natural processes appear to dominate sediment composition and proportions of grain-size while anthropogenic processes appear to be of minor importance at ‘Āhihi Kīna‘u’s inshore environment. Such natural processes include a combination of physical, chemical, and biological contributions to sediment composition and grain-size. The differences in sediment composition were more noticeable between years than among sites. Overall the size variation was relatively consistent between years within each site although size characteristics appeared to vary among sites.

Water Temperature

Change in sea temperature is an important abiotic factor affecting ecological and biological activities on coral reefs at various spatio-temporal scales. It affects the health,

mortality, physiology, and reproduction of reef-building corals. Optimal growth of Hawaiian corals occurs at a thermal range near 26-27°C while lower and upper lethal levels are approximately 18 to 31°C (Jokiel and Coles 1974; 1977; 1990; Jokiel 2008). The interaction between increased temperature and high light intensity together sustains physiological damage and accelerates bleaching of reef corals (Coles and Jokiel 1978; Jokiel and Coles 1990). Bleaching can be initiated when corals are exposed to above-normal ambient summer temperatures of 3-4°C for 1-2 days or by 1-2°C for several weeks (Jokiel and Coles 1990). Hawai‘i’s mean maximum summer temperature is 27.0-28.0°C and the bleaching threshold is expected to be 29-30°C (Jokiel and Coles 1990). Temperature anomalies can also facilitate infectious coral diseases (Rosenberg and Ben-Haim 2002) and disease prevalence (Bruno *et al.* 2007; Williams *et al.* 2010) that leads to loss of coral tissue and total coral cover.

The short term risk of decreased coral cover by temperature change was expected to be minimal in 2008-2010. The highest mean monthly temperatures observed from July to October in 2008 and 2009 (Fig. 2.26a and 2.26b), were within the normal ambient range for all sites. The highest means were less than the mean maximum summer temperatures reported for Hawai‘i by Jokiel and Coles (1990). Water temperatures remained near 26-27°C, which is the optimal range for skeletal growth in Hawaiian shallow reef corals and below the threshold for bleaching.

Temperatures above 28.0°C were seldom observed, 0.6% of total recorded hours at Kanahena Cove and 0.4% at *Montipora* Pond during summer and fall months. Such occasions lasted for relatively short periods, generally less than a day. Temperatures exceeded 28.0°C mostly in the afternoon through early evening and appeared to be within

the range of daily fluctuation combined with light wind conditions. Preliminary climate data (National Weather Service Honolulu, NOAA) recorded relatively low average wind speeds (6.4-12.4 km/h) from the NNE (10-30°) direction at Kahului Airport between October 4 and 9, 2009. Low average wind speeds were also observed from the 24 to 26th of the same month, but from a more normal trade wind (40-60°) direction. In general, prevailing trade winds help cool coastal surface waters during the afternoon at ‘Āhihi Kīna‘u. However such light wind conditions, especially from the northerly direction, appeared to keep peak temperatures higher for longer than usual. In addition, Kanahena Cove is more protected from prevailing trade winds therefore a minimal cooling effect would be expected. Thus, it appeared to have slightly higher means and instantaneous measurements than other sites. Highly fluctuating temperatures at the sheltered *Montipora* Pond is perhaps determined by trade wind patterns in combination with shallow depth and reduced mixing.

The sea surface temperature (SST) anomaly, affecting coral reefs at broad spatio-temporal scales (e.g. Hoegh-Guldberg 1999; Hughes *et al.* 2003; Jokiel and Brown 2004), has been widely discussed and monitored for the last 15 years. However, data are often lacking for inshore reefs at fine spatio-temporal scales, which may be more relevant to local level management teams. Jokiel and Brown (2004) indicate that temperature of inshore coral reefs can differ substantially from oceanic SST determined by local geographic, oceanographic, and climatic characteristics. Broad-scale information lacks data density and accuracy for detecting bleaching events such as those that occurred in Hawai‘i at finer spatio-temporal scales (Jokiel and Brown 2004). This data set collected at ‘Āhihi Kīna‘u is an integral part of long-term monitoring and resource management.

Temperature monitoring helps assess benthic cover change and the health of inshore shallow corals due to environmental change and/or direct effects of human trampling. It can also serve as a baseline for determining any future temperature changes.

Conclusions

The database developed in this project will be invaluable as a description of the resource and as a baseline for future comparisons. No discernable impact or recovery of corals from trampling and snorkeling was observed at Kanahena Cove, Kalaeloa, or Mokuhā after the two-year closure. There were no apparent changes for other functional benthic organisms at these sites. The time-lag between impact and recovery of the coral community, in terms of benthic cover, is likely to be longer than the time frame of this study. However, benthic surveys showed substantial decreases in live corals, and increases in dead corals, tunicates, turf, and macroalgae at *Montipora* Pond during the closure. Unexpectedly, these negative changes occurred in less than two years, despite the lack of anthropogenic impacts. While differences may be a result of natural processes, potential impacts of past and present environmental and anthropogenic stressors should also be considered. Fish abundance and biomass varied considerably at all sites between open- and closed-access periods, making it difficult to establish statistical differences with time. High variability naturally exists in survey data of highly mobile organisms such as fishes. Therefore, it is challenging to infer the relationship between the influence of non-extracting recreational activities and the frequency of habitat use especially at Kalaeloa and Mokuhā.

Sediment characteristics are largely influenced by geographic characteristics and associated natural processes with minimal anthropogenic factors at all inshore sites. Overall, inshore sediment composition and grain-size were similar to results from previously surveyed sites in ‘Āhihi Kīna‘u. Terrigenous material decreased 34-67% between 2008 and 2010 at all sites, especially at Mokuhā. Grain-size was not substantially different between years, yet showed substantial variation among sites.

Inshore temperatures between July 2008 and May 2010 fell within the normal ambient range for all of Hawai‘i’s shallow reefs. No major bleaching from elevated temperature was observed. While a few excessively high temperatures above 28°C were observed at two sites, these were within the range of short-term fluctuation (0.4-0.6% of the time) affected by local climatic conditions and landscape characteristics.

Monitoring at various time scales and frequency would provide further information about changes and the response of inshore biological resources, since recovery times may vary at different sites and exceed two years. While no direct study of trampling and recovery was included, Connell (1997) reviewed 23 long-term studies (>4 years) on disturbance and recovery of coral cover in the Indo-Pacific and Western Atlantic Ocean. Among 65 examples from these studies, 19 examples of recovery were found ranging from one to fourteen years after acute or chronic disturbances in the Indo-Pacific. The average observation period after disturbance for recovered examples was 5.2 years and 12.4 years for non-recovered examples. In Hawai‘i recovery occurred from 6 to 13 years in Kāne‘ohe Bay (Hunter and Evans 1995) while virtually no recovery occurred 13 years after an intense Kona storm off West Hawai‘i in 1980 (Dollar and Tribble 1993). Therefore benthic conditions should be monitored for several years,

especially at *Montipora* Pond, Kanahena, and Kalaeloa, where coral is abundant in very shallow water. Fish monitoring at various temporal scales and at greater frequency would also better capture patterns of habitat utilization by popular resource fishes as well as large charismatic species at representative sites. Environmental variables such as temperature and salinity (as measured by electrical conductivity) would provide an important reference to better understand the effects of natural fluctuations and its influence on benthic conditions at fine spatial scales. Monitoring water quality and nutrients may identify anthropogenic effects on the anchialine pond and adjacent *Montipora* Pond. Identifying groundwater input and hydrologic patterns may provide evidence for presence or absence of connectivity between these ponds.

During this study, there was no strong evidence to indicate that the two-year closure facilitated an increase of fishes or coral cover within the inshore reef community. While the lack of non-extractive recreational activities may not have resulted in an increase of inshore biological resources during the 2-year closure period, it is important to continue long-term monitoring to help detect acute and chronic environmental dynamics for future management measures. ‘Āhihi Kīna‘u NARS has limited local impacts such as overfishing, sedimentation or eutrophication that affect the majority of other sites in the Main Hawaiian Islands. This will help separate the global from the local impacts as they become more apparent. Continuation of seasonal and annual monitoring will provide quantitative data to identify both spatial and temporal changes that will undoubtedly occur with increased temperatures and shifts in ocean chemistry (Gattuso *et al.* 1999; Kleypas *et al.* 1999; Orr *et al.* 2005; Hoegh-Guldberg *et al.* 2007;

Jokiel *et al.* 2008). Adaptive and creative management efforts will be necessary to deal with these changing times.

CHAPTER 3

CHARACTERIZING SPATIAL PATTERNS OF CORAL REEF AT A BROAD SCALE, ‘ĀHIHI KĪNA‘U, MAUI

Introduction

Spatial Patterns in Heterogeneous Landscape

A landscape is often perceived as a spatially heterogeneous area (Turner 1989), involving complex and variable system properties in space and time (Li and Raynolds 1995) at a given scale. General causes of a heterogeneous spatial pattern include local uniqueness such as abiotic variability or unique land use by humans, phase differences of spatial patterns due to disturbances, and dispersal of organisms (Levin 1976; Turner *et al.* 2001). Environmental factors and variation in population dynamics create the spatial pattern within species or communities (Legendre and Legendre 1998). Spatial patterns may be created by both inherent ecological processes among biological communities and/or external, natural and anthropogenic environmental processes in a heterogeneous landscape. Spatial heterogeneity is also a function of scale (Wiens 1989). These processes may operate similarly, differently, or across spatio-temporal scales creating diverse landscapes.

Identifying spatial patterns is a first step to understanding the relationship between spatial heterogeneity and processes. Landscape structure must be identified and quantified in meaningful ways before the interactions between the landscape patterns and ecological processes can be understood (Turner 1989). There are many examples where knowledge of the spatial pattern is applied. These examples are commonly found in environment and natural resource management, and spatial planning. For many years, terrestrial and aquatic ecosystems have been managed with single-resource objectives and

yet multiple resource consequences were present (Risser *et al.* 1984). However, over the last few decades informed, management approaches began emphasizing ecosystem-based systems, integrating multi-resource objectives into decision making. Shifting to complex and adaptive management approaches, it is critical to identify spatial patterns of multiple resource distributions, uses, and their changes. With spatially explicit information, it is possible to assess where management need exists in space, to prioritize allocation of limited resources and efforts to the area of the greatest interest, and to make sound decisions. Pattern identification is the key for the environment and natural resource management, possibly indicating a shift in processes and its geographic extent.

Turner *et al.* (2001) described two primary categories of pattern quantification including landscape metrics and spatial statistics or geostatistics. Common landscape metrics include a proportion of each cover type, relative richness of cover types, diversity and dominance of cover types describing spatial composition. Other landscape metrics, such as contagion, patch area and perimeter, and connectivity, are common measures of spatial configuration. Contagion is a measure of clumpiness while patch area and perimeter describe patch shapes and complexity. Spatial configuration is also referred as spatial structure. Fortin and Dale (2005) presented forms of spatial structures in an ecological context. These forms included gradient, trend, aggregation, clumping, patchness, random, uniform, or over-dispersion that result in levels of spatial dependence. The term ‘spatial dependence’ used by Fortin and Dale (2005) refers to the similarity (or dissimilarity) of response patterns as a function of distances among locations. It implies levels of responses to both external or environmental processes and inherent ecological processes. The inherent processes such as competitions and dispersal of organisms may

result in autocorrelation (i.e., correlation of a variable itself). Legendre and Legendre (1998) also defined two types of spatial structures, autocorrelation and spatial dependence, in specific meaning with statistical context. Autocorrelation referred to components of non-independent errors due to distance between paired observation points. Spatial dependence may be considered as the influence of spatially structured explanatory variables on the response variable which may not be necessarily autocorrelated among observations but manifested in a spatially structured pattern. These explanatory variables with spatial structure are called trends. In this case, the error components are assumed to be independent among observations at various locations. The term ‘spatial structure’, including autocorrelation and spatial dependence, is used following Legendre and Legendre (1998) in subsequent sections.

Spatial Statistical Approach

One way to identify and characterize spatial patterns is to apply spatial statistical analysis. The spatial statistical approach takes the presence of spatial relationships among observations into account. A non-spatial approach does not incorporate presence of spatial structures among observations and these are assumed to be independent. The non-spatial approach is effective in estimating properties when the spatial pattern is homogeneous, and when spatial structures and locations are not of interest. It can also reveal causes, processes, and interactions among factors in manipulative experiments when confounding factors and co-linearity are controlled. In many situations, however, spatial patterns are heterogeneous in a landscape, and observed patterns may have spatial relationships among them. Locations and geographical extent may also be useful

information for those who manage landscapes. Thus the spatial approach can be useful for dealing with the environment and natural resources, revealing spatial structures, estimating and predicting values, and possibly reducing estimated variances by accounting for spatial structures of the environment and resources.

Spatial analysis allows researchers to explore possible explanatory processes that may need to be considered, and to incorporate a spatial and/or additional source of variation as a part of ecological processes (Legendre 1993). It assesses relevant scales for ecological functions and organisms (Turner *et al.* 2001), and estimates value and uncertainty of unsampled locations (Goovaerts 1997). For example, geostatistics is a sub-branch of spatial statistics (Diggle and Ribeiro 2006), offering methods to describe the spatial continuity that is an essential feature of many natural phenomena, and provides adaptations of classical regression techniques to take advantage of this continuity (Isaaks and Strivastava 1989). It has been the primary tool for mining geologists since the 1960's allowing them to estimate spatial structure of minerals and predict their location at an unmeasured position on a surface.

In soil science, the geostatistical approach was used for estimation and prediction of soil property, quality, and infiltration processes (e.g., Delisle 2007; Verger 2008). It can be also used as a tool to modify or improve field sampling designs considering limiting costs and logistics. Yost *et al.* (1993) evaluated geostatistical and soil classification approaches for reducing estimated variances of organic carbon, and developing effective sampling size and locations for the Pearl Harbor recharge area, Oahu. With the geostatistical approach, an estimate of variance was reduced at

maximum sampling distance of 1.2 km while variance estimated by the soil taxonomic approach remained high.

Application of spatial statistics has also been known among other fields of study. Goovaerts (1997) stated that use of geostatistics has been expanded among diverse fields such as mining, petroleum, soil science, oceanography, hydrogeology, remote sensing, and environmental science. It allows one to model the uncertainty of unknown values through the alternative realization that all honor the data and reproduce aspects of the patterns of spatial dependence or other statistics deemed consequential for the problem (Goovaerts 1997). In geography, spatial statistics has been widely applied. Anselin (2006) reviewed the historic development and applications of spatial statistics in regional sciences and economics, namely spatial econometrics, focusing on the spatial relationships among socio-geographic and environmental variables. Spatial statistics has also been of prime interest to ecologists, because most ecological phenomena investigated by sampling geographic space are structured by forces that have spatial components (Legendre and Legendre 1998). These spatial analyses have been applied to studying landscapes (e.g., Sales *et al.* 2007) as well as seascapes (e.g., Petitgas 1996, Pittman *et al.* 2007) indicating its potential and usefulness in the marine environment.

Mapping is an integral part of quantifying landscape (Gustafson 1998) and spatial statistics are valuable for the analysis and visual representation of the outcome. For example, geostatistics commonly employ the spatial prediction and interpolation method called ‘kriging’. Kriging was named after a South African mining engineer, D.G. Krige by Matheron who was one of actual contributors to the development of this method in the early 1960’s (Cressie 1993). It is known as the best single unbiased linear local

estimation model from existing data incorporating spatial structure. Surfaces of kriged estimates and uncertainty for un-sampled locations are produced using GIS software and spatial statistical packages. These statistical outputs can be further used in spatial modeling, stochastic simulations, and visual representations which are potentially useful for management applications.

Characterizing Spatial Patterns of Crustose Coralline Algae and Corals at ‘Āhihi Kīna‘u

Application of spatial analysis is relevant to Hawai‘i’s sub-tidal seascapes. Crustose coralline algae and coral are abundant and key functional groups constituting coral reef seascapes, particularly in ‘Āhihi Kīna‘u where the abundance of fleshy macroalgae is < 1% (Rodgers *et al.* 2009). These organisms are ecosystem engineers, they provide valuable ecosystem services and goods, and maintain integrity of marine resources and seascapes. CCA is a dominant calcifying organism that plays a major role in cementing carbonates and providing a framework for coral reefs (Adey 1998), and a preferred settlement substrate and natural inducer for larval metamorphosis of marine invertebrates including corals (Morse *et al.* 1988; Heyward and Negri 1999). CCA is found to be abundant on the reef when herbivores are present and enriched with nutrients (Smith *et al.* 2001; 2010). CCA therefore has an important role indicating current states of processes on the reef community structure. Corals significantly influence habitat complexity and availability for reef fishes (Friedlander *et al.* 2003; DeMartini *et al.* 2010) supporting food webs and biodiversity. They are also sentinels for identifying environmental change and degradation since they require specific water quality, temperature, and light conditions for survival (Jokiel and Coles 1990; Jokiel 2006, 2008).

These calcified organisms should be monitored for changes in their patterns, as shifts in temperature and ocean chemistry occur (Kleypas *et al.* 1999; Orr *et al.* 2005; Hoegh-Guldberg *et al.* 2007; Jokiel *et al.* 2008).

Scleractinian corals have been researched for over a half a century. Yet, few studies quantify how random or non-random their distributions are over space. If spatial patterns are discussed at all, they tend to be qualitative or implicit. Patterns of distributions are scale dependent. However, it is not very often that a scale of operation or relevant scale for the organism is addressed. Spatial characteristics and scale are basic but important issues to link to the dominant processes affecting the pattern in the context of conservation effort and management measures. In addition, explicit quantitative spatial information may result in additional or new knowledge that could be integrated in further exploration, hypothesis development, or ecosystem models of the coastal environment.

Characterizing spatial patterns of sub-tidal benthic cover such as CCA, corals, and other benthic organisms, however, can be challenging at a scale of around 10 km². In most cases, detailed patterns of benthic cover and distributions of organisms are primarily determined by *in-situ* visual estimates using a quadrat or through photographic images. While this sampling technique provides high spatial resolution data and is suited for fine-scale replication, it requires high labor input, equipment, extensive support, and substantial time commitments. These logistical challenges add up to a high total cost as the area of interest increases. Broadband multispectral satellite imagery is useful for identifying geomorphological patterns for coarse to intermediate habitat classes (Green *et al.* 1996; 2000) at state-wide or regional scales, yet it lacks high spectral resolution and

may not be the best for obtaining detailed ecological information (e.g., Mumby *et al.* 1997; Hochberg and Atkinson 2003; Mumby *et al.* 2004b). Airborne hyper- or multispectral imagers such as the Compact Airborne Spectrographic Imager (CASI) are attractive options for discriminating benthic types with high spectral resolution and overall accuracy (Mumby *et al.* 1997; Hochberg and Atkinson 2003; Mumby *et al.* 2004b). The total cost of acquisition and processing of CASI were estimated to be £34,000-57,000 (approximately \$54,000-90,000 U.S.) for covering 150 km² about a decade ago (Green *et al.* 2000). While CASI is relatively cost effective and has been successfully used for detailed benthic cover classification in Caribbean reefs (Mumby *et al.* 1997; Green *et al.* 2000), it is not a common application for Hawaiian reefs employed by management agencies. If a reasonable number of comparable samples is readily available in the area, these can be employed in spatial statistical analysis for characterizing spatial patterns of functional benthos at a local scale of around 10 km².

Objectives

Spatial patterns of coral and CCA cover in ‘Āhihi Kīna‘u were examined at the areal scale of approximately 10 km². The study aimed to characterize patterns of coral and CCA distributions and effects of potential seascape predictors using a spatial statistical approach. Study questions included:

- Are coral and CCA spatial distributions random or structured?
- Is there a scale that is associated with their distributions, abundance, or spatial structure?
- What external factors affect spatial patterns of coral and CCA?

The objectives are 1) to identify potential spatial structure (i.e., autocorrelation and spatial dependence) within each cover type, 2) to determine the representative statistical models that may characterize variability and estimate parameters, and 3) to produce prediction maps of CCA and coral distributions.

Materials and Methods

Study Area

The study area focused on nearshore reefs of south Maui, encompassing Maluaka point, approximately 0.7 km north of Pu‘uola‘i through ‘Āhihi Bay, ‘Āhihi Kīna‘u Natural Area Reserve System (NARS), Keoni‘ō‘io (Le Perouse Bay), Kamanamana to Pōhakueaea (Fig. 3.1).

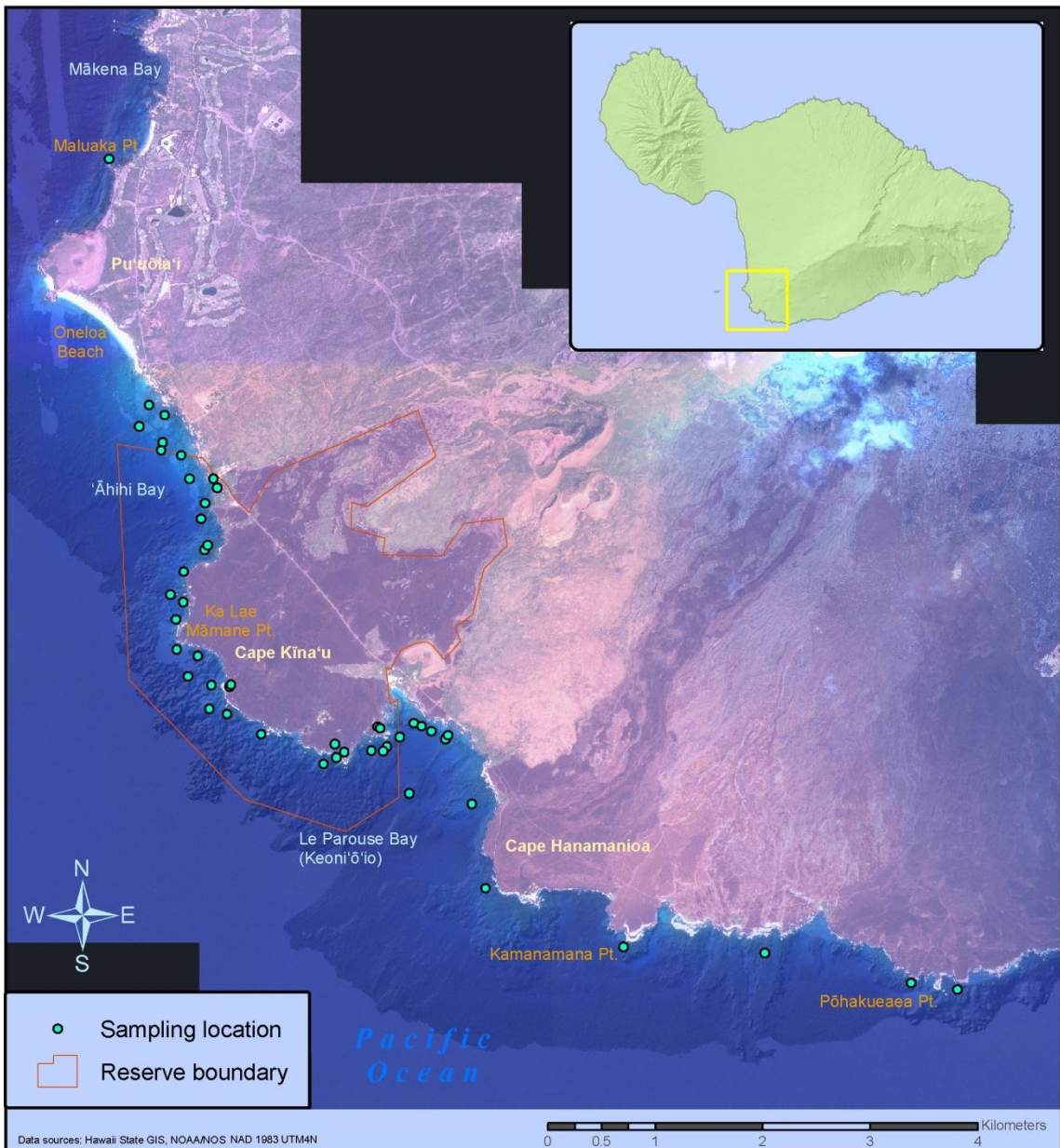


Fig. 3.1 Survey sites, south Maui, 2007 and 2009.

In general, the terrestrial study area experiences little human use due to limited road access and topography. Geologically, the area is dominated by basalts originating from the Hāna Volcanic series (Stearns 1985; Macdonald *et al.* 1990). Surficial basalts were created during the Holocene and Pleistocene periods, with four distinct geologic ages, ranging from 50,000 to less than 1500 years old (Sherrod *et al.* 2007). Northern flows from Pu‘uola‘i to Maluaka point are estimated to be 30,000-50,000 years old, while Cape Kīna‘u, Cape Hanamanioa, and Pōhakueaea point were created by the latest volcanic activity, estimated to be less than 1500 years old (Sherrod *et al.* 2007).

Topography of older shorelines (Pu‘uola‘i, ‘Āhihi, Keoni‘ō‘io, and Kamanamana) are characterized by low outcrops, talus, benches, and sea cliffs less than 10 m high (AECOS 1979). Cape Kīna‘u, Cape Hanamanioa, and Pōhakueaea have more complex shorelines with medium to high sea cliffs, ranging from approximately 3 m to greater than 10 m (AECOS 1979).

Vegetation is abundant along shorelines from Pu‘uola‘i through ‘Āhihi and Keoni‘ō‘io, while the relatively rough young lava flows host very little vegetation at Cape Kīna‘u and Cape Hanamanioa. The southeastern shorelines encompass four sparsely vegetated points and gullies. Recent remote sensing imagery (Battista *et al.* 2007) reveals changes in land cover and land use north of Pu‘uola‘i. Resorts and golf courses are obvious in the recent imagery while the shoreline was primarily covered by vegetation in 1979 (AECOS 1979).

The southeastern shorelines and reefs between Ka Lae Māmane and Pōhakueaea, are exposed to strong tradewinds funneling through the Alenuihaha Channel, between the Kohala Mountains and around the south flank of Mount Haleakalā. Annual prevalence of

the northeast tradewinds is 65% (Haraguchi 1979). According to Haraguchi (1979), moderate tradewind speed range from approximately 30 to 37 km h⁻¹ in the southeastern position of the study while the prevailing wind speed is 15-20 km h⁻¹ in the northwestern position of the study area. The sea is often rough in the southeastern positon of the study area due to waves generated by prevailing tradewinds.

Data

Coral and CCA cover were measured at 47 survey sites (Fig. 3.1). Predictor variables measured included sediment composition (proportion of organic materials) and grain-size (proportions of fine/very fine sands and silt/clay), topographic relief (rugosity), and spatial coordinates (northing and easting) obtained from the field sampling. These variables were chosen based on prior knowledge from past studies (e.g., Jokiel *et al.* 2004). Additional landscape data of interest included slope and aspect as covariates. These were generated from bathymetric data by the airborne Scanning Hydrographic Operational Airborne Lidar Survey (SHOALS) Light Detecting and Ranging (LIDAR) system of the U.S. Army Corps Engineering in 1999-2000 (Irish 2000).

General Field Sampling Protocol

Field sampling was conducted on nearshore reefs of the study area in 2007 and 2009. Data were collected by SCUBA diving and snorkeling, using the Rapid Assessment Techniques (RAT) designed by CRAMP (Jokiel *et al.* 2004; Rodgers 2005; Rodgers *et al.* 2009).

Prior to field sampling, geographic positions of sampling sites were randomly

generated within the domain defined with selection criteria. The criteria included stratified depths (1 m, 3 m, 5 m, and 10 m) with a maximum of 12 m, and habitat with >10% coral cover. The domain was defined using the SHOALS LIDAR data and NOAA benthic habitat map (Battista *et al.* 2007) in ArcGIS to meet criteria. The ‘Generate Random Points’ tool of Hawth’s Analysis Tools extension (Beyer 2004) was used for generating random geographic positions within the domain.

In the field, starting positions were determined using a Garmin GPSMAP 76CSx and 76, providing less than \pm 3 m accuracy when Wide Area Augmentation System (WAAS) was enabled. Once a predetermined site was located by the GPS unit, a Pelican float was immediately deployed for visual marking of the starting point for each transect. In addition, physical features of transect points were qualitatively described and documented for reference.

Shallow inshore reefs were accessed from the shoreline while outer reefs were accessed by boat. Actual sampling depths ranged between 1 and 9.4 m. Generally, 25 m-long transect lines were used at each site for a concurrent fish survey. Benthic and topographical relief (rugosity) data were obtained from the first 10 m of each transect. Bulk sediment was collected at each site. Detailed field sampling methods for each data type are described in the following sections.

Benthic Sampling

Approximately 20 high resolution digital images were taken along a 10 m transect using a Panasonic FX35 zoom digital camera within a Panasonic MCFX35 underwater housing, or Olympus 5050 zoom digital camera with an Olympus PT050 underwater

housing for assessing the characteristics of fine scale benthic seascapes structures. The Panasonic camera was assembled with an aluminum monopod frame, 0.5 m from the substrate for use in shallow inshore reefs providing a 50 x 69 cm image. To obtain the same image extent, the Olympus system required a 0.7 m-long monopod. A 6-cm bar on the monopod base serves as a measurement scale.

The software program PhotoGrid (Bird 2001) was used for quantifying percent cover of biotic functional groups and abiotic substrate. Twenty non-overlapping images were imported into PhotoGrid where 50 randomly selected points were displayed onto each image. Processed data were exported as a comma separated value (CSV) file. These files were organized and managed in Microsoft Office Excel 2007, and imported into Microsoft Access XP for database management.

Topographic Relief (Rugosity) and Depth

Rugosity was measured to determine topographical relief and spatial complexity. A 15 m chain marked at 1 m intervals with 1.3 cm links was draped along the length of the transect (10 m) following the bottom contours. An index of rugosity, the ratio of the reef contour distance as measured by the chain length to the horizontal linear distance, was calculated for each transect (McCormick 1994). Hand-held and vessel mounted electronic depth sounders were also used for estimating depth at sites deeper than 1.5 m. Approximate depth was estimated using the 0.5 m-monopod and a transect line for extremely shallow areas between 0.5 and 1.0 m.

Sediment Sampling

Replicate sediment samples were collected at each of four sites in both 2008 and 2010. Three samples were collected at Kanahena Cove, and two samples were each collected at Kalaeloa, Mokuhā, and *Montipora* Pond annually. Each Fisher brand 9 x 18 cm sample bag was filled with approximately 500 cm³ of sediment in the field. Composition and grain-size of sediment were determined following sedimentological methods described in Rodgers (2005). Sediment in each bag was thoroughly mixed for subsequent processing and analysis. For each sample percentages of sediment composition and grain-size were calculated using Microsoft Excel. Results were summarized in descriptive statistics.

Sediment Composition

Terrigenous and organic matter was partitioned from marine carbonates by incinerating them at different temperatures (Dean 1974; Parker 1983; Bengtsson and Enell 1986; Craft *et al.* 1991; Sutherland 1998; Heiri *et al.* 2001). Approximately 10 g of sediment was finely ground using a mortar and pestle, prior to determination of inorganic-organic carbon fractions. Subsamples were taken from each replicate to reduce variability. These were dried in crucibles to remove moisture for 10 h at 100 °C then placed in a desiccator and weighed. Samples were then incinerated in a muffle furnace for 12 h at 500 °C to remove organic matter. Following incineration, samples were placed in a desiccator and weighed. For removal of carbonate material, samples were again placed in a muffle furnace for 2 h at 1000°C. These were cooled in a desiccator and weighed. The percent loss on ignition (LOI) was calculated based on mass changes

at each step. LOI₅₀₀ was used as an index of organic matter and LOI₁₀₀₀ was primarily an index of the calcium carbonate (CaCO₃).

Sediment Grain-size

Subsamples were taken from each of two or three replicates collected from each site. These were wet sieved (McManus 1988) using standard brass sieves. Mesh sizes included 2.8 mm, 500 µm, 250 µm, and 63 µm (USA Standard Testing Sieve: A.S.T.M.E.-11 specifications). A brass catch pan collected the silt/clay sized fraction (<63 µm). Five size fractions were determined: granule (> 2.8 mm), very coarse and coarse sand (500 µm-2.8 mm), medium sand (250-500 µm), fine and very fine sand (63-250 µm), and silt/clay (<63 µm) in accordance with the Wentworth scale (Folk 1974). Each size fraction was filtered through pre-weighed Whatman 114 wet strength filters and air-dried. These were then weighed on three separate days to determine the proportion of each size fraction. Extremely large pebbles or cobbles were removed before sieving to minimize variability and skewed weights.

Data and Statistical Analysis

Figure 3.2 shows general steps of data and statistical analysis performed in this study. Benthic data were analyzed for spatial structure and the relationships between their seascapes predictors using a general linear regression and geostatistical approaches. Following the initial exploratory data analysis, response and explanatory variables were transformed to meet assumptions of normal distributions for subsequent statistical analyses. Proportions of CCA and corals were arcsine-square root transformed. Organic

material and silt were arcsine-quad root transformed, and fine sand was arcsine-cube root transformed. Statistical and spatial analyses were performed by Minitab 15.1 (Minitab Inc. 2007), ArcGIS with Spatial Statistics, and Geostatistical Analyst extensions (ESRI 2003), GeoDa (Anselin *et al.* 2006), and R using “geoR” package (Ribeiro and Diggle 2001).

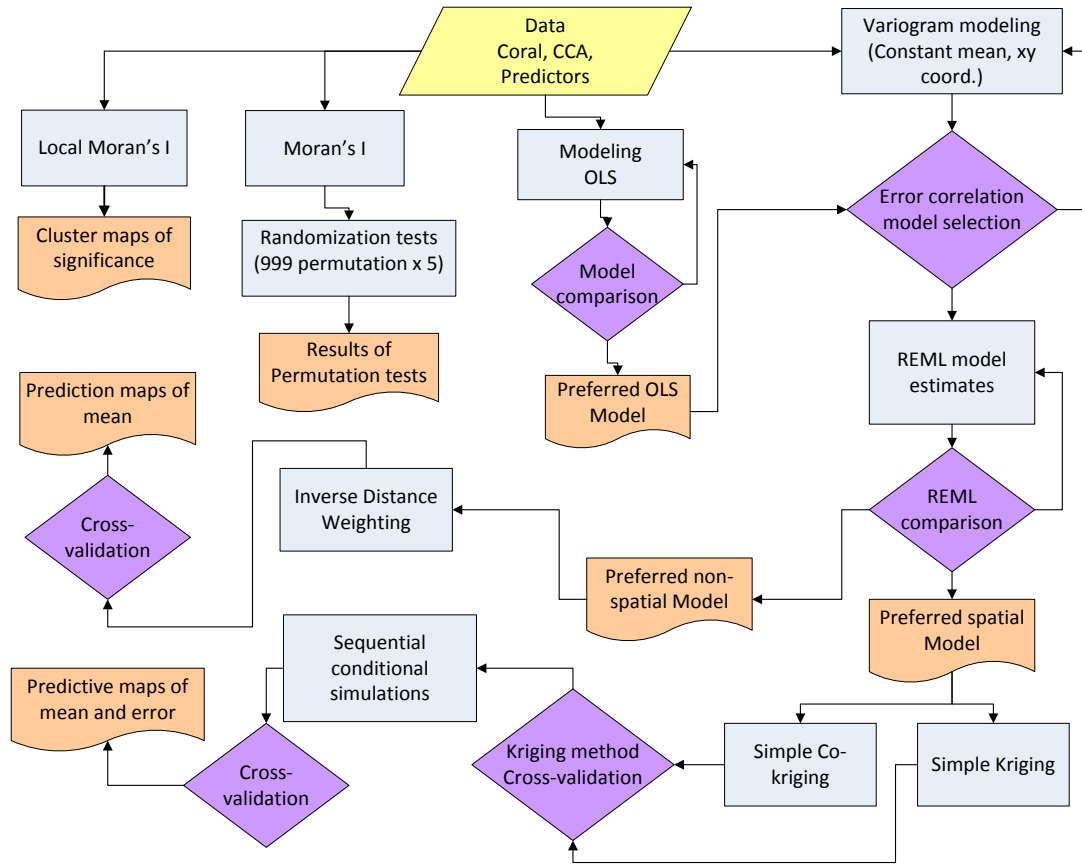


Fig. 3.2. A flowchart of data and statistical analysis. OLS = ordinary least square regression; REML= the Restricted Maximum Likelihood.

Analysis of Spatial Structures

First, assuming stationarity (constant mean and/or variance at all locations), Moran's *I* statistics (Moran 1950) were calculated for the response variables to determine

whether autocorrelation was present using inverse distance weighting and neighborhood weights, following (Anselin 1995):

$$I = \frac{\frac{n}{S_0} \sum_i \sum_j w_{ij} z_i z_j}{\sum_i z_i^2}$$

where n is number of observations, S_0 is the sum of all weights, w_{ij} is the weighting between observation i and j , z_i , z_j are deviations from the mean for observation at site i and j . A possible range of Moran's I statistics is generally ± 1.0 where 0 indicates no autocorrelation (spatial randomness). However, Moran's I values greater than 1 or lesser than -1 may occur occasionally (Legendre and Legendre 1998). Significance of Moran's I statistics was tested by a randomization test under a null hypothesis stating random spatial distribution of observed values. A significantly positive or negative value indicates non-random spatial distribution. The positive I statistic indicates the presence of autocorrelation in a region while the negative I statistic indicates that negative autocorrelation or dispersion exists. Five randomization tests of Moran's I statistics were conducted with 999 permutations for assessing consistency of resultant p -values. Randomization tests were repeated for each of five different neighborhood weights.

Presence of local spatial clusters was also examined on maps based on Local Morans' I statistics which is a type of a Local Indicator of Spatial Association (LISA) suggested by Anselin (1995). A LISA is defined as any statistic that identifies spatial clusters of similar values, and the sum of all LISAs is proportional to a global statistic of spatial association. While Morans' I is a global statistic and may average or smooth local variations, Local Morans' I indicates local clustering of similar values and may be used

to assess the influence of individual locations on the magnitude of the global statistic as an outlier (Anselin 1995). It is defined as:

$$I_i = z_i \sum_j w_{ij} z_j$$

where w_{ij} is the weighting between site i and j , z_i , z_j are deviations from the mean, and the summation over j includes only neighboring values.

Sample semivariograms, a graphical representation of semivariance, were also examined for the presence of possible spatial structure. Semivariance is a measure of the average dissimilarity between data separated by lag distance h . Semivariances were calculated following (Goovaerts 1997):

$$\gamma(h) = \frac{1}{2N(h)} \sum_{i=1}^{N(h)} [z(x_i) - z(x_i + h)]^2$$

where $\gamma(h)$ is the semivariance for separation distance or lag h , $N(h)$ is the number of pairs of measured values separated by lag distance h , $z(x_i)$ is a datum value at site i , and $z(x_i + h)$ is a datum value at site $i + h$.

Components of semivariograms include nugget, range, and sill (Fig. 3.3b and c). A nugget effect implies a presence of variability (i.e., non-zero value) for $h = 0$, the origin of semivariogram, while the theoretical expectation is $\gamma(0) = 0$. It reflects fine scale variations that occur at less than the closest paired-distance of sampling points, measurement errors, or combination of these. Range is the distance at which the spatial correlation no longer exists. Sill is the asymptotic plateau of the semivariogram and represents the total observed variance.

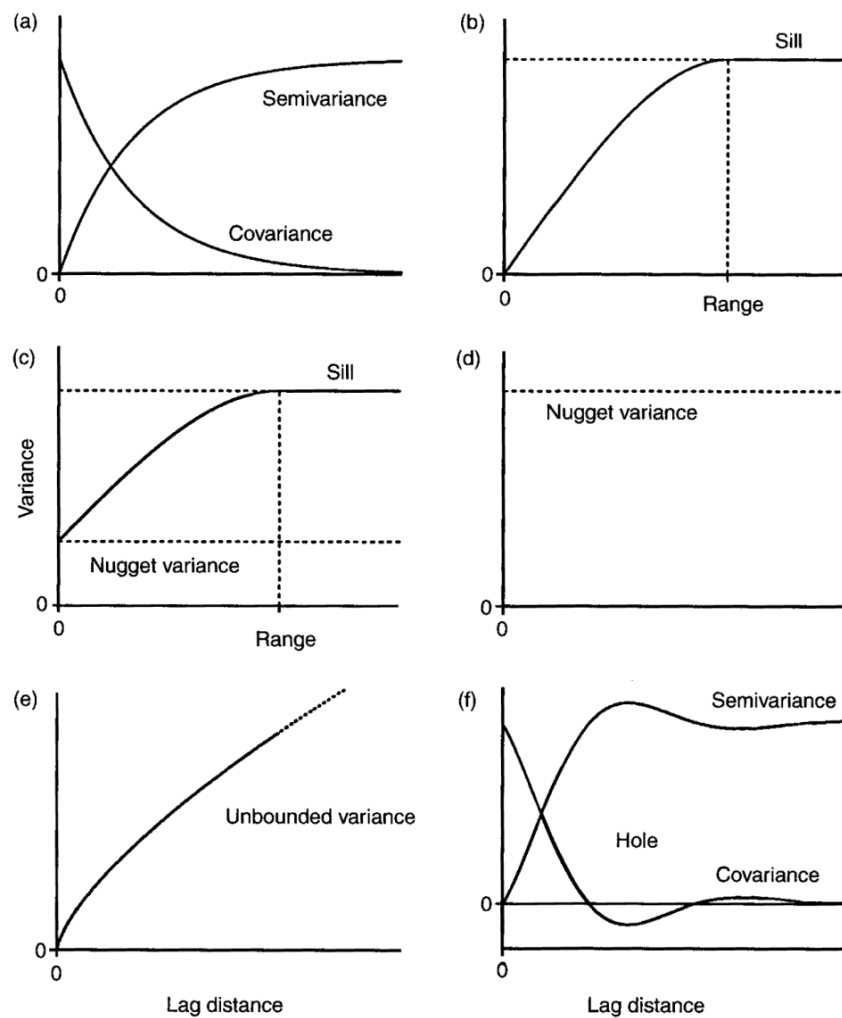


Fig. 3.3. Theoretical functions for spatial correlation: a) typical variogram and equivalent covariance function; b) bounded variogram showing the sill and range; c) bounded variogram with a nugget variance; d) pure nugget variogram; e) unbounded variogram; f) variogram and covariance function illustrating the hole effect (Webster and Oliver 2007).

Alternatively, the covariance function and correlation statistics can be measured to assess a spatial structure in terms of similarity for lag h . Assuming second-order stationarity, in which the probability of the mean and variance are constant at all locations, the covariance function is expressed following (Webster and Oliver 2007):

$$C(h) = cov[Z(x), z(x + h)]$$

where $C(h)$ is the covariance function of lag h . Autocorrelation is then defined as:

$$\rho(h) = C(h)/C(0)$$

where $C(0)$ is the covariance at lag 0, and corresponds to σ^2 . When second-order stationarity is assumed, the covariance and semivariogram $\gamma(h)$ are equivalent, and the relationship is:

$$\gamma(h) = C(0) - C(h)$$

shown in Fig. 3.3a. The standardized semivariance $\gamma(h)$ can be also expressed with the autocorrelation coefficient $\rho(h)$ following:

$$\gamma(h) = \sigma^2\{1 - \rho(h)\}$$

When a nugget effect is present, the sill is a sum of the nugget and additional variance from spatial structure that is a function of range and distance. Thus the sill corresponds to the total observed variance $\tau^2 + \sigma^2$, where τ^2 is a nugget variance and σ^2 is the covariance with a distance function. With presence of a nugget, σ^2 is equivalent to a semivariance value termed as a partial sill in geostatistics. The range relates to a correlation ρ , the spatially structured component.

Anisotropy (directional patterns of covariance parameters) and stationarity were also examined from sample variograms. Lag size, number of lags, and maximum pair-wise distance for the variogram analysis were determined from distribution frequency of pair-wise distance classes attaining an adequate number of pairs in each class for precision. A minimum of 30 paired distances is suggested for computing a semivariogram value (SAS Institute Inc., 1999) for each distance class.

Model Selection and Comparison

Model selections and comparisons were conducted in two phases (Fig. 3.2). First, ordinary least squares (OLS) regression models were fit with fixed explanatory variables to identify candidate models assuming independent errors. These follow a general form of linear model, $Y = X\beta + \varepsilon$ where Y is a vector of the response variable, β is a vector of coefficients, X is a matrix of fixed predictor variables, and a remaining error component is ε when $\sim N(0, \sigma^2)$. The model selection was undertaken with “best subsets” procedure using selection criteria (see Kutner *et al.* 2005). These criteria included Mallow’s C_p , adjusted coefficient of determination (adjusted R^2), and root-mean-squared error (RMSE). Subsequent diagnostics for influential observations and multi-collinearity were also examined upon selection.

Second, the linear models were compared in terms of independent and spatially correlated errors. The error components ε of the linear model $Y = X\beta + \varepsilon$, included matrices of covariance $\sigma^2 [f(d_{ij})]$ where $f(d_{ij})$ is a correlation function based on the distance between site i and j in the spatial model. An independent error model has a conventional matrix, $\sigma^2 I$ assuming equal variances and no correlation. Thus these were referred to as non-spatial models in latter sections. Common correlation functions, including exponential, Gaussian, spherical, and wave or hole effect, were examined. For example, using the linear mixed model approach, the variance-covariance structure with a nugget and exponential function is written as follows (Littell *et al.* 2006):

$$\begin{aligned}Var[\varepsilon_i] &= \sigma^2 + \sigma_n^2 \\Cov[\varepsilon_i, \varepsilon_j] &= \sigma^2 [f(d_{ij})] \\f(d_{ij}) &= \exp(-d_{ij}/\rho)\end{aligned}$$

Similarly, semivariance $\gamma(h)$ with a nugget using the exponential function could be expressed as (Webster and Oliver 2007):

$$\gamma(h) = c_0 + c_1 \left\{ 1 - \exp\left(-\frac{h}{r}\right) \right\}$$

where c_0 is the nugget variance, c_1 is the partial sill, r is a distance parameter defining the spatial extent, consisting of the total observed variance (sill).

Four basic types of linear models were specified: 1) constant mean, 2) first-order spatial trend, 3) seascape predictors selected in OLS model selection, and 4) the first-order spatial trend and seascape predictors in OLS model selection. The constant mean and the first-order trend models were fit using various correlation functions (e.g., exponential and spherical) and compared to non-spatial models within each model type. Models specified with additional trends or predictors were fitted using a selected correlation function. Errors of these non-stationary, trend models were fitted accounting for effects of predictors and geometric anisotropy to see if the adjustment for such effects would further improve a model. The best-fitting theoretical variogram (or correlation function) was initially explored and determined for spatial models based on cross-validation in Geostatistical Analyst (ESRI 2003). Initial parameter estimates were also obtained in Geostatistical Analyst.

The restricted maximum likelihood (REML) approach was subsequently used for obtaining final estimates of parameters, Akaike Information Criterion (AIC), and log-likelihood values using an R-package (R Development Core Team 2011) called ‘geoR’ (Diggle and Ribeiro 2007). The maximum likelihood methods are based on the probability distribution density. The methods estimate parameters that correspond to the greatest value of likelihood function on the density curve. If the parameter value is consistent with the sample data, the densities will be relatively large and correspond to a large value of likelihood function, while it will be small if the parameter is not consistent with the data (Kunter *et al.* 2005). The REML approach is commonly used because it results in unbiased estimates of parameters as it accounts for the lost degrees of freedom from estimating fixed effects in β (West *et al.* 2007). REML estimates of parameters could be also obtained through the linear mixed model framework (see Littell *et al.* 2006; Pinheiro and Bates 2009). It allows one to incorporate a complex matrix of different variances,

covariances, and correlation values, not limited by the identity matrix as a general linear model assumes.

AIC and log-likelihood values were used as comparison criteria between spatial and non-spatial models as well as among various spatial models. Small AIC and large log-likelihood values indicate a preferred model. Spatial and non-spatial models were also evaluated by the likelihood ratio test (LRT) within each model type. In LRT, the likelihood function value of the full model is compared to the likelihood function value of the reduced model which contains a subset of parameters in the full model. The ratio of these values is a test statistic, denoted as G^2 , and it was calculated following (Kunter *et al.* 2005):

$$G^2 = -2\log_e \left[\frac{L(R)}{L(F)} \right] = -2[\log_e L(R) - \log_e L(F)]$$

where $L(R)$ is a likelihood function value for the reduced model and $L(F)$ is a likelihood function value for the full model. The null hypothesis states that the reduced model fits data just as same as the full model does. Under the null hypothesis, G^2 follows an approximate χ^2 distribution with degrees of freedom equal to number of parameters in the full model minus the number of parameters in the reduced model. A large G^2 value with small degrees of freedom will result in rejecting the null hypothesis.

While the OLS models in the former subsection estimated coefficient parameters for slope and predictors, spatial models required additional parameters to be estimated for spatial structures. Additional estimates included range (spatial correlation), partial sill (variance excluding residual variance), nugget (residual) variance, and anisotropic angle for transformation. Parameter estimates were obtained for characterization of spatial patterns. Estimates included range, partial sill, nugget variance, and anisotropic transformation angles for observed response variables and the residuals.

Visual Representation of Predicted Values

To describe spatial distributions of coral and CCA, predicted values were interpolated and visually represented as continuous surfaces on maps. Interpolation methods were evaluated and applied based on results from the preceding model selection processes and estimated parameters. ‘Inverse distance weighting’ method (IDW), a deterministic local interpolator, was applied when a non-spatial model was selected for prediction. Root-mean-squared prediction errors (RMSPE) were compared for determining the best neighborhood search method and settings for IDW. ‘Kriging’ was applied if spatial models were selected predicting a response variable at unsampled locations accounting for spatial structure. A kriging surface provides the best local estimate from one realization. A kriging surface was further employed in the sequential Gaussian conditional simulation for obtaining global estimates with characteristics of kriging’s statistical properties through randomly simulated multiple realizations. Unlike kriging, a stochastic simulation, such as the sequential Gaussian conditional simulation, allows one to assess probabilistic spatial variations in predicted mean and error values from multiple realizations. Moreover, kriging tends to overestimate smaller values and underestimate larger values than the average (Goovaerts 1997; Webster and Oliver 2007). To conduct the conditional simulations, the data were first de-trended, de-clustered, and normal-score transformed to fulfill kriging assumptions. The data were then fitted to the variograms based on the results of preceeded model selections and interpolated by simple kriging or co-kriging. Cross-validation statistics, including mean prediction error (MPE), RMSPE, average kriging standard error (AKSE), mean standardized prediction error (MSPE), root-mean standardized prediction error (RMSTDPE) were compared for selecting the final kriging estimates. The selected kriging surface was subject to the conditional simulations producing a final map for characterizing the spatial distributions. Four trials of the conditional simulations were conducted with a different number of realizations. Number of realizations included 5, 100, 500, and 1000. The differences in descriptive statistics

were assessed to select the most representative map. All interpolation methods were conducted by ArcGIS with Geostatistical Analyst extensions (ESRI).

Results

Total number of sampling points were 47 within the northing (min. 2277249, max. 2284973) and easting coordinates (min. 766068.3 , max. 773966.1) (Fig. 3.4 and 3.5). The minimum and maximum neighborhood distance included 21.7 and 11047 m averaging 272 m. High frequency of paired distance distribution occurred approximately between 22 and 4000 m (Fig. 3.6). Lag size of 200 m, lag numbers of 21, and maximum lag distance of 4000 m provided over 30 paired points in each distance class. Table 3.1 shows the overall descriptive summary of raw response variables.

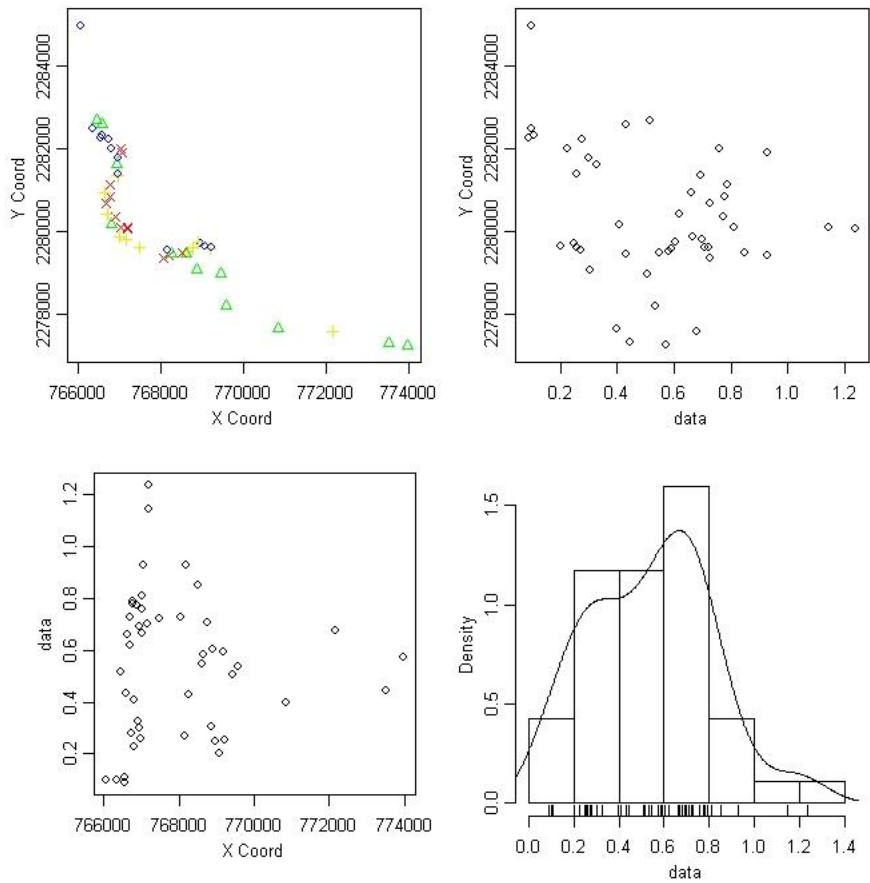


Fig. 3.4. Scatterplots of a) sampling sites in Y (N-S) and X (E-W) coordinates. Blue circles (1st quartile), green triangles (2nd quartile), yellow vertical crosses (3rd quartile) and red diagonal crosses (4th quartile) correspond to the quartiles of the empirical distribution of measured values (Diggle and Ribeiro 2007). b) coralline algae cover against Y coordinate, c) crustose coralline algae cover against X coordinate, d) histogram of transformed mean proportion of coralline algae.

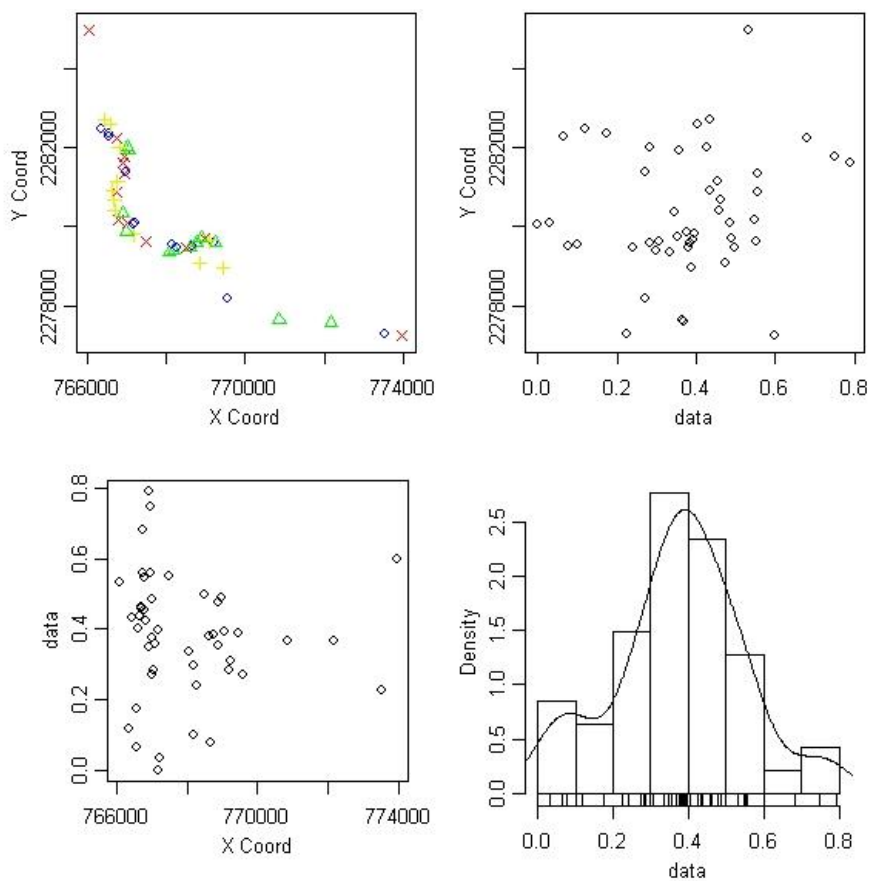


Fig. 3.5. Scatterplots of a) sampling sites in Y (N-S) and X (E-W) coordinates. Blue circles (1st quartile), green triangles (2nd quartile), yellow vertical crosses (3rd quartile) and red diagonal crosses (4th quartile) correspond to the quartiles of the empirical distribution of measured values (Diggle and Ribeiro 2007). b) coral cover against Y coordinate, c) coral cover against X coordinate, d) histogram of transformed mean proportion of corals.

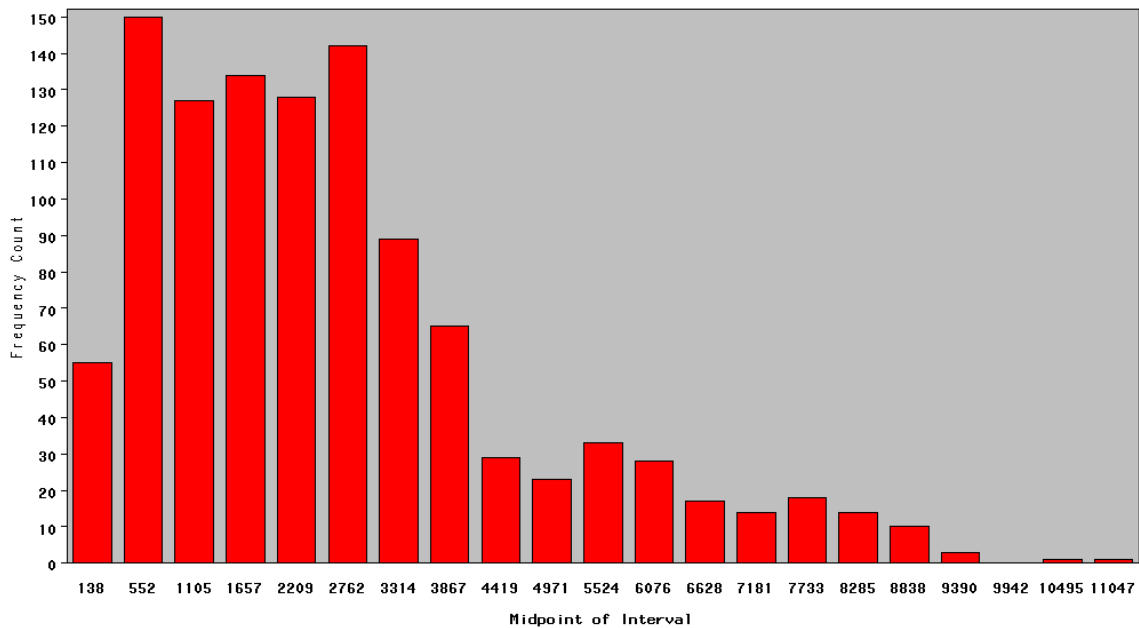


Fig. 3.6. Distribution of pairwise distances among 47 sampling sites. Distance is in meters.

Table 3.1. Descriptive statistics of crustose coralline algae and coral cover proportions.

Variable	Mean	SE Mean	Min	Q1	Median	Q3	Max
Coralline algae	0.296	0.0320	0.0080	0.0880	0.292	0.442	0.892
Coral	0.158	0.0168	0.0000	0.0780	0.140	0.218	0.506

Analysis of Spatial Structures

Based on inverse distance weighting, observed Moran's *I* statistic was 0.2800 ± 0.005 ($p < 0.001$) for CCA and 0.0982 ± 0.005 ($p = 0.093$) for corals while the expected value was -0.0217.

Results of randomization tests are summarized for CCA (Table 3.2) and corals (Table 3.3).

Resultant *p*-values from five randomization tests were statistically significant for CCA indicating the presence of spatial structure. The *p*-values from five randomization tests for CCA were stable

when number of neighborhoods was less than 20. The p -values were slightly unstable when 30 neighborhoods were used. All randomization tests were statistically not significant at $\alpha = 0.05$ for corals using the range of k-neighborhood values.

Table 3.2. Results of randomization tests for mean coralline algae cover. k = number of neighborhoods included; I_o = Global Moran's I statistic, p = p -value calculated for the 5th randomization test.

k	I_o	p
3	0.407	0.001
5	0.3563	0.001
10	0.2382	0.001
20	0.1077	<0.01
30	0.0061	0.05

Table 3.3. Results of randomization tests for mean coral cover. k = number of neighborhoods included; I_o = Global Moran's I statistic, p = p -value calculated from 5th randomization test.

k	I_o	p
3	0.0670	0.192
5	-0.0162	0.589
10	-0.0180	0.591
20	0.0170	0.104
30	-0.0253	0.485

Significance and cluster maps for CCA (Fig. 3.7 and 3.8), plotted from local Moran's I statistics, indicated similar values (shown by different colors) at sampling sites. These clusters indicated a presence of local spatial structure. Similar values were observed in the north-west direction, starting near the southern-most site at Cape Kīnau (Fig. 3.7). High proportions of CCA were clustered near the southern-most site at Cape Kīnau while low proportions were clustered at the northern most ‘Āhihi Bay area (Fig. 3.8).

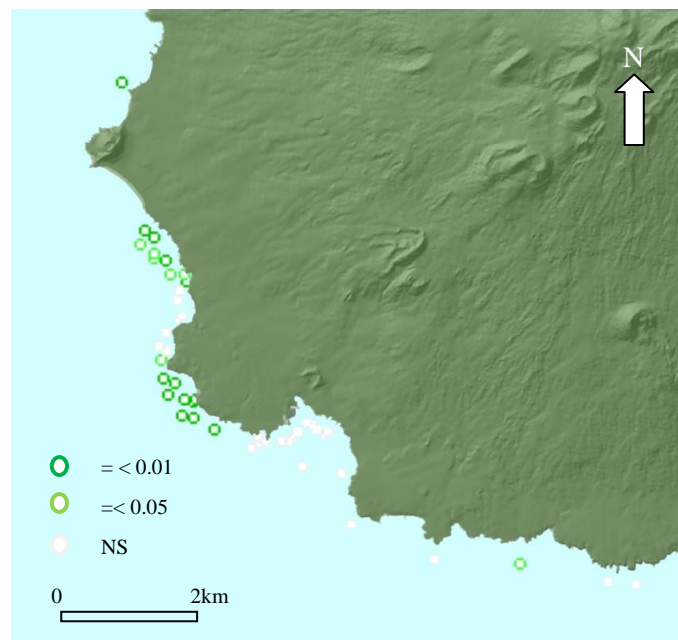


Fig. 3.7. A significance map of similarity for coralline algae cover in proportion based on local Moran's I statistics using $k = 10$. Dark green symbols indicate sites with $p =$ or < 0.01 while light green symbols indicate sites with $p =$ or < 0.05 . NS = not significant.

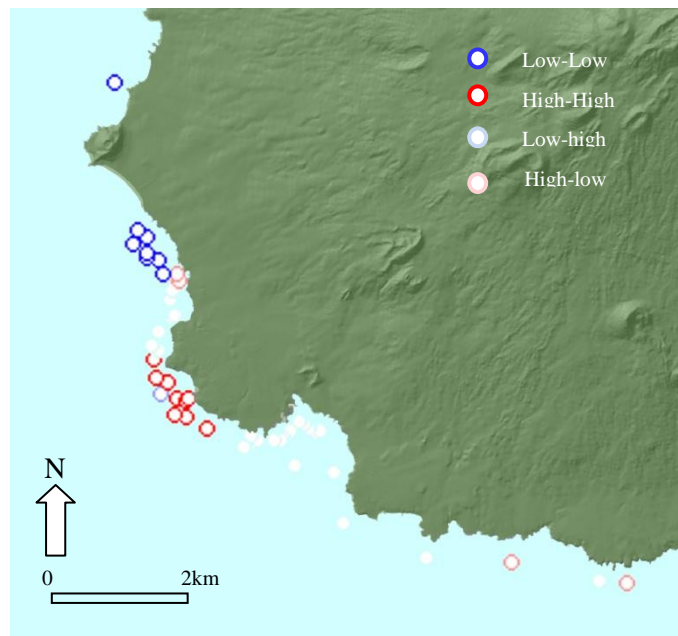


Fig. 3.8. A map of similarity cluster types for crustose coralline algae cover in proportion based on local Moran's I statistics using $k = 10$. Dark red symbols indicate sites surrounded by similar high values while dark blue symbols indicate sites surrounded by similar low values. Light red and light blue symbols are outliers indicating high values surrounded by low and low surrounded by high.

A cluster of similar coral proportions existed at the northwestern corner of Cape Kīnau (Fig. 3.9). The clustered area was far smaller than clusters of coralline algae. A cluster consisted of high values for corals (Fig. 3.10). Clustering was much less extensive for corals than CCA.

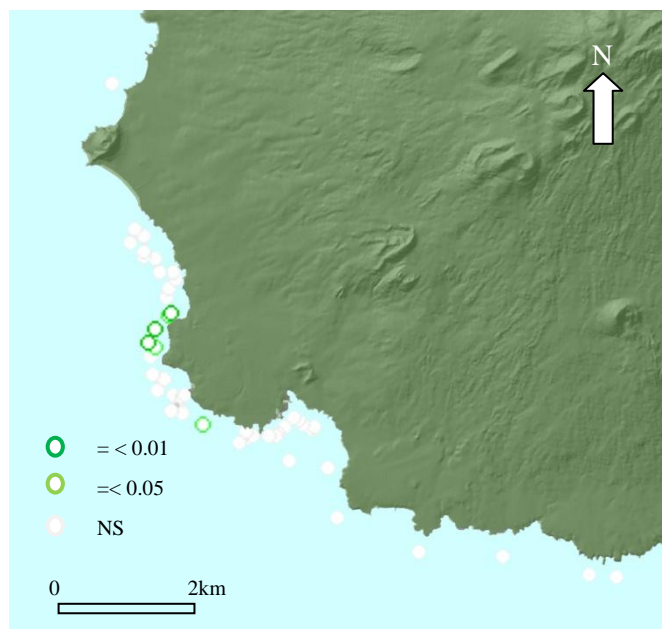


Fig. 3.9. A significance map of similarity for coral in proportion based on local Moran's I statistics using $k = 10$. Dark green symbols indicate sites with $p = < 0.01$ while light green symbols indicate sites with $p = < 0.05$. NS = not significant.

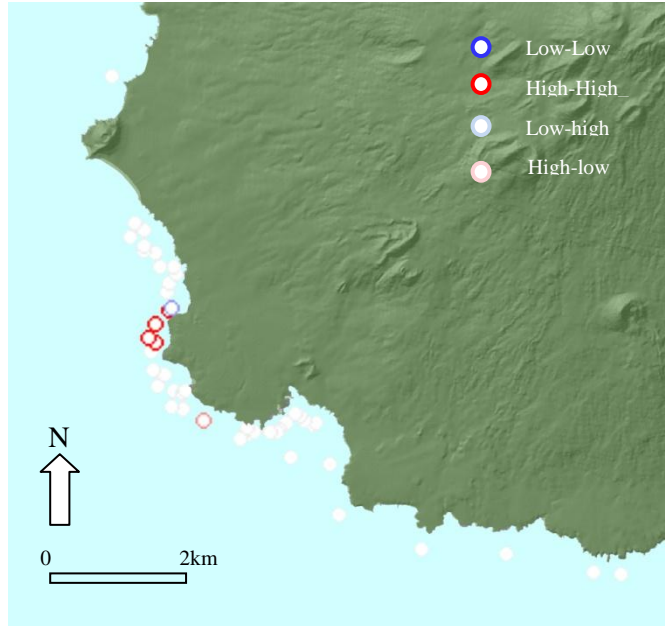


Fig. 3.10. A map of similarity cluster types for corals in proportion based on local Moran's I statistics using $k = 10$. Dark red symbols indicate sites surrounded by similar high values. Light red and light blue symbols are outliers indicating high values surrounded by low and low surrounded by high.

The omnidirectional sample variograms (Fig. 3.11a and 3.11b) of CCA were visually explored by fitting to a spherical and wave (or hole effect) variogram models. The sample variogram appeared to have a gradual monotonic increase indicating a presence of spatial structure. A four-directional sample variogram of CCA (Fig. 3.12) was plotted for further exploration of directional patterns. It showed significant trend in the N-S direction (0°) and the W-E direction (90°), indicated by exceeding semivariance above the sample variance (0.074) as the distance increased. Semivariance fluctuated about every several hundred meters beyond 1000 m to 3500 m.

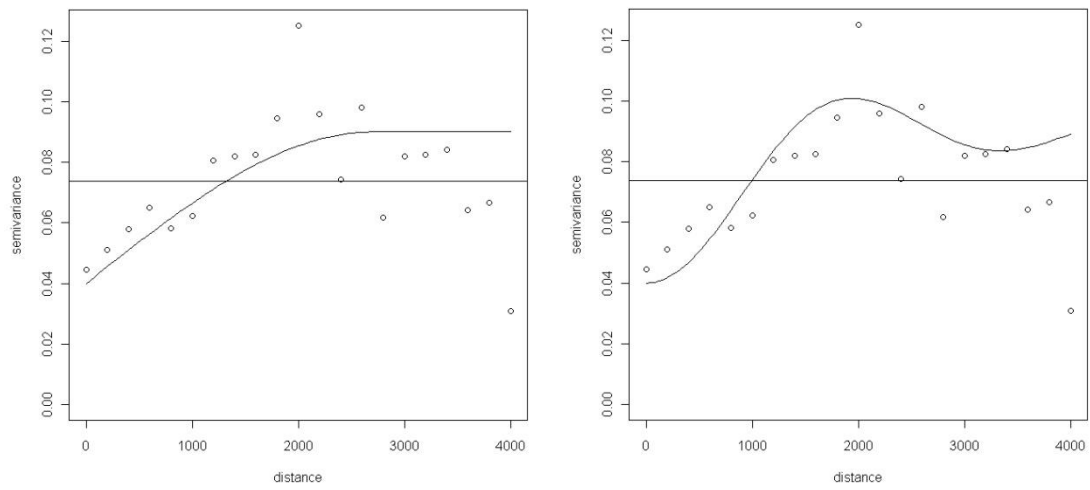


Fig. 3.11. Omnidirectional sample variograms fitted a) with spherical model, and b) with wave model for coralline algae cover in proportion. The horizontal line indicates the sample variance in proportion-squared. Distance is in meters.

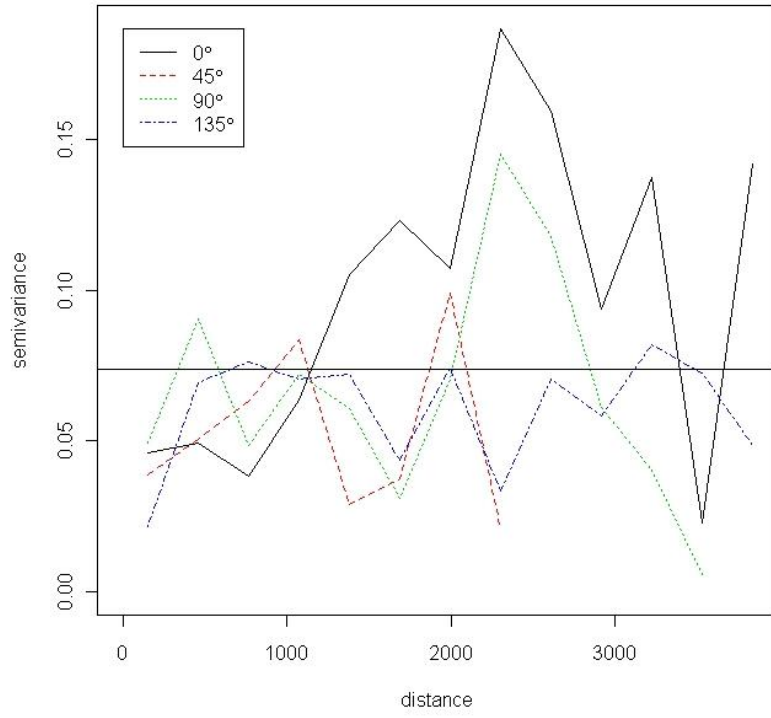


Fig. 3.12. Sample variogram of coralline algae cover in proportion in four directions. The horizontal line indicates the sample variance in proportion-squared. Distance is in meters.

Omnidirectional sample variograms (Fig. 3.13a and 3.13b) of corals were explored and visually fit to gaussian and spherical variogram models. The sample variogram might exhibit a steep monotonic increase at shorter distance, approximately around 200 m. A four-directional sample variogram of corals (Fig. 3.14) was noisy, but it might be anisotropic and indicates a trend in the N-S direction (0°) and the NW-SE direction (135°) as semivariance values greatly exceeded the sample variance (0.031). According to these analyses, CCA abundance had a spatial structure over a relatively long distance. Coral abundance might have a minimal, localized weak spatial structure within a very short distance.

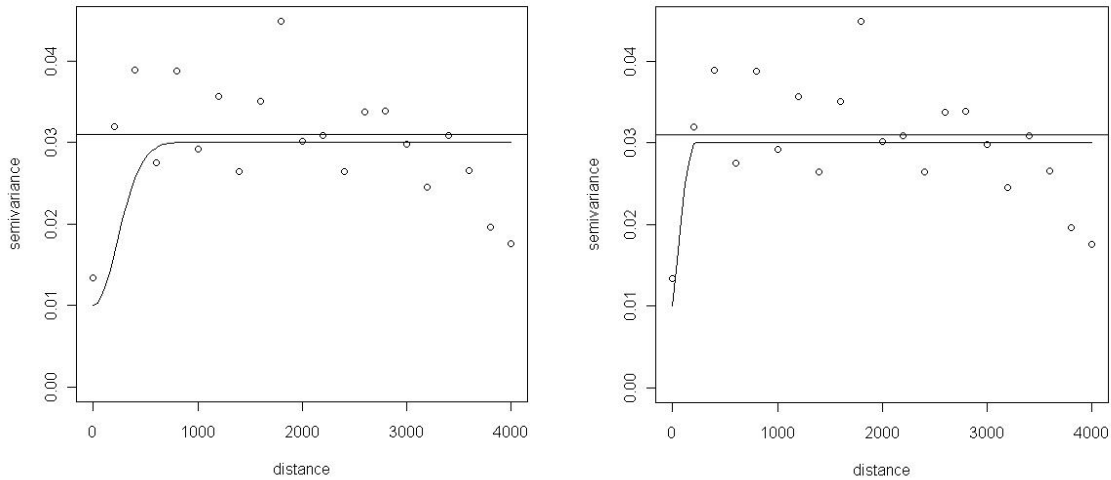


Fig. 3.13. Omnidirectional sample variograms for coral cover in proportion, a) fitted with gaussian model, and b) with spherical model. The horizontal line indicates the sample variance in proportion-squared. Distance is in meters.

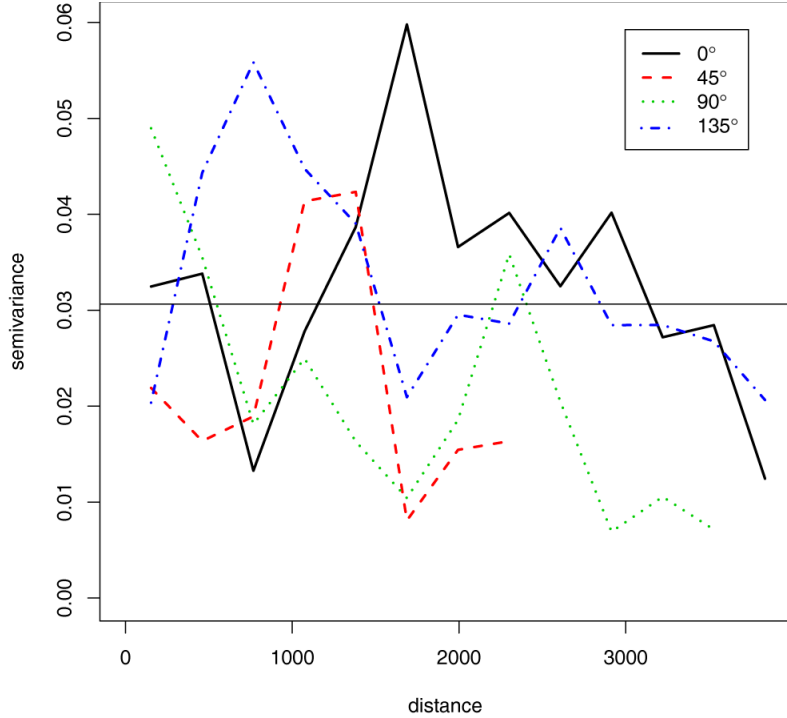


Fig. 3.14. Sample variogram of coral cover in proportion in four directions. The horizontal line indicates the sample variance in proportion-squared. Distance is in meters.

Model Selection and Comparison

Non-spatial Models with Independent Errors

Three OLS models were selected as candidates examining the relationship of CCA and corals to seascape variables. Spatial structures were not accounted for in these models. The best candidate was the 6-parameter model for both CCA and corals indicated by the smallest Mallow's C_p and the largest adjusted R^2 values (Table 3.4). No interaction terms were significant among predictors, and thus omitted from these models. These models explained approximately 49% of variability for CCA ($F = 7.86$; $df = 5$) and 51% for corals ($F = 8.37$; $df = 5$). These models also had the smallest internal cross-validation values including prediction error sum of squares (PRESS) and RMSE which

implied better prediction. Spatial coordinate terms (i.e., X as the easting coordinates and Y as the northing coordinates) were selected as predictor variables in most candidate models.

Table 3.4. Selected OLS models for CCA and corals with 4, 5, and 6 parameters (p) including intercepts. Model parameters included: the intercept; X = the easting coordinate; Y = the northing coordinate; Organic = organic material in sediment; Slope = mean slope within 25 m radius of sampling point; Rugosity² = quadratic term of Rugosity; Cp = Mallow's Cp criterion value; Adj. R² = adjusted R² (R² value that is adjusted for parsimony for number of parameters used); RMSE = root mean square error.

Response	p	Models	Cp	Adj. R ²	RMSE
CCA	4	X, Y, Depth	8.7	0.399	0.21039
CCA	5	X, Y, Depth, Rugosity	6.9	0.362	0.21683
CCA	6	X, Y, Depth, Rugosity, Organic	5.8	0.427	0.20538
Corals	4	Depth, Rugosity, Slope	8.9	0.359	0.14020
Corals	5	Y, Rugosity, Rugosity ² , Organic	5.1	0.422	0.13309
Corals	6	X, Y, Rugosity, Rugosity ² , Depth	4.5	0.445	0.13046

While the depth resulted in the greatest F statistic, both northing and easting coordinates were also highly significant for CCA. The northing coordinate was highly significant and had the greatest F- value for corals. The relationship between the abundance of CCA and easting coordinates, northing coordinates, depth, and proportion of organics were negative while rugosity was positive (Table 3.5) for the best candidate model.

For corals, models had smaller Mallow's Cp and the larger adjusted R² values when a quadratic term of rugosity was included. Coral abundance decreased with decreasing values of spatial coordinates implying the northwest direction while it increased with depth and rugosity (Table 3.6).

Table 3.5. Estimated parameters and their standard errors of explanatory variables for CCA abundance with the six parameter OLS model. X = the easting coordinate; Y = the northing coordinate; Adj SS = adjusted sum of squares. Bold type indicates statistical significance ($p < 0.01$).

Predictor	Coefficient	Adj SS	F	p
X	-0.00010 ± 0.00004	0.29070	6.89	0.012
Y	-0.00015 ± 0.00004	0.59176	14.03	0.001
Depth	-0.07765 ± 0.01814	0.77303	18.33	0.000
Rugosity	0.21490 ± 0.11640	0.14377	3.41	0.072
Organic material	-3.89200 ± 2.22000	0.12969	3.07	0.087

Table 3.6. Estimated parameters and their standard errors of explanatory variables for coral abundance with the six parameter OLS model. X = the easting coordinate; Y = the northing coordinate; Adj SS = adjusted sum of squares. Bold type indicates statistical significance ($p < 0.01$).

Predictor	Coefficient	Adj SS	F	p
X	-0.00004 ± 0.00002	0.05707	3.35	0.074
Y	-0.00008 ± 0.00002	0.18792	11.04	0.002
Rugosity	1.78380 ± 0.61280	0.14420	8.47	0.006
Rugosity ²	-0.43790 ± 0.18460	0.09577	5.63	0.022
Depth	0.01793 ± 0.00984	0.05653	3.32	0.076

Spatial Models with Correlation Functions

The selected OLS models of CCA and corals, from the previous section, were used for non-spatial and spatial model comparison. The first-order spatial trend and seascapes predictors were accounted for in the selected models. Semivariances of residuals from the selected OLS models were graphically examined for spatial structure in omni- and four directions for CCA (Fig. 3.15 and 3.16) and corals (Fig. 3.17 and 3.18).

Sample variance of residuals was 0.038, nearly a half of the observed CCA sample variance (0.074). Sample semivariances of residuals appeared to have a steep monotonic increase for a short distance, approximately around 200 m (Fig. 3.15). Spatial structure appeared to depend on directions (Fig. 3.16). Strong variability was observed in the 135° direction near 1200 m. The spherical variogram showed the best overall cross-validation results for models with trends. For example, cross-validation indicated the closest standardized mean prediction error value to zero (0.000026), a reasonably small RMSE (0.1814) with the minimum dispersion from the average standard error value (0.1817), and the closest standardized RMSE (1.004) to 1. Therefore the spherical correlation function was used for obtaining final parameter estimates, AIC, and log-likelihood values for comparison between isotropic and anisotropic models.

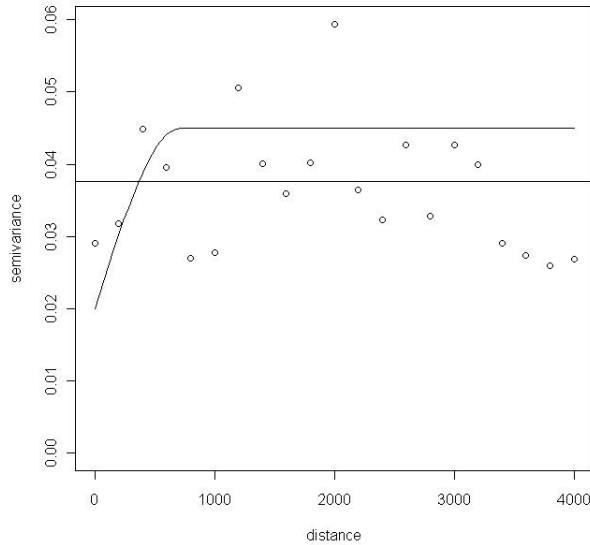


Fig. 3.15. Omni-directional sample variogram of the selected OLS residuals for coralline algae cover in proportion, fitted to the spherical model. The horizontal line indicates the sample variance in proportion-squared. Distance in meters.

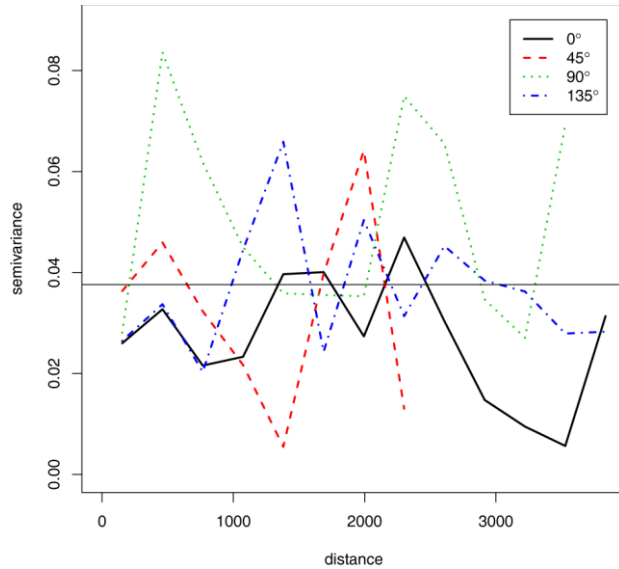


Fig. 3.16. Sample variogram of the selected OLS residuals for coralline algae cover in proportion in four directions. The horizontal line indicates the sample variance in proportion-squared. Distance in meters.

For corals, sample variance of residuals was 0.015 while the observed variance of coral was 0.031. The omni-directional sample variogram of residuals appeared to represent a form of pure nugget with no detectable spatial structure (Fig. 3.17). The four-directional sample variogram showed the extremely high semivariance (>0.05) around the distance, approximately 1500 m (Fig. 3.18). The initial semivariogram modeling in Geostatistical Analyst estimated zero for the partial sill value.

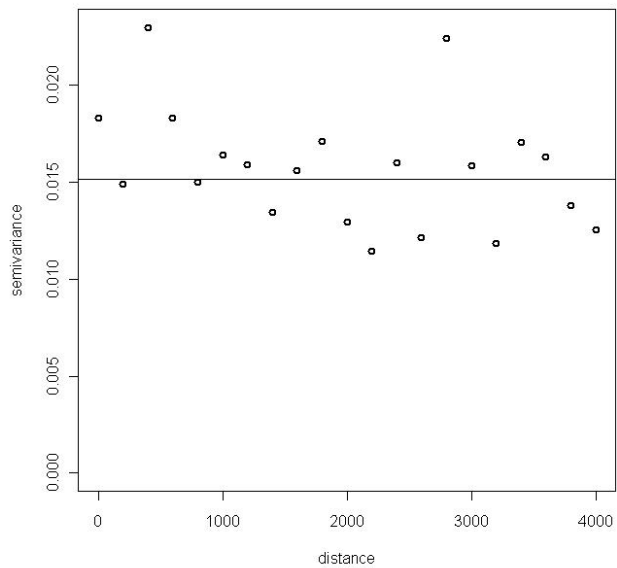


Fig. 3.17. Omni-directional sample variogram of the selected OLS residuals for coral cover in proportion. The horizontal line indicates the sample variance in proportion-squared. Distance in meters.

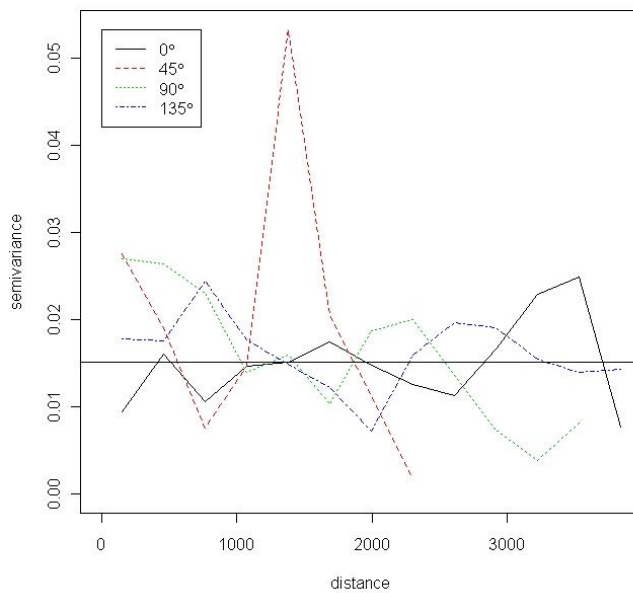


Fig. 3.18. Sample variogram of the selected OLS residuals for coral cover in proportion in four directions. The horizontal line indicates the sample variance in proportion-squared. Distance in meters.

Spatial models with fewer covariates were also explored in terms of correlation structures and anisotropy. Types of spatial models, AIC, log-likelihood values, and parameter estimates are summarized in Table 3.7. Spatial models of CCA resulted in the smaller AIC and greater log-likelihood values than non-spatial models when compared within each type of model. Eight of 12 spatial models had statistically significant, greater log-likelihood ratios than non-spatial models. The smallest AIC value (-2.92) was found for the anisotropic models specified with the first-order trend plus seascape predictors among all spatial models. The AIC of the non-spatial model with the same predictors (i.e., the selected OLS model) was 0.56. The log-likelihood ratio between these spatial and non-spatial models was statistically significant ($\chi^2 = 9.48$, $df = 3$; $p=0.02$). Therefore, the null hypothesis, stating that the full (spatial) model does not fit differently from the reduced (non-spatial) model, was rejected. The spatial model fitted differently from the non-spatial model. The anisotropic model with spatial and seascape trends showed the better fit than the non-spatial model with the same predictors. The isotropic and anisotropic seascape predictor models also had highly significant log-likelihood ratios (Table 3.7) between the non-spatial models.

The exponential and spherical variogram models resulted in similar AIC and log-likelihood values, while the wave function showed larger AIC and smaller log-likelihood values for the constant mean and the first-order trend models. Results of cross-validations, from preliminary variogram modeling agreed with theoretical variogram selection based on AIC and log-likelihood values. Thus the exponential or spherical variograms are preferred correlation models for CCA.

Table 3.7. Summary of geostatistical models for coralline algae cover. Geostatistical models were specified with a constant mean, the first order spatial trends, seascape predictors, a combination of the first order spatial trend and seascape predictors assuming isotropy or geometric anisotropy. p(f) = number of estimated parameters for the full (spatial) model; X = easting coordinate; Y = northing coordinate; Dep = depth; Rug = rugosity; Organic = organic material in sediment; iso = isotropic (omni-directional), aniso = geometric anisotropy transformation; Error = a type of error correlation function used, exp = exponential, wv = wave, sph = spherical; AIC = Akaike Information Criterion; Log-likelihood = log-likelihood function value by REML; p(r) = number of estimated parameters for the reduced (non-spatial) model; P-sill = partial sill; Angle = angle of geometric anisotropy transformation.

Model	p(f)	Error	AIC	Log-likelihood	p(r)	P-sill (σ^2)	Range (ρ)	Nugget (τ^2)	Angle
Constant	4	exp	5.79	1.13**	2	0.053	316.4	0.018	-----
		wv	8.48	-0.24**		0.034	810.6	0.050	-----
		sph	5.72	1.14**		0.052	668.0	0.020	-----
X, Y (iso)	6	exp	5.50	3.25	4	0.055	84.0	0.000	-----
		sph	6.12	2.94		0.039	556.8	0.022	-----
X, Y (aniso)	7	exp	0.56	6.72**	4	0.054	73.2	0.000	147°
		wv	10.25	1.87		0.034	810.6	0.050	203°
		sph	2.62	5.69*		0.043	593.3	0.020	147°
Dep, Rug, Organic (iso) (aniso)	7	sph	0.66	6.47**	5	0.045	1132.0	0.019	-----
	8	sph	-2.42	9.21**		0.037	744.3	0.019	145°
X, Y, Dep, Rug, Organic (iso) (aniso)	9	sph	-0.73	9.37	7	0.026	624.5	0.019	-----
	10	sph	-2.92	11.46*		0.025	714.6	0.020	145°

*Likelihood Ratio Test (LRT), approximating $\chi^2(3)$, resulted in p<0.05 when the full (spatial) and reduced (non-spatial) models were compared.

**LRT approximating $\chi^2(2)$ or $\chi^2(3)$ resulted in p<0.01 when the full (spatial) and reduced (non-spatial) models were compared.

In general, smaller AIC values were found with more complex models including seascape predictors (i.e., depth, rugosity, and organic materials) than simpler models with the constant mean or the first-order trend. The anisotropic model with the first-order trend plus seascape predictors resulted in the smallest AIC and largest log-likelihood values among all spatial models.

The log-likelihood ratios between the isotropic and anisotropic models of the first-order trend plus seascape predictors were statistically significant ($\chi^2 = 4.18$, $df=1$; $p=0.04$). The likelihood ratios between the isotropic and anisotropic models for the first-order trend ($\chi^2 = 5.50$, $df=1$; $p=0.02$) and seascape predictor models ($\chi^2 = 5.48$, $df=1$; $p=0.02$) were also statistically significant.

Estimated sills ($\sigma^2 + \tau^2$) were similar within each model type, but ranges varied depending on the spatial models. The estimated sill was 0.045 with the nugget variance 0.020, and 715 m for the range of the 10 parameter model. The estimates were in reasonable agreement with the sample variogram (Fig. 3.14). The partial sill (σ^2) of the 10 parameter model was reduced to approximately a half of the constant mean model. However, there was no substantial change in the value of range. For example, the range of the constant mean model with the spherical function was about 668 m while the 10 parameter model was about 715 m. The spatial structure among errors was evident at a distance of approximately 715 m, although spatial dependence on trends were already removed. Therefore the CCA abundance has positive autocorrelation and/or spatial dependence on unknown variables that were not included in the model.

The 10-parameter model was preferred among all spatial and non-spatial models. Overall, the OLS models for CCA improved when predictors and directional spatial structures were taken into account.

Table 3.9 is a summary of spatial models and results for corals. Results of spatial and non-spatial model comparisons varied. Four of 13 spatial models had statistically significant, larger log-likelihood ratios than non-spatial models. These models included the constant mean with Gaussian function, the constant mean with the wave function, the isotropic first-order trend with the spherical function, and the anisotropic first-order trend with Gaussian function. While the smallest AIC value (-35.0) was found for the anisotropic models specified with the first-order trend plus seascape predictors among all spatial models, the non-spatial model (-36.6) resulted in smaller AIC than the smallest of spatial models. The log-likelihood ratio between this spatial and non-spatial models was not statistically significant ($\chi^2 = 4.38$, $df = 3$; $p = 0.22$).

Overall, the Gaussian and spherical variogram models resulted in relatively similar AIC and log-likelihood values for the constant mean and the first-order trend models while the wave function showed larger AIC and smaller log-likelihood values. The wave variogram model resulted in a comparable AIC value to the Gaussian model when the model included only a constant mean.

No particular theoretical variogram was fitted well to the isotropic and anisotropic first-order trend models. The cross validation did not suggest strong preference over Gaussian or spherical variograms for both isotropic and anisotropic first-order trend models. AIC for Gaussian and wave models fluctuated from small to large depending on inclusion or exclusion of the anisotropy transformation. AIC of the

Table 3.8. Summary of geostatistical models for coral cover. Geostatistical models were specified with a constant mean, the first order spatial trends, seascape predictors, a combination of the first order spatial trend and seascape predictors assuming isotropy or geometric anisotropy. p(f) = number of estimated parameters of the full (spatial) model; X = easting coordinate; Y = northing coordinate; Dep = depth; Rug = rugosity; Or = organic materials in sediment; iso = isotropic (omni-directional) model, aniso = a model with geometric anisotropy transformation; Error = a type of error correlation function used, gau = Gaussian function, wv = wave function, sph = spherical function, exp = exponential function; AIC = Akaike Information Criterion; Log-likelihood = log-likelihood function value by REML; p(r) = number of estimated parameters of the reduced (non-spatial) model; P-sill = partial sill; Angle = angle of geometric anisotropy transformation.

Model	p(f)	Error	AIC	Log-likelihood	p(r)	P-sill (σ^2)	Range (ρ)	Nugget (τ^2)	Angle
Constant	4	gau	-28.40	18.19*	2	0.022	125.3	0.007	----
		wv	-29.10	18.53*		0.029	222.6	0.000	----
		sph	-22.50	15.26		0.003	442.9	0.028	----
X, Y (iso)	6	gau [†]	-15.71	13.85	4	0.000	547.0	0.031	----
		wv	-16.46	14.23		0.003	413.5	0.029	----
		sph	-22.71	17.35*		0.030	220.5	0.000	----
X, Y (aniso)	7	gau	-24.00	19.00*	4	0.028	39.3	0.001	1°
		wv [†]	-13.70	13.85		0.000	869.9	0.031	0°
		sph	-19.20	16.61		0.013	410.9	0.017	1°
Rug, Rug ² , Dep (iso) (aniso)	7	sph	-32.80	23.39	5	0.008	913.5	0.014	----
	8	sph	-30.40	23.22		0.006	1847.0	0.016	115°
X, Y, Rug, Rug ² , Dep (iso) (aniso)	9	exp [†]	-32.66	25.33	7	0.000	7918.0	0.017	----
	10	exp	-35.04	27.52		0.011	60.1	0.007	10°

*LRT approximating $\chi^2(2)$ or $\chi^2(3)$ resulted in $p<0.05$ when the full (spatial) and reduced (non-spatial) models were compared.

†Consideration of a non-spatial model was suggested by the software as partial sill were estimated as zero.

spherical variogram was relatively stable when compared to Gaussian or wave variograms in this model type. The ‘geoR’ suggested consideration of a non-spatial model upon fitting three different models with predictors (Table 3.9) since the estimated sill was less than the one hundredth of the total variance.

Residuals of the seascape predictor model and the model specified with first-order trend plus seascape predictors were fitted to the theoretical variograms. The spherical function showed the best overall cross-validation results for models with seascape predictors. Cross-validation statistics indicated the closest standardized mean prediction error value to zero (0.0155), a reasonably small RMSE (0.1428) with the minimum dispersion from the average standard error value (0.1418), and the closest standardized RMSE (1.000) to 1. Therefore the spherical correlation function was used for obtaining final parameter estimates, AIC, and log-likelihood values for comparison between isotropic and anisotropic models with seascape predictors. The exponential variogram was selected for the model specified with the first-order trend and seascape predictors. Cross-validation statistics included the standardized mean prediction error (0.0024), RMSE (0.1327), the average standard error (0.1331), and the standardized RMSE (0.9966).

In general, smaller AIC values were found with more complex models specified with seascape predictors (i.e., rugosity and depth) than simpler models with the constant mean or the first-order trend. The anisotropic model with the first-order trend plus seascape predictors resulted in the smallest AIC and largest log-likelihood values among all spatial models. The log-likelihood ratios between the isotropic and anisotropic models of the first-order trend plus seascape predictors were statistically significant ($\chi^2 =$

4.38, $df=1$; $p=0.04$). However, there was no statistically significant difference between the isotropic and anisotropic models for the first-order trend, and for seascape predictors alone.

Estimated sills ($\sigma^2 + \tau^2$) and ranges varied depending on the spatial models. Estimates from eight models had greater nugget variances than sills indicating the absence of spatial structure. Estimates from the remaining five models showed spatial structure with distances ranging approximately between 39 and 223 m.

The estimated sill was 0.018 with the nugget variance 0.007, and 60.1 m for the range of the 10-parameter model. The partial sill (σ^2) of the 10-parameter model was reduced to approximately half of the constant mean model. The spatial structure among errors might exist according to this model when the spatial trend and seascape predictors were already accounted. The coral abundance might be positively autocorrelated at the distance of approximately 60 m. However the effect of autocorrelation was statistically negligible.

The 10-parameter model was the preferred spatial model taking the directional spatial structure into account. The model including constant mean and spatial components improved moderately when trends (i.e., spatial coordinates and seascape predictors) were removed. However, the non-spatial model with positional coordinates and seascape predictors did not substantially improve when spatial structures were taken into an account, and no additional variability was explained by autocorrelation.

Visual Representation of Predicted Values and Uncertainty

Simple kriging and co-kriging interpolations were applied to CCA cover. The data were modeled with a spherical correlation structure. Rugosity, depth, and proportion of organic material were included as covariates for co-kriging. Predicted mean proportion values across the area resulted in 0.259 for kriging and 0.258 for co-kriging. Although overall predicted means were similar, the spatial distribution patterns of means were not similar, particularly in the northern area of Cape Kīna‘u where means range from 0.001 to 0.261(Fig. 3.19a and 3.19c). Maps of prediction standard errors also exhibited the differences in the direction of spatial structures between kriging and co-kriging (Fig. 3.19b and 3.19d). Prediction standard errors are deviations of the prediction from the actual value at a given point (ESRI 2003). The spatial structure was apparent in the NW-SE direction for kriging, while the spatial structure was oriented in the N-S direction for co-kriging with covariates. Relatively high predicted standard errors were obvious in the area where less neighboring points were present.

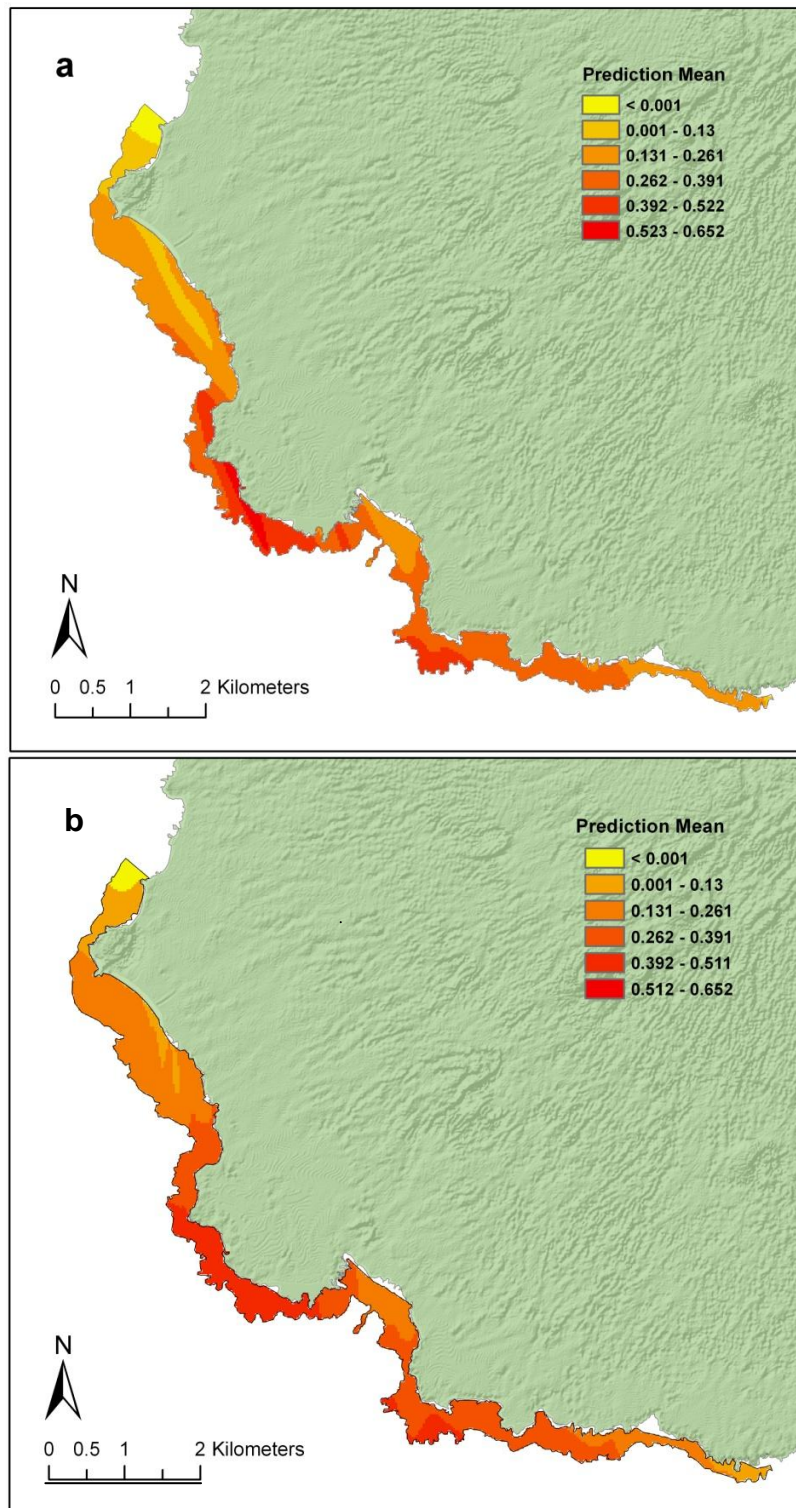


Fig. 3.19. Maps of predicted mean proportion of crustose coralline algae by a) simple kriging, and b) simple co-kriging.

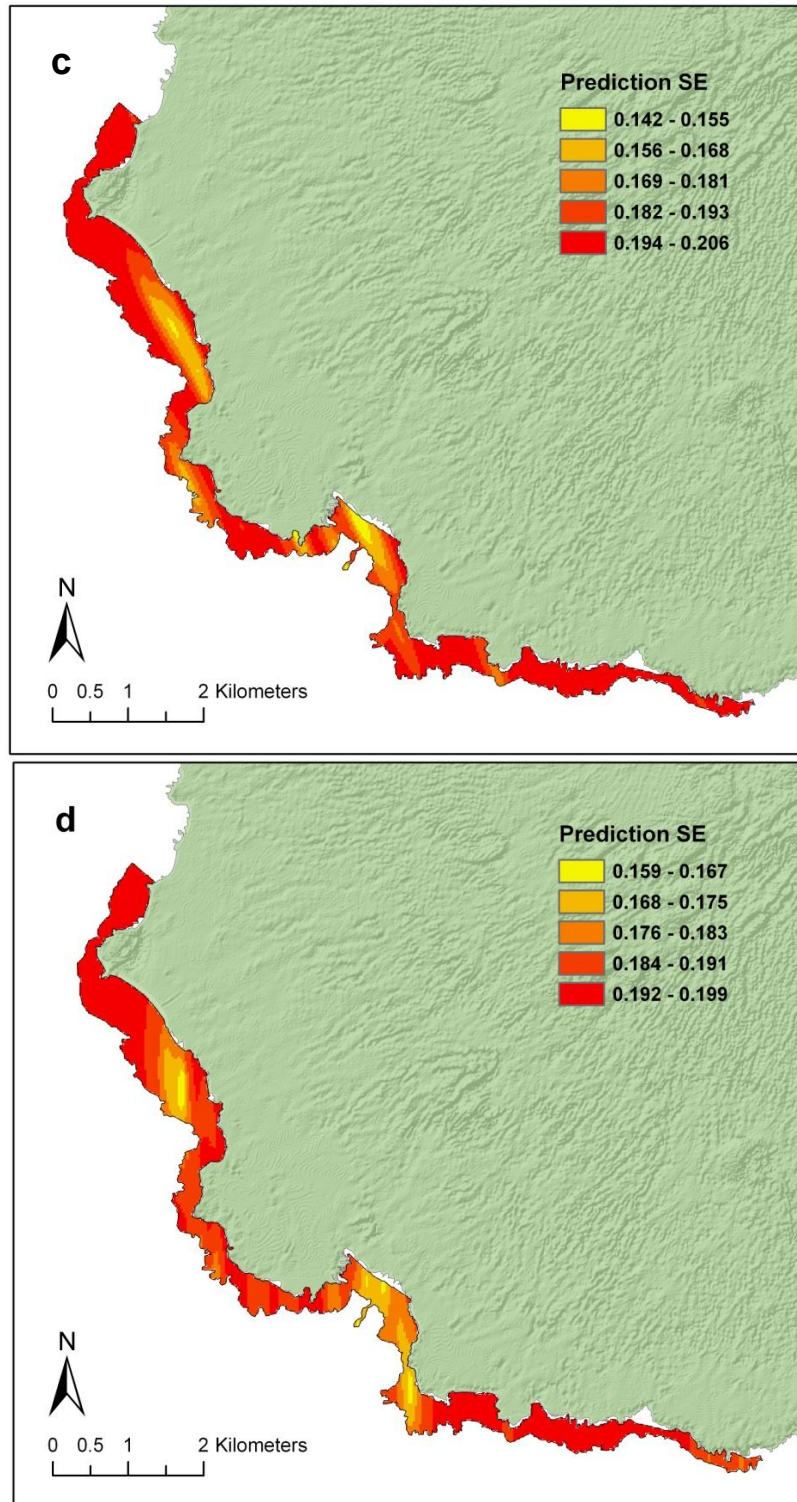


Fig. 3.19. Maps of prediction standard error of crustose coralline algae proportion by c) simple kriging, and d) simple co-kriging.

Table 3.9 summarizes results of cross-validations for kriging and co-kriging of CCA. The selection criteria included similar values between the root-mean-square prediction error (RMSPE) and the average kriging standard errors (AKSE), mean standardized prediction error near zero, and the root-mean standardized prediction error near one (ESRI 2003). Either a kriging or co-kriging model could be used for prediction of CCA. However the co-kriging model requires greater number of estimated parameters and thus computationally more complex than kriging model. In this analysis the co-kriging model did not result in substantial improvement for prediction and interpolation. Therefore the results of the kriging model were used in the subsequent conditional simulations.

Table 3.9. Summary of cross-validation results for kriged coralline algae cover. SK = simple kriging; SCK = simple co-kriging; MPE = mean prediction error; RMSPE = root-mean-square prediction error; AKSE = average kriging standard error; MSPE = mean standardized prediction error; RMSTD = root-mean standardized prediction error.

Kriging	MPE	RMSPE	AKSE	MSPE	RMSTD
SK	-0.0066	0.1828	0.1823	-0.0323	1.0080
SCK	0.0190	0.1786	0.1816	0.1106	0.9663

Predicted means of CCA cover were similar among different interpolations (Table 3.10). Kriging and co-kriging variances were less than the one-third of variances from the conditional simulations. While kriging estimates are the best unbiased linear estimates at individual local points, they tend to smooth a surface overly by underestimation of large values and overestimation of small values (Goovaerts 1997). Smoothing effects of kriging and co-kriging estimates were evident.

Table 3.10. Descriptive statistics for simulated coralline algae cover. Int = interpolation trial; SK = simple kriging; SCK = simple co-kriging; Number = number of realizations; Mean = mean of all cells in all realizations within the polygon; SD = standard deviation of all cells in all realizations within the polygon; Var = variance; CV = coefficient of variation (%).

Int	Number	Mean	Var	CV
SK	1	0.2589	0.0163	49.4
SCK	1	0.2575	0.0143	46.4
s1	1000	0.2598	0.0508	86.7
s2	500	0.2570	0.0512	88.1
s3	100	0.2562	0.0511	88.2
s4	5	0.2548	0.0515	89.0

Figure 3.20a through 3.20d are maps of mean CCA cover with varying numbers of realizations generated by the sequential Gaussian conditional simulations. CCA distributions were generally low in the northwestern position of the study area, especially in the embayment, and high around Cape Kīna‘u in the southeast. While the general distribution patterns of CCA were similar among all four maps, the distributions of mean values were more defined and smoothed for maps generated from 500 and 1000 realizations than maps from five and 100 realizations. Similarly standard deviations showed more defined and smoothed spatial patterns with maps generated from 500 and 1000 realizations than a map generated from five and 100 realizations (Fig. 3.21a through 3.21d). The narrowest range of standard deviation was found with 1000 realizations while the standard deviation of five realizations was the broadest. Variance slightly increased as number of realizations decreased (Table 3.10). There were no obvious differences between maps of mean cover and standard deviation generated from 500 and 1000 realizations. Maps of means and standard deviations generated from 500 and 1000

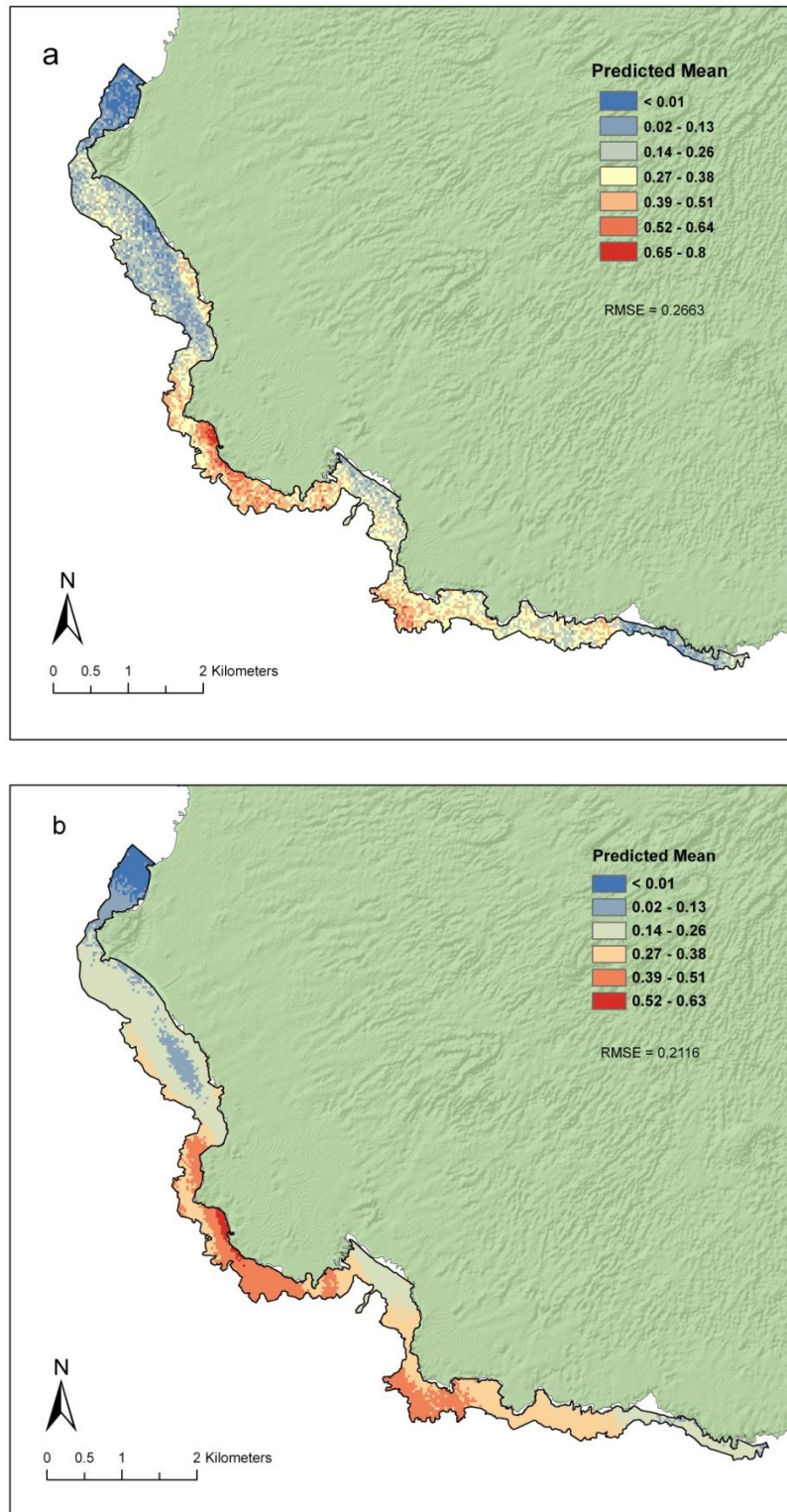


Fig. 3.20. Maps of mean proportion of crustose coralline algae cover generated, from a) five realizations, and b) 100 realizations by the Gaussian conditional simulations.

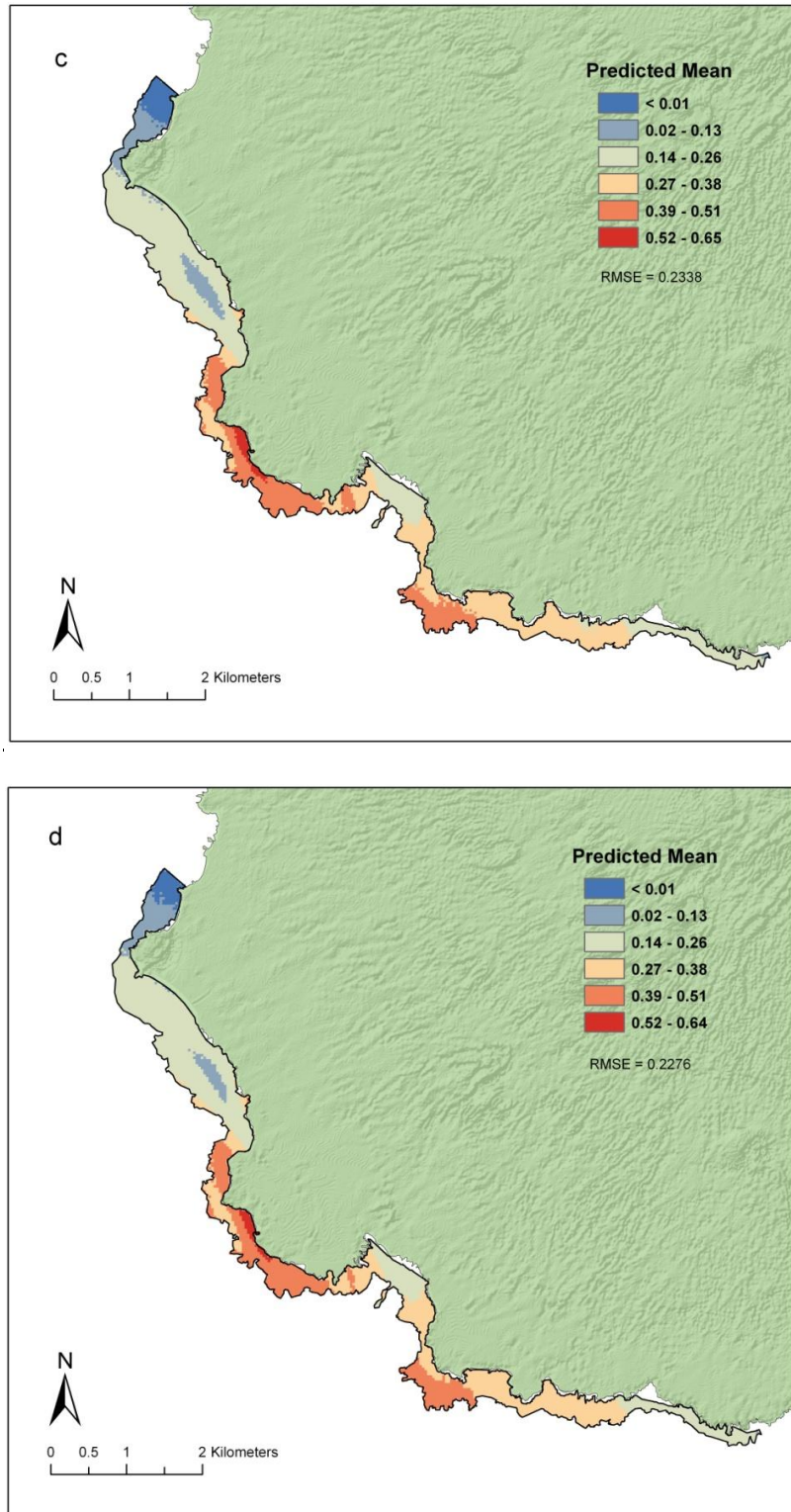


Fig. 3.20. Maps of mean proportion of crustose coralline algae cover, generated from c) 500 realizations, and d) 1000 realizations by the Gaussian conditional simulations.

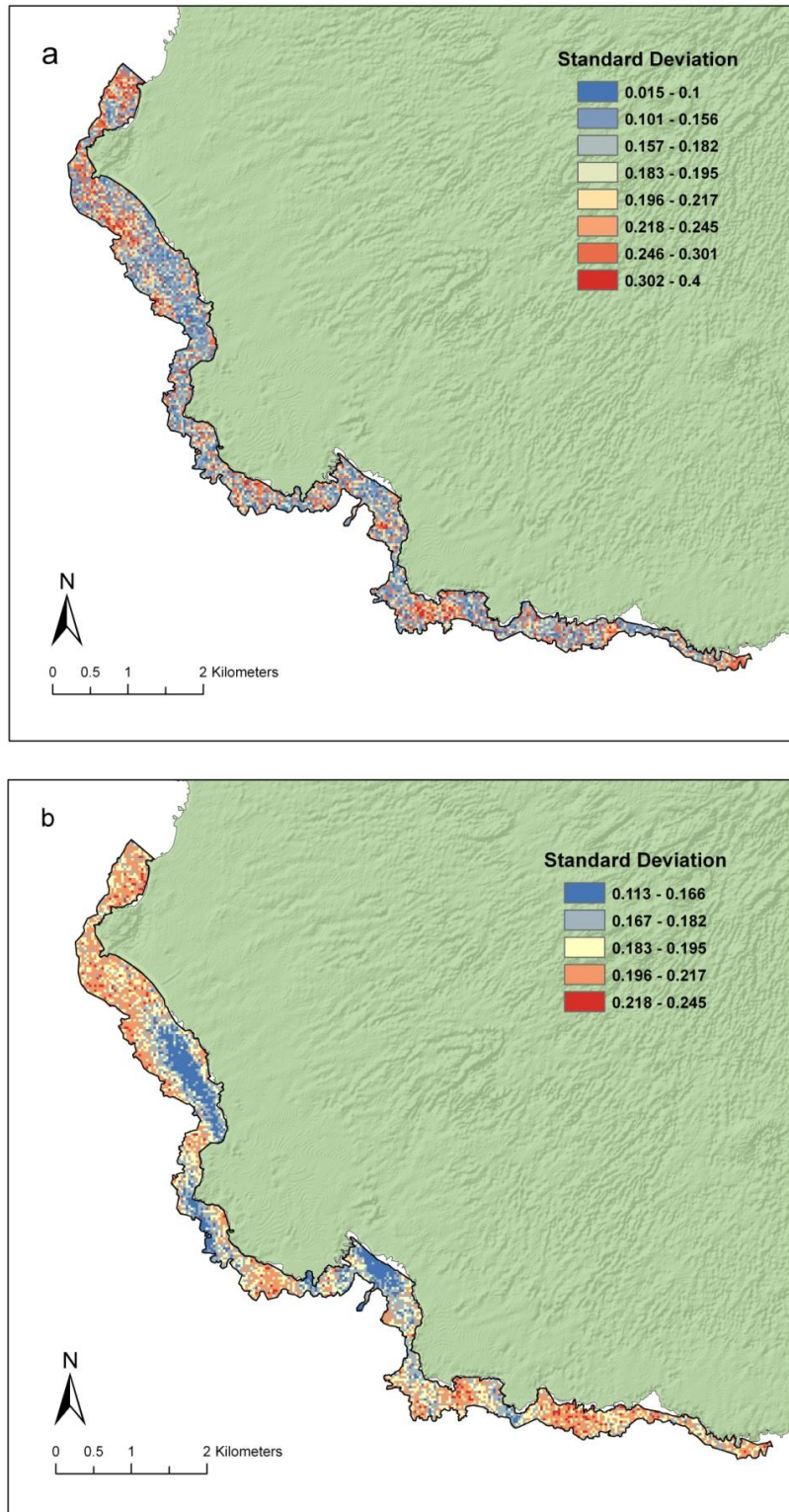


Fig. 3.21. Maps of standard deviation for crustose coralline algae proportion, generated from a) five realizations, and b) 100 realizations by the Gaussian conditional simulations.

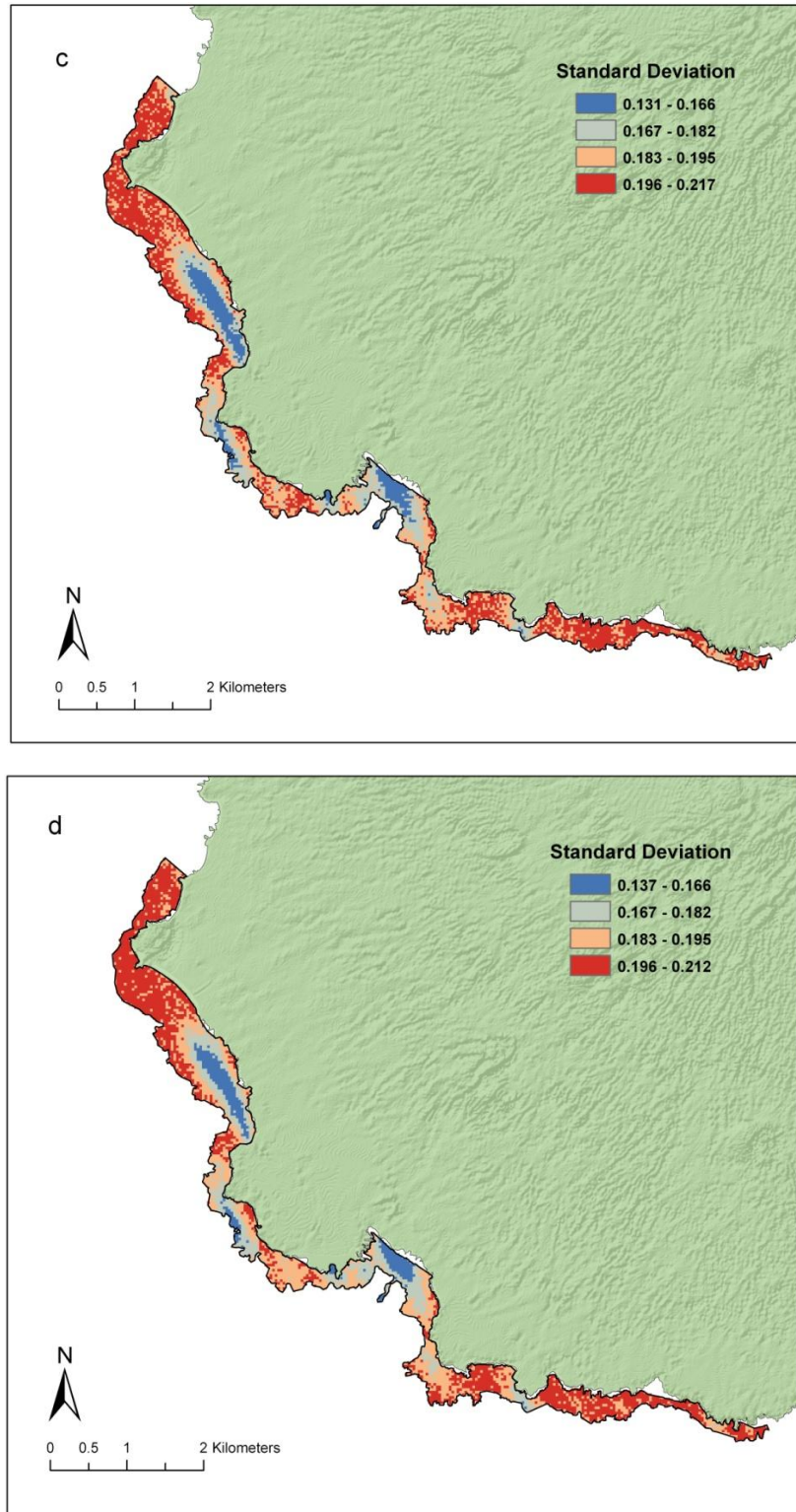


Fig. 3.21. Maps of standard deviation for crustose coralline algae proportion, generated from c) 500 realizations, and d) 1000 realizations by the Gaussian conditional simulations.

realizations resembled maps of kriged mean and standard deviation. The RMSPE calculated with the validation data ($n = 7$) was the lowest with mean generated from 100 realizations (0.2116). RMSPE were 0.2276, 0.2338, and 0.2663 for a map from 1000 realizations, 500 realizations, and five realizations, respectfully. According to RMSPE from the validation data, the map of mean CCA cover generated from 100 realizations represented its spatial distribution the best.

Inverse distance weighting interpolation (IWD) was applied to represent the spatial distribution of coral cover. The preferred spatial model with the smallest AIC value did not differ significantly from the independent error model (Table 3.8). In addition, estimated spatial correlation parameters substantially differed among models depending on the choice of theoretical variogram for fitting. A cluster of significantly similar values was localized and small in its extent (Fig. 3.9). Such clusters may be overly smoothed by kriging interpolation.

Comparisons of IDW with different neighborhood search methods and settings indicated that the smallest RMSPE resulted when power was optimized for 1.09, anisotropy, and an ellipse model was included in neighborhood definition (Table 3.11). Its mean prediction error was the closest to zero.

Table 3.11. Comparisons of Inverse Distance Weighting interpolation (IDW) methods for coral cover. OP = computed optimized power value; Smoothing = smoothing factor value; MPE = mean prediction error; RMSPE = root-mean-squared prediction error.

Map ID	Method	OP	Anisotropy	Smoothing	MPE	RMSPE
a	Standard	1.09	Yes	n/a	-0.01174	0.1094
b	Standard	3.56	No	n/a	-0.02307	0.1130
c	Smooth	3.48	No	0.2	-0.02233	0.1118

The mean coral cover map generated by IDW (Fig. 3.22a) appeared different than the other two maps (Fig. 3.22b and 3.22c) due to the effect of anisotropy. RMSPE was calculated with the validation data ($n = 7$) for the map a (Fig. 3.20a). It resulted in 0.0630 that was substantially lower than RMSPE of the training data ($n = 47$).

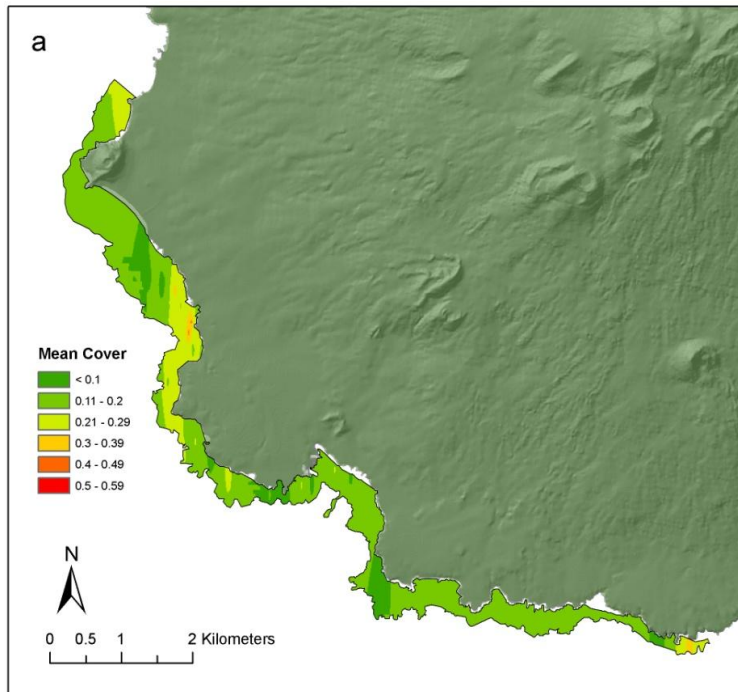


Fig. 3.22. Maps of predicted mean proportion of coral cover interpolated by IDW, determined by a) standard method, anisotropy, and optimized power of 1.09.

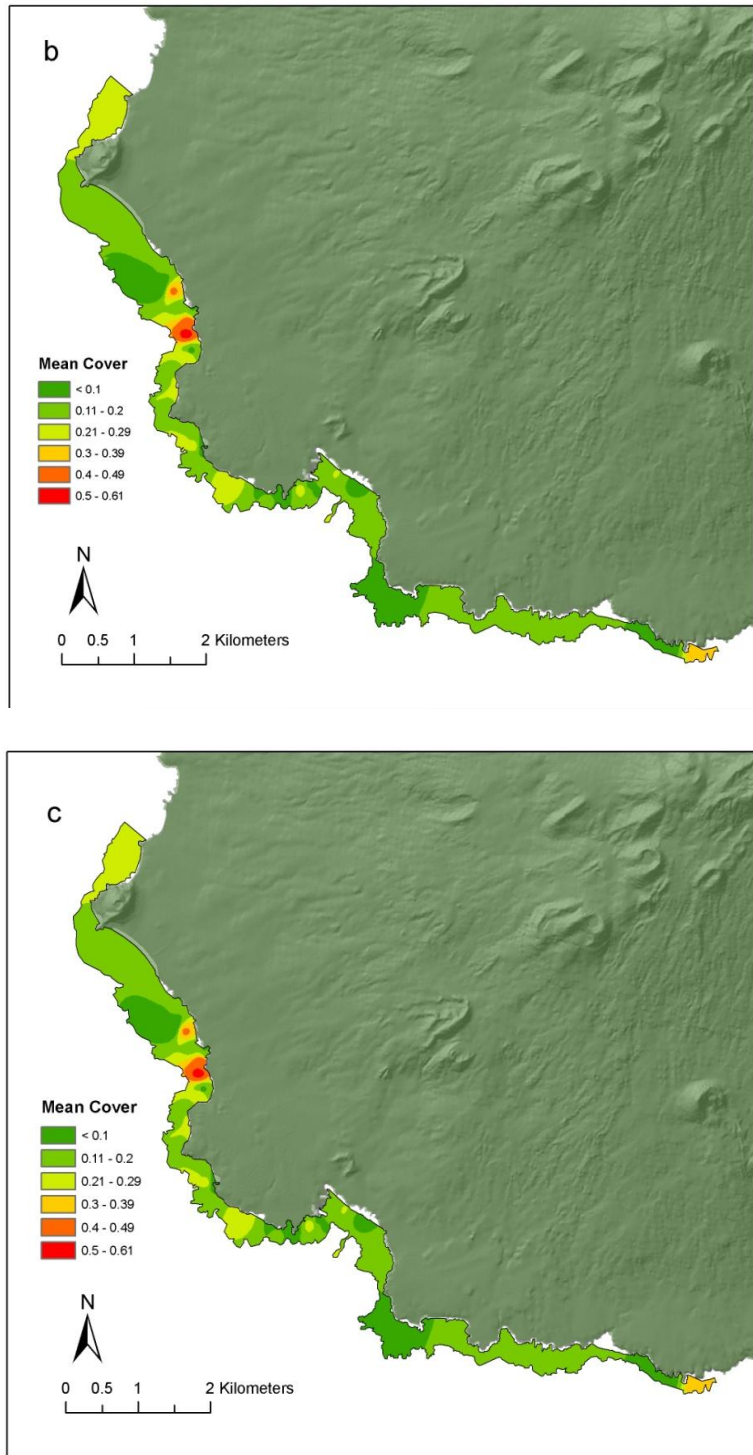


Fig. 3.22. Map of predicted mean proportion of coral cover interpolated by IDW, determined by b) standard method, isotropy, and optimized power of 3.56, and c) smoothing method, isotropy, and optimized power of 3.48.

Discussion

Analysis of Spatial Structures

Moran's *I* statistics were obtained as a preliminary step to identify possible presence of spatial structure for the observed CCA and coral cover data. Conducting the multiple permutation tests allowed the assessment of how consistent the probable occurrence of spatial structure was. Resultant p-values from the multiple permutation tests were consistent, and indicated that CCA abundance was spatially structured while coral was not.

Moran's *I* test alone however does not provide insights into the scale of distance that may be associated with spatial structure. Variogram analysis allowed the scale of spatial structure and presence of spatial trends to be characterized. It also allowed examination of the magnitude of directional effects. The assumption of stationarity is more stringent for Moran's *I* test than for the variogram approach that employs the intrinsic hypothesis. The combination of Moran's *I* tests and variogram analysis were found to be more robust, and complementary approaches in assessing spatial structure. Results of the variogram analysis indicated that CCA abundance was spatially structured. According to the variogram results, a potential fine-scale spatial structure might exist for coral abundance, yet its magnitude may be weak relative to CCA.

Moran's *I* test does not decompose contributors to spatial structures such as trends, local clustering, spatial dependence, or an actual autocorrelation. Local Moran's *I* tests and associated cluster maps were useful in assessing where clusters of similar values occurred and their strength. High abundance of CCA was spatially correlated at the southern most area of Cape Kīnau while low abundance was spatially correlated at the

north of ‘Āhihi Bay. This result lead to further exploration using Local Moran’s *I* tests and associated cluster maps for rugosity and organic material. The cluster patterns of rugosity resembled the spatial pattern of CCA clusters indicating potential spatial dependence of CCA on rugosity. The clusters of high organic material values were also partially overlapped with clusters of high CCA abundance. Cluster maps helped to assess the nature of spatial structure present in CCA cover.

Model Selection and Comparison

Non-spatial Models with Independent Errors

The 6-parameter model (Table 3.4) resulted in the best non-spatial predictive model for coral cover at ‘Āhihi area showing the lowest Mallow’s *Cp* (4.5). This model included spatial coordinates, rugosity, and depth. Jokiel *et al.* (2004) concluded that there was a significant relationship between coral cover and rugosity, depth, and fine sands based on samples collected at state wide locations in Hawai‘i. The results from the present study agree with Jokiel *et al.* (2004) regarding positive effects of rugosity and depth on coral cover. However effects of fine sands as well as sediment composition were not significant factors for corals in the current study. The overall average fraction of fine sands was fairly low (7.3%) and composition was dominated by coarser carbonate sands (86.9%).

The best non-spatial predictive model, with the lowest Mallow’s *Cp*, also included six parameters including depth, rugosity, and organic material for CCA cover. Spatial coordinates were consistently selected for the best models including 4-, 5-, and 6-parameter models indicating strong predictors for CCA cover at this scale.

Results (Table 3.5) revealed the positive effects of rugosity, and negative effects of depth and organic material on CCA at ‘Āhihi area. In the best non-spatial model, rugosity was statistically significant ($p = 0.072$) at $\alpha[2] = 0.10$, but not at the arbitrary $\alpha[2] = 0.05$. Rugosity was selected for the 5-parameter model which was the second best non-spatial model with the lowest Cp value as well. The 6-parameter model supported the positive relationship between CCA and rugosity assessed on cluster maps. It has been known to have a positive relationship between corals, and reef fish (Friedlander and Parrish 1998, Friedlander *et al.* 2003) which affect grazing pressure and the relative dominance of CCA cover (Litter and Litter 1984). Therefore, rugosity is appropriate to include in the predictive model.

The negative effect of organic material was contrary to my expectation since CCA was found to be abundant with nutrient enrichment (Litter and Litter 1984; Smith *et al.* 2001; 2010), as organic materials generally associate with greater nutrient storage, cycling, and availability. The effect of organic material may be confounded with depth, since the depth and organic material had a significant negative correlation ($r = -0.54$, $p < 0.001$). The depth has stronger effects ($p < 0.001$) on the abundance of CCA than effects of organic materials ($p = 0.087$) on average.

According to Fabricius and De’ath (2001), CCA cover on the Great Barrier Reef (GBR) showed a strong inverse pattern ($R^2 = 62\%$) to thickness of sediment deposit, and a strong positive pattern with relative distance across the shelf ($R^2 = 81\%$). The regression tree model with these variables explained 85% of total variability. The regression tree model of physical variables resulted in a positive relationship to water clarity, slope, and negatively related to sediment deposition explaining 78% of total

variability. They suggested that the relative cross-shelf distance, calculated from geographic coordinates, was a strong surrogate for the confounding physical factors such as water clarity affecting CCA cover. Similarly, in this study, spatial coordinates would be considered as surrogates for physical and additional unknown factors affecting CCA cover.

Fabricius and De'ath (2001) also suggested that sediment accumulation accounts for substantial local variation in CCA cover not explained by relative cross-shelf distance. Thickness of sediment deposit was not quantified in this study. Based on a qualitative observation, sediment deposits were generally very thin or negligible on the reef substrate at 'Āhihi area. How sediments play a role in the relationship among nutrients, organic materials, and CCA cover dynamics would be interesting to examine in the future. A manipulative experiment would help determine causal effects of organic materials in sediment on CCA cover.

There have been few studies that describe the abundance, distribution, and relationships of CCA to the environment and reef communities in Hawai'i, despite of its ecological and geological significance. Patterns of CCA abundance and distribution were influenced by depth, water motion, light intensity, nutrient levels, grazing pressure, and species composition at a habitat scale (Litter 1973; Adey *et al.* 1982; Litter and Litter 1984). Litter and Litter (1984) contrasted benthic cover and compositions at two different locations, Waikīkī reef flat and Kealakekua Bay. These locations reflected different levels of nutrients and grazing pressure. Geologically younger Kealakekua Bay represented a reef system with low nutrients and high grazing pressure by herbivorous fish and sea urchins while the older Waikīkī reef was relatively eutrophic and overfished.

The distribution and abundance pattern of CCA substantially differed along depth gradients between the two locations. There was a rapid decline in cover from approximately 75% at depths <3 m to less than 20% cover around 7 m in Kealakekua Bay. Overall, CCA cover decreased with increasing depth in ‘Āhihi’s reef as similar to Kealakekua Bay. However, at the southern-most area of Cape Kīnau, the clusters of high CCA cover (approximately 40-89%) consistently occurred at varying depths ranging from 1-8 m. The best non-spatial model of CCA for ‘Āhihi area resulted in a substantially lower coefficient of determination (~51%) than the models for GBR. Thus patterns of CCA cover on ‘Āhihi’s reef differs from ones on Waikīkī reef and Kealakekua Bay, as well as GBR as its patterns may respond to varying intensity of environmental and ecological processes at different scales. Additional variables which were not included in the model need further consideration, for example, sediment deposition depth, survival rate, grazing pressure, and/or nutrient input through potential submarine ground water. Such data were not available for this study but could be investigated in a future study of CCA abundance and distribution.

Spatial Models with Correlation Functions

Coral cover exhibited no autocorrelation, but there was evidence of weak spatial dependence on seascape predictors such as rugosity and northing coordinate in ‘Āhihi area. Evidence suggested that residuals of coral cover had negligible, or no autocorrelation when effects of spatial trends and seascape predictors were removed.

Lag distance of this analysis was 200 m, thus potential spatial structure of coral abundance less than 200 m may not be detected. The estimated range for the best spatial

model (Table 3.8) with the least AIC was 60 m. This result might imply autocorrelation of coral abundance at this distance, yet several outcomes suggested considering non-spatial models during the analysis. Lag distance for coral abundance may be made shorter and re-analyzed for the potential spatial structure at a scale less than 200 m, if a suitable enough number of pairs are available for each lag class within the data set. However, because of irregular pair-wise distances between sampling points, shorter lag distances might be difficult to achieve without losing the number of pairs for each distance class. The precision may be lost with altered lag distances from the current setting.

In order to investigate spatial structure of coral cover with a geostatistical approach, samples might be collected at a systematic distance or lattice. A systematic sampling scheme over the entire study area might be more efficient in terms of spatial prediction. The greater coverage and greater number of samples per unit effort that can be achieved by a systematic scheme may be important from a management perspective wherever a geographic unit of management is large. Diggle and Rebeiro (2007) pointed out two practical considerations for the lattice sampling scheme. Unlike a random sampling design, a general lattice design does not have closely paired positions. However, having replicated measurements at a close or identical position will provide useful information when a substantial nugget variance is present. The second consideration is that closely paired positions are particularly useful for parameter estimations to determine the covariance structure of the model (Diggle and Rebeiro 2007). To accommodate these considerations, closely paired random points, or fine-scale hierarchical lattice can be imposed within proximity of a randomly chosen node or grids.

Such a sampling design may be considered for reevaluating potential spatial structures for coral cover with finer scale than 200 m. Yet it is necessary to evaluate effectiveness and efficiency of the suggested sampling design as it increases the number of samples thus costs will increase.

CCA residuals showed a long distance spatial structure around 715 m after trends were removed and directional correlation among errors was accounted for in the model. Thus the abundance of CCA is spatially dependent and also autocorrelated in the ‘Āhihi area.

The spatial model with first-order trend and seascape covariates was a reasonable model. The anisotropic pattern implies the orientation of hard substrate stretching from the northwest to southeast. It was not possible to sample in the northeast and southwest direction due to the land mass and the depth beyond the sampling protocol, thus the direction was constrained.

Wave and water circulation affects spatial patterns of physical, chemical, and biological processes. Litter and Litter (1984) stated that CCA predominates in areas of heavy grazing or wave shear. According to field experience and observations, wind and wave exposure regime could be drastically different at the north or south of Ka Lae Māmane point (Fig. 3.1). The southern proximity of this point showed a strong spatial structure of high CCA cover, while the locale of low cover concentrated in the northern area. These results may indicate that the spatial pattern and structure of CCA corresponds to indirect effects of exposure to wind, wave, and fluid dynamics at ‘Āhihi’s reef. While the field observations generally agreed with the study conducted by

Haraguchi (1979), quantitative data of wind-wave exposure and fluid dynamics measured at site-level would help assess the spatial and non-spatial relationship to CCA cover.

Visual Representation of Predicted Values and Uncertainty

Although parameter setting of simple co-kriging was based on the best subset non-spatial and spatial model, its root-mean-squared prediction error was greater than simple kriging. This approach indicated no substantial improvement for prediction and interpolation by adding depth, rugosity, and organic material. The correlation between CCA cover and covariates were perhaps not strong enough to improve prediction using co-kriging. Using depth and rugosity derived from the digital elevation model, based on LIDAR data, may improve prediction by co-kriging as continuous data provide smooth data points of covariates where the cover data don't exist. Kriging with external drift (KED) may be another option to consider for improvement in prediction if covariates' data are smooth, not punctual as are the point data used. KED accommodates non-stationarity and incorporates secondary variables into the kriging system, similar to the universal kriging accounting for spatial coordinates as trends (Webster and Oliver 2007).

CCA distributions predicted by kriging would be represented differently depending on how kriging weights were determined by regularly or irregularly spaced data. While the available data were spaced irregularly, the potential change in representation and its accuracy might be explored with regularly spaced data. It is not surprising that kriging standard deviations were high in the areas with less dense neighboring points. Increased sample numbers in such areas will reduce errors and represent the distribution more accurately.

The conditional simulations assessed probabilistic patterns of the population distribution with statistical properties of the sample distribution of CCA. Prediction maps generated from the varying number of realizations demonstrated probable representation of the CCA's spatial distribution with uncertainty. This may be a reasonable visualization for the distribution patterns of the population at one point in time. High mean CCA cover was found on the capes, which are exposed to wind and waves. The areas of lower mean cover were found to be in the more protected embayments. This distribution pattern was also observed with sampled data. Sample data around Cape Kīnau fairly represent the population distribution of CCA while the northern area of the cape may not be well represented by samples since higher uncertainty was observed. About 100 to 500 realizations would give representative distribution patterns of mean CCA with associated uncertainty. As an extent of conditional simulations, the Bayesian kriging method may be also explored in the future. This is a kriging method that utilizes existing prior information and the probability distribution and combines with sample data to estimate and predict posterior probability distributions of the outcome.

In this study, the spatial pattern of coral distribution was represented in a non-geostatistical manner, using the deterministic approach for prediction and interpolation. Regardless, it was a reasonable representation when using the inverse distance weighting method based on the cross-validation statistic, the root-mean-squared prediction error calculated from the validation data points. However, another approach may be explored by building the separate geostatistical models or layers for predictors and combine them into a function to predict the distribution patterns of corals.

Conclusions

This study demonstrated the application of spatial statistical analysis to characterize the spatial patterns of CCA and coral abundance at ‘Āhihi’s nearshore reefs. In addition to insights gained from the non-spatial approach, the spatial approach identified degrees of spatial structure in CCA and coral cover. This approach utilized currently available analytical tools from geostatistics and spatial statistics to add new spatially explicit information for benthic covers on ‘Āhihi’s reef at a local yet broad scale.

CCA cover was better described and predicted by a spatial model that accounted for spatial structure. The estimation and prediction of coral cover did not improve dramatically when the spatial relationship was incorporated in the model. This may imply that coral cover was spatially independent from the distance class ≥ 200 m, but depended on spatial structures of rugosity and depth. A hot spot as well as cold spot of CCA cover existed as unique spatial patterns that may relate to varying environmental and ecological processes, seascape characteristics, and internal processes of CCA. Each cover type is likely to operate at a different scale. Coral cover appeared to operate at a finer scale than CCA.

The context and implication of selected models is limited to the studied area. Different covariates from the ones used in this study may be tested in predictive models for both CCA and coral covers as indicators of space-specific processes. Much future study using spatial statistical approaches is needed to assess how general or unique observed patterns of CCA and coral cover in the environment.

Spatial information provided by this analysis will contribute to future spatial planning and monitoring of ‘Āhihi’s nearshore reef. With this new information, one can

identify where biological importance, human use, and natural impacts may overlap.

Results from this study will facilitate efforts to consider and gauge spatial scales of CCA and coral cover responses when designing sampling and monitoring methods. This applied information will also aid in assessing the spatial extent of management needs, and prioritize allocation of available resources and efforts to the area of greatest interest.

Results of this study can support decision making for sustainable use and preservation of ‘Āhihi’s coral reef seascape in future endeavors.

CHAPTER 4

SUMMARY AND CONCLUSION

The overarching goals of this thesis were to produce temporal and spatial information needed to assist the management and conservation of ‘Āhihi Kīna‘u NARS, and to explore the conceptual framework of landscape ecology to further our understanding of relationships between the seascape pattern, local impacts, and distributions of marine resources within ‘Āhihi Kīna‘u NARS, thereby guiding future conservation and management decisions. ‘Āhihi Kīna‘u NARS is the only NARS that encompasses a relatively large marine jurisdictional area (3.27 km^2), and offers the highest level of protection from destruction of the marine environment and extraction of organisms in the Main Hawaiian Islands since its designation in 1973. Seascapes of the reserve consist of ecologically-important habitats, unique biotic and abiotic forms and structures, and restricted human use. The surrounding areas of the NARS receive limited anthropogenic modification, thus keeping its seascape far less impacted than other coastal seascapes on Maui. Therefore, it would be an excellent reference site for long-term environmental and ecological research and monitoring, and should be managed properly to preserve its unique seascape. Prior to the current study, only limited scientific information was available for this area to support management decisions for uses of the inshore reef. Through this study, new detailed temporal and spatial information was produced to support management and preservation of ‘Āhihi Kīna‘u.

This thesis explored and established linkages between landscape ecological perspectives and ‘Āhihi Kīna‘u’s coral reef seascape in a broad sense. A holistic view of

biotic, abiotic, and human interactions and dynamics in a physically explicit space is a fundamental perspective in landscape ecology. Evaluating spatio-temporal patterns and heterogeneity of a landscape across scales is also emphasized in its trans-disciplinary perspectives as heterogeneous patterns and processes of these factors interplay among them. Chapter 2 of this thesis focused on the potential influence of management regimes based on shoreline access closure and recreational activities, and abiotic components on biotic resources. The objectives were to quantify and document potential temporal changes to inshore fish and benthic characteristics resulting from shoreline access closure, and to quantify abiotic environmental variables (i.e., rugosity, sediment composition, grain-size, and temperature) that influence biotic factors. Linkage of this chapter to landscape ecology was featured in assessment of temporal differences in biotic resources affected by management regimes and/or the natural environment. Each study area exhibited varying features of seascape, and was quantified for spatial composition and topography at a fine scale of <0.2 km.

Results in chapter 2 indicated no strong evidence that the shoreline closure facilitated an overall increase or decrease in marine biological resources. Distributions of fish abundance and biomass were highly variable in both 2008 and 2010. While direct effects of the shoreline-closure were not obvious on the fish assemblage, the effects of a long history of legal protection from fishing, relatively isolated and undeveloped shoreline, and suitable habitats are evident. Numeric abundance of fish was considerably higher ($9.7\text{-}45.1 \text{ ha}^{-1} \times 1000$) at inshore sites when compared to sites 3 to 10 m deep in ‘Āhihi Kīna‘u NARS. The mean abundance of inshore fish was $26.7 (\text{ha}^{-1} \times 1000)$ in 2008, and $25.1 (\text{ha}^{-1} \times 1000)$ in 2010. Density ranged from 3.8 to $21.6 (\text{ha}^{-1} \times 1000)$.

1000) among 25 transects at sites 3 to 10 m deep with an average of 11.0 ($\text{ha}^{-1} \times 1000$). Highly-prized species of inshore fish (e.g., Flagtail, Sharpnose Mullet, Parrotfishes, and Yellow Tang) were abundant and frequent at two of the most remote inshore sites, while the lowest numbers were observed at one site, Kanahena Cove with open shoreline access between 2008 and 2010. No temperature or sedimentation anomaly was observed during the years of study. Decline or recovery of coral cover by trampling was not detectable following the two-year closure, as the time-lag between impact and recovery of coral cover is likely to be longer than the time frame of this study. Benthic composition and abundance of other functional organisms remained similar between years of the open- and closed shoreline access. However, coral cover declined substantially at *Montipora* Pond following the closure period (37% decrease in 2010). The decline of live coral cover may be attributed to delayed and/or cascading effects of anthropogenic and natural factors. In addition, high prevalence of *Montipora* White Syndrome was observed during the study period. Results from this study were alarming, and influential in the subsequent NARS management plan to establish and implement monitoring protocol at *Montipora* Pond to further understand processes affecting degraded condition. Findings from this temporal evaluation provided a practical baseline for inshore marine resources, and contributes to a broader discussion of shoreline access closures and coastal resource management.

To understand effects of factors and processes, the landscape ecological approach aims to quantify potential spatial patterns and relationships of phenomena as a first step. In chapter 3, the study identified and characterized spatial patterns of crustose coralline algae (CCA) and coral abundance and distribution in ‘Āhihi area. The strength of spatial

and non-spatial models to best describe these patterns was also evaluated. The scale of study was local yet much broader than the scale of study in chapter 2, describing spatial patterns in continuous seascape beyond delineated inshore study area. The objectives included identifying potential spatial structure within each cover type, determining the representative statistical models that may characterize variability and estimate parameters, and producing prediction maps of CCA and coral distributions. This chapter was linked to the spatial analytical tools employed in landscape ecological approaches. These analytical techniques were used to estimate spatial patterns and examine relationships of CCA and coral distributions to surrounding seascape variables and predict them with estimates of uncertainty.

The resultant explicit spatial information provided new insights into the abundance and distribution of CCA in this area. Crustose coralline algae exhibited spatial structure at greater distances than corals. The spatial dependence and autocorrelation were important components of a predictive model for CCA cover in addition to the seascape variables. Unique clusters of high and low CCA cover were identified. Although coral abundance and distribution appeared independent from autocorrelation when separated by distances greater than 200 m, it was inconclusive regarding its potential autocorrelation at the separation distance less than 200 m. The result also suggested that the distribution of corals appeared to be affected by the spatial patterns of rugosity and depth. The optimal spatial model of CCA was also utilized to represent a probabilistic distribution pattern by employing conditional simulations. Such information can be applied for the development or evaluation of sampling designs and formulation of hypotheses to best understand the relationship between patterns and

processes. Its application also includes a basis for spatial planning and prioritizing management goals in a particular area.

The holistic approach of landscape ecology should be extended to development and implementation of NARS long-term monitoring that integrates assessments of key functional organisms, habitat conditions, water quality, temperature, and human use to determine the relative importance of natural or anthropogenic processes on marine resources. Quantitative spatial analysis and mapping approaches of landscape ecology will help understand processes that interact with resource patterns and distributions, and provide useful, spatially-explicit information for designing a monitoring program, planning and evaluating the extent of existing management measures.

Concepts of landscape ecology provide a bridge between researchers, stakeholders, and managers integrating a holistic view of seascapes components for preservation and sustainable uses of the marine environment. However, one may ask if landscape approaches are needed as specific and practical research aspects to better understand spatial heterogeneity, patterns, and processes. Obviously, a landscape approach is necessary when a researcher expects a significant influence of landscape structure (i.e., spatial composition and configuration) on the response of interest. While application of a landscape approach depends upon the study questions being asked, it may not always be necessary. Fahrig (2005) states that a landscape approach can be time- and money-consuming in research and is not always needed when a sufficient proportion of variation in the response variable is explained with local variables only. However, one may not know if local variables would explain a sufficient variation in the response variable over a heterogeneous landscape, or across different spatial scales unless

an ecological study is conducted in a framework of landscape ecology. Many past ecological studies primarily focused on local variables, and few studies expanded foci on effects of landscape structures. Fahrig (2005) also suggests that a landscape perspective can be ignored in situations where the landscape structure itself is highly dynamic or when the amount of habitat exceeds a threshold. A landscape approach may not help understand patterns and processes of the response variable when a landscape is relatively homogeneous. However, effects of landscape structure are worth being tested for different landscapes including coral reef seascapes, as management strategy has been shifting toward ecosystem-based models, i.e., those dealing with multiple environmental and resource issues.

The integrity of coral reef ecosystems continues to be compromised by anthropogenic impacts, changing climate and ocean chemistry, and cascading effects of these factors at multiple spatial and temporal extents. Therefore, it is important to evaluate various aspects of landscape components to understand ecological systems as a whole, and to develop and implement sound management plans for preservation and sustainable use. Overall, conceptual framework and analytical techniques of landscape ecology present relatively new perspectives in coral reef studies, and may support adaptive and creative management efforts while dealing with dynamic environmental and anthropogenic processes affecting Hawai‘i’s coral reef seascapes.

REFERENCES

- Adey, W.H., Townsend, R.A., and Boykins, W.T. 1982. The Crustose Coralline Algae (Rhodophyta: Corallinaceae) of the Hawaiian Islands. Smithsonian Contribution to the Marine Sciences, No. 15. Washington DC: Smithsonian Institution Press 74p.
- Adey, W.H. 1998. Coral reefs: Algal structured and mediated ecosystems in shallow, turbulent, alkaline waters. *Journal of Phycology* 34(3): 393-406
- Aeby, G.S. 2006. Baseline levels of coral disease in the Northwestern Hawaiian Islands. *Atoll Research Bulletin* 543:471-488
- Aeby, G. S., Ross, M., Williams, G.J., Lewis, T.D, and Work, T.M. 2010. Disease dynamics of *Montipora* white syndrome within Kāne‘ohe Bay, Oahu, Hawai‘i: Distribution, seasonality, virulence, and transmissibility. *Diseases of Aquatic Organisms* 91(1): 1-8
- AECOS, Inc. 1979. Maui Coastal Zone Atlas, Hawaii Coral Reef Inventory Part C, Island of Maui. Kāne‘ohe: AECOS, Inc. 86p.
- Allison, W.R. 1996. Snorkeler damage to reef corals in the Maldives Islands. *Coral Reefs* 15: 215-218
- Anselin, L. 1995. Local indicators of spatial association, LISA. *Geographical Analysis* 27(2): 93-115
- Anselin, L., Syabri,I., and Kho, Y. 2006. GeoDa: An introduction to spatial data analysis. *Geographical Analysis* 38(1): 5-22.
- Battista, T.A., Costa, B.M., Anderson, S.M. 2007. Shallow-water benthic habitats of the main Hawaiian islands (DVD). Silver Spring, MD.
- Bellwood, D.R. 1995. Carbonate transport and within reef patterns of bioerosion and sediment release in parrotfishes (family Scaridae) on the Great Barrier Reef. *Marine Ecology Progress Series* 117: 127-136
- Bengtsson, L. and Enell, M. 1986. Chemical analysis. In Handbook of Holocene Palaeoecology and Palaeo-hydrology. Ed. Berglund, B.E. Chichester: John Wiley & Sons pp. 423-451
- Beyer, H. 2004. Hawth's Analysis Tools for ArcGIS (downloadable on-line software). Spatial Ecology.com <http://www.spatialecology.com/index.php>

- Bird, C. E. 2001. PhotoGrid: ecological analysis of digital photographs (downloadable on-line software). University of Hawai‘i Mānoa, Honolulu, HI.
<http://www.photogrid.netfirms.com/>
- Birkeland, C. 1982. Terrestrial runoff as a cause of outbreaks of *Acanthaster planci* (Echinodermata, Asteroidea). *Marine Biology* 69(2): 175-185.
- Boggs, S. 1995. Principles of Sedimentology and Stratigraphy. 2nd ed. New Jersey: Prentice-Hall 774p.
- Brock, R.E. 1982. A critique of the visual census method for assessing coral reef fish populations. *Bulletin of Marine Science* 32: 269-276
- Brock, V.E. 1954. A preliminary report on a method of estimating reef fish populations. *Journal of Wildlife Management* 18: 297-308
- Brown, B. 1997. Disturbances to reefs in recent times. pp. 354-379 Birkeland, C. ed. In: Life and Death of Coral Reefs. New York: Chapman and Hall
- Bruggemann, J.H., van Kessel, A.M., van Rooji, J.M., and Breeman, A.M. 1996. Bioerosion and sediment ingestion by the Caribbean parrotfish *Scarus vetula* and *Sparisoma viride*: Implication of fish size, feeding mode and habitat use. *Marine Ecology Progress Series* 134: 59-71
- Bruno, J.F., Selig E.R., Casey K.S., Page C.A., Willis B.L., Harvell, C.D., Sweatman, H., and Melendy, A.M. 2007. Thermal stress and coral cover as drivers of coral disease outbreaks. PLoS Biol 5(6): e124.doi:10.1371/journal.pbio.0050124
- Bryant, D., Burke, L., McManus, J., and Spalding, M. 1998. Reefs at Risk. A Map-based Indicator of Threats to the World’s Coral Reefs. Washington, DC: World Resources Institute 60p.
- Cesar, H.S.J., and van Beukering, P.J.H. 2004. Economic valuation of the coral reefs of Hawai‘i. *Pacific Science* 58(2): 231-242
- Chabanet, P., Adjeroud, M., Andréfouët, S., Bozec, Y., Ferraris, J., García-Charton, J., and Schrimm, M. 2005. Human-induced physical disturbances and their indicators on coral reef habitats: A multi-scale approach. *Aquatic Living Resources* 18: 215-230
- Claisse, J.T., Kienzle, M., Bushnell, M.E., Shafer, D.J., and Parrish, J.D. 2009. Habitat- and sex-specific life history patterns of yellow tang *Zebrasoma flavescens* in Hawai‘i, USA. *Marine Ecology Progress Series* 389: 245-255

Coles, S.L and Jokiel, P.L. 1978. Synergistic effects of temperature, salinity, and light on the hermatypic coral *Montipora verrucosa*. *Marine Biology* 49: 187-195

Connell, J. H. 1978. Diversity in tropical rain forests and coral reefs. *Science* 199: 1302-1310

Connell, J.H. 1997. Disturbance and recovery of coral assemblages. *Coral Reefs* 16 (Suppl.): S101-S113

Connell, J.H., Hughes, T.H., Wallace, C.C. 1997. A 30-year study of coral abundance recruitment, and disturbance at several scales in space and time. *Ecological Monographs* 67 (4): 461-488

Costanza, R., D'Arge, R., De Groot, R., Farber, S., Grasso, M., Hannon, B., Limburg, K., Naeem, S., O'Neill, R.V., Paruelo, J., Raskin, R.G., Sutton, P., Van Den Belt, M. 1997. The value of the world's ecosystem services and natural capital. *Nature* 387: 253-260

Craft, C.B., Seneca, E.B. and Broome, S.W. 1991. Loss on ignition and Kjeldahl digestion for estimating organic carbon and total nitrogen in estuarine marsh soils: Calibration with dry combustion. *Estuaries* 14: 175-179

Cressie, N.A. 1993. Statistics for Spatial Data. Revised Edition. New York: John Wiley & Sons 900p.

Dean, W.E. 1974 Determination of carbonate and organic matter in calcareous sediments and sedimentary rocks by loss on ignition: Comparison with other methods. *Journal of Sedimentary Petrology* 44(1): 242-248

Delisle, L. 2007. A Spatial Approach to Estimating Soil Carbon Stocks at the Field Level. M.S. Thesis. Department of Agronomy and Soil Science, University of Hawai‘i Mānoa, Honolulu. 146p.

DeMartini, E.E., Anderson, T.W., Kenyon, J.C., Beets, J.P., Friedlander, A.M. 2010. Management implications of juvenile reef fish habitat preferences and coral susceptibility to stressors. *Marine and Freshwater Research* 61: 532-540

DeMello, J.K. 2004. Commercial marine landings from fisheries on the coral reef ecosystem of the Hawaiian Archipelago. pp. 157-170. Friedlander, A. ed. In: Status of Hawai‘i’s Coastal Fisheries in the New Millennium, Proceedings of the 2001 Fisheries Symposium, American Fisheries Society, Hawai‘i Chapter. 2004.

- Department of Business, Economic Development and Tourism (DBEDT), State of Hawai‘i. 2010. web. Accessed June, 2011.
http://hawaii.gov/dbedt/info/census/Census_2010/Apportionment/Hawaii_2010_population_Summary.pdf
- Diggle, P.J. and Ribeiro Jr., P.J. 2007. Model-based Geostatistics. New York: Springer 228p.
- Division of Forestry and Wildlife (DOFAW), Natural Area Reserve System (NARS), Department of Land and Natural Resources (DLNR), State of Hawai‘i. 2008. web. Accessed September, 2008.
<http://hawaii.gov/dlnr/dofaw/nars/reserves/maui/ahihikinau>
- Dollar, S.J. 1982. Wave stress and coral community structure in Hawai‘i. *Coral Reefs* 1: 71-81
- Dollar, S.J. and Tribble, G.W. 1993. Recurrent storm disturbance and recovery: a long-term study of coral communities in Hawai‘i. *Coral Reefs* 12: 223-233
- ESRI. 2003. Using ArcGIS Geostatistical Analyst. Redlands, CA: Environmental Systems Research Institute, Inc.
- Eversole, D. and Fletcher, C.H. 2003. Longshore sediment transport rates on a reef-fronted beach: Field data and empirical models Kaanapali Beach, Hawai‘i. *Journal of Coastal Research* 19(3): 649-663.
- Ewel K.C., Cressa C., Kneib R.T., Lake P.S., Levin L.A., Palmer M.A., Snelgrove P. and Wall D.H. 2001. Managing critical transition zones. *Ecosystems* 4: 452-460
- Fabricius, K. and De’ath, G. 2001. Environmental factors associated with the spatial distribution of crustose coralline algae on the Great Barrier Reef. *Coral Reefs* 19: 303-309
- Fabricius, K. E. 2005. Effects of terrestrial runoff on the ecology of corals and coral reefs: Review and synthesis. *Marine Pollution Bulletin* 50(2): 125-146
- Fahrig, L. 2005. When is a landscape perspective important? pp. 3-9 In Issues and Perspectives in Landscape Ecology. Eds. Wiens, J.A., and Moss, M.R. New York: Cambridge University Press
- Fielding, E. The Nature Conservancy. Personal communication. Makawao, Hawaii. October 30, 2008
- FishBase. 2000. Global information systems on fishes. www.fishbase.org

Fletcher, C. 2010. Hawai‘i’s changing climate: Briefing sheet. Center for Island Climate Adaptation and Policy, Sea Grant College Program, University of Hawai‘i. Honolulu, HI. 7p.

Forman, R.T.T. 1983. An ecology of the landscape. *BioScience* 33: 535

Forman, R.T.T. 1995. Some general principles of landscape and regional ecology. *Landscape Ecology* 10: 133-142

Forman, R.T.T, and Godron, M. 1986. *Landscape Ecology*. New York: John Wiley & Sons 620p.

Fortin, M.-J., and Dale, M.R.T. 2005. *Spatial Analysis: A guide for ecologists*. Cambridge: Cambridge University Press 365p.

Friedlander, A.M. and Parrish, J.D. 1998. Habitat characteristics affecting fish assemblages on a Hawaiian coral reef. *Journal of Experimental Marine Biology and Ecology* 224(1): 1-30

Friedlander, A.M., Brown, E.K., Jokiel, P.L., Smith, W.R., Rodgers, K.S. 2003. Effects of habitat, wave exposure, and marine protected area status on coral reef fish assemblages in the Hawaiian archipelago. *Coral Reefs* 22: 291-305

Friedlander, A.M., Aeby, G., Brown, E., Clark, A., Coles, S., Dollar, C., Hunter, C., Jokiel, P.J., Smith, B., Walsh, W., Williams, I., and Wiltse, W. 2005. The state of coral reef ecosystems of the Main Hawaiian Islands. pp. 222-269. Waddel, J. ed., In: *The state of coral reef ecosystems of the United States and Pacific freely associated states: 2005*. NOAA Technical Memorandum NOS NCCOS 11. NOAA/NOCCS Center for Coastal Monitoring and Assessment's Biogeography Team. Silver Spring, MD.

Gattuso, J.P., Allemand, D. and Frankignoulle, M. 1999. Photosynthesis and calcification at cellular, organismal and community levels in coral reefs: a review on interactions and control by carbonate chemistry. *American Zoologist* 39: 160-183.

Gilmour, J. 1999. Experimental investigation into the effects of suspended sediment on fertilization, larval survival and settlement in a scleractinian coral. *Marine Biology* 135: 451-462

Glynn, P.W. 1974. Rolling stones among the scleractinia: Mobile coralliths in the Gulf of Panama. pp. 183-200. Cameron, A.M., Cambell, B.M., Cribb, A.B., Endean, R., Jell, J.S., Jones, O.A., Mather, P., and Talbot, F.H. eds. In: *Proceedings of the Second International Coral Reef Symposium Vol. 2*. The Great Barrier Reef Committee, Brisbane, Australia.

- Godwin, S.L. Papahānaumokuākea National Marine Monument. Personal communication. Honolulu, HI. January 22, 2010.
- Goovaerts, P. 1997. Geostatistics for Natural Resource Evaluation. New York: Oxford University Press 483p.
- Gosline, W.A., and Brock, V.E. 1960. Handbook of Hawaiian Fishes. Honolulu: University Press of Hawai‘i 372p.
- Green, E.P., Mumby, P.J., Edwards, A.J., and Clark, C.D. 1996. A review of remote sensing for the assessment and management of tropical coastal resources. *Coastal Management* 24(1): 1-40
- Green, E.P., Mumby, P.J., Edwards, A.J., and Clark, C.D. 2000. Remote Sensing Handbook for Tropical Coastal Management. Edwards, A.J. ed. Paris: United Nations Educational, Scientific and Cultural Organization 316p.
- Grigg, R.W. 1983. Community structure, succession and development of coral reefs in Hawai‘i. *Marine Ecology Progress Series* 11:1-14
- Grigg, R.W. and Dollar, S.J. 1990. Natural and anthropogenic disturbance on coral reefs. pp. 439-452 Dubinsky, Z. ed. In: *Ecosystems of the World 25, Coral Reefs*. New York: Elsevier Science Publishing Company
- Grober-Dunsmore, R., Frazer, T.K., Beets, J.P., Lindberg, W.J., Zwick, P. Funicelli, N.A. 2008. Influence of landscape structure on reef fish assemblages. *Landscape Ecology* 23: 37-53
- Guinther, E., and Bartram, P. 1979. Maui Coastal Zone Atlas. Hawai‘i Coral Reef Inventory, Island of Maui (MICRI), Part C. Kāne‘ohe: AECOS, Inc.
- Gustafson, E.J. 1998. Quantifying landscape spatial pattern: what is the state of the art? *Ecosystems* 1:143-156
- Guzner, B., Novoplansky, A., Shalit, O., and Chadwick, N.E. 2010. Indirect impacts of recreational scuba diving: Patterns of growth and predation in branching stony corals. *Bulletin of Marine Science* 86(3): 727-742
- Hamnet, M., Lui, M., and Johnson, D. 2006. Fishing, Ocean Recreation, and Threats to Hawaii’s Coral Reefs. Social Science Research Institute, University of Hawai‘i at Mānoa. Honolulu, Hawai‘i 6p.
- Haraguchi, P. 1979. Weather in Hawaiian Waters. Honolulu: Pacific Weather 107p.

Harborne, A.R., Mumby, P.J., Zychaluk, K., Hedley, J.D., Blackwell, P.G. 2006.
Modeling the beta diversity of coral reefs. *Ecology* 87(11): 2871-2881

Hawai'i Cooperative Fisheries Research Unit (HCFRU). 2008. Biology of Parrotfish in
Hawai'i. Final Report for the Western Pacific Regional Fishery Management
Council, Hololulu, Hawai'i. January, 2008. 37p.

Hawai'i Tourism Authority (HTA). 2003. Natural Resource Assessment, Report vol. 1.
274p.

Hawai'i Tourism Authority (HTA). 2009. Visitor Satisfaction and Activity Report.
184p. web. Accessed June, 2011. <http://hawaii.gov/dbedt/info/visitor>

Hawkins J.P. and Roberts, C. M. 1993. Effects of recreational scuba diving on coral
reefs: trampling on reef-flat communities. *Journal of Applied Ecology* 30: 25-30

Hawkins, J.P., Roberts, C.M., Van't Hof, T., DeMeyer, K., Tratalos, J., and Aldam, C.
1999. Effects of recreational scuba diving on Caribbean coral and fish
communities. *Conservation Biology* 13(4): 888-897

Heiri, O., Lotter, A.F., and Lemcke, G. 2001. Loss on ignition as a method for
estimating organic and carbonate content in sediments: Reproducibility and
comparability of results. *Journal of Paleolimnology* 25: 101-110

Heyward, A.J. and Negri, A.P. 1999. Natural inducers for coral larval metamorphosis.
Coral Reefs 18(3): 273-279

Hinchey, E.K., Nicholson M.C., Zajac R.N. and Irlandi E.A. 2008. Preface: Marine and
coastal application of landscape ecology. *Landscape Ecology* 23: 1-5

Hochberg, E.J., and Atkinson, M.J. 2003. Capabilities of remote sensors to classify coral,
algae, and sand as pure and mixed spectra. *Remote Sensing of Environment* 85:
174-189

Hodgson, G. 1990. Tetracycline reduces sedimentation damage to corals. *Marine
Biology* 104(3): 493-496

Hoegh-Guldberg, O. 1999. Climate change, coral bleaching and the future of the
world's coral reefs. *Marine and Freshwater Research* 50: 839-866

Hoegh-Guldberg, O., Mumby, P. J., Hooten, A. J., Steneck, R. S., Greenfield, P., Gomez,
E., Harvell, C. D., Sale, P. F., Edwards, A. J., Caldeira, K., Knowlton, N., Eakin,
C. M., Iglesias-Prieto, R., Muthiga, N., Bradbury, R. H., Dubi, A. and Hatziolos,
M. E. 2007. Coral reefs under rapid climate change and ocean acidification.
Science 318: 1737-1742

- Hoover, J.P. 2007. Hawaii's Fishes: A guide for snorkelers and divers. 2nd ed. Honolulu: Mutual Publishing 181p.
- Hughes, T.P., and Connell, J.H. 1999. Multiple stressors on coral reefs: A long-term perspective. *Limnology and Oceanography* 44: 932-940
- Hughes, T.P., Baird, A.H., Bellwood, D.R., Card, M., Connolly, S.R., Folke, C., Grosberg, R., Hoegh-Guldberg, O., Jackson, J.B.C., Kleypas, J., Lough, J.M., Marshall, P., Nyström, M., Palumbi, S.R., Pandolfi, J.M., Rosen, B., and Roughgarden, J. 2003. Climate change, human impacts, and the resilience of coral reefs. *Science* 301: 929-933
- Hunter, C.L. and Evans, C.W. 1995. Coral reefs in Kāne‘ohe Bay, Hawai‘i: two centuries of western influence and two decades of data. *Bulletin of Marine Science* 57: 501-515
- Irish, J.L. 2000. An introduction to coastal zone mapping with airborne LIDAR: The SHOALS system. Proceedings 21. In: Techincheper la Diffesa Dallinquimento, Cosenza, Italy. web. Accessed June, 2011.
<http://shoals.sam.usace.army.mil/Publications.aspx>.
- Isaaks, E.H., and Strivastava, R.M. 1989. Applied Geostatistics. New York: Oxford University Press 561p.
- Jokiel, P.L. 2006. Impact of storm waves and storm floods on Hawaiian reefs. pp. 390-398. In: Proceedings of 10th International Coral Reef Symposium, Okinawa, Japan. June 28-July 4, 2004.
- Jokiel, P.L. 2008. Biology and ecological functioning of coral reefs in the Main Hawaiian Islands. pp. 489-517. Riegl, B.M. and Dodge, R.E. eds. In: *Coral Reefs of the USA*. New York: Springer
- Jokiel, P.L. and Coles, S.L. 1974. Effects of heated effluent on hermatypic corals at Kahe Point, Oahu. *Pacific Science* 28:1-18
- Jokiel, P.L. and Coles, S.L. 1977. Effects of temperature on mortality and growth of Hawaiian reef corals. *Marine Biology* 43: 201-208
- Jokiel, P.L. and Coles, S.L. 1990. Response of Hawaiian and other Indo-Pacific reef corals to elevated temperature. *Coral Reefs* 8: 155-162
- Jokiel, P.L. and Brown, E.K. 2004. Global warming, regional trends and inshore environmental conditions influence coral bleaching in Hawaii. *Global Change Biology* 10: 1627-1641

- Jokiel P.L., Brown E.K., Friedlander A., Rodgers S.K. and Smith W.R. 2004. Hawai'i coral reef assessment and monitoring program: Spatial patterns and temporal dynamics in reef coral communities. *Pacific Science* 58: 159-174
- Jokiel, P.L., Rodgers, K., Kuffner, I., Andersson, A., Cox, E.A and Mackenzie, F. 2008. Ocean acidification and calcifying reef organisms: A mesocosm investigation. *Coral Reefs* 27: 473-483.
- Kay, A.M and Liddle, M.J. 1989. Impact of human trampling in different zones of a coral reef flat. *Environmental Management* 13(4): 509-520
- Kerbiriou C., Leviol I., Jiguet F. and Julliard R. 2008. The impact of human frequentation on coastal vegetation in a biosphere reserve. *Journal of Environmental Management* 88: 715-728
- Kiene, W.E. 1988. A model of bioerosion on the Great Barrier Reef. pp. 449-454. Choat, J.H., D. Barnes, MA. Borowitzka, J.C. Coll, P.J.Davies, P. Flood, B.G. Hatcher, D. Hopley, P.A. Hutchings, D. Kinsey, G.R. Orme, M. Pichon, P.F. Sale, P. Sammarco, C.C. Wallace, C. Wilkinson, E. Wolanski and O. Bellwood eds. In: Proceedings of the 6th International Coral Reef Symposium Vol. 3. Townsville, Australia.
- Kleypas, J. A., Buddemeier, R. W., Archer, D., Gattuso, J.-P., Langdon, C. and Opdyke, B. N. 1999. Geochemical consequences of increased atmospheric carbon dioxide on coral reefs. *Science* 284: 118-120
- Kördel, W., Dassenakis, M., Lintelmann, J., and Padberg, S. 1997. The importance of natural organic material for environmental processes in waters and soils. Technical Report. *Pure and Applied Chemistry* 69(7): 1571-1600
- Kunter, M.H., Nachtsheim, C.J., Neter, J., and Li, W. 2005. Applied Linear Statistical Models. 5th ed. New York: McGraw-Hill/Irwin 1396p.
- Leeder, M.R. 1982. Sedimentology: Process and Product. London: George Allen & Unwin (Publishers) Ltd, 344p.
- Legendre, P. 1993. Spatial autocorrelation: trouble or new paradigm? *Ecology* 74(6): 1659-1673
- Legendre, P., and Legendre, L. 1998. Numerical Ecology. 2nd ed. Amsterdam: Elsevier Science 853p.
- Lepczyk C.A., Lortie C.J. and Anderson L.J. 2008. An ontology for landscapes. *Ecological Complexity* 5: 272-279

- Levin, S.A. 1976. Spatial patterning and the structure of ecological communities. *Lectures on Mathematics in the Life Science* 8: 1-35
- Levin, S.A. 1992. The problem of pattern and scale in ecology. *Ecology* 73(6): 1943-1967
- Li, H. and Raynolds, J.F. 1995. On definition and quantification of heterogeneity. *Oikos* 73:280-284
- Liddle, M.J. and Kay, A.M. 1987. Resistance, survival and recovery of trampled corals on the Great Barrier Reef. *Biological Conservation* 42(1): 1-18.
- Littell, R.C., Milliken, G.A., Stroup, W.W., Wolfinger, R.D., and Schabenberger, O. 2006. SAS for Mixed Models. 2nd ed. Cary, North Carolina: SAS Institute, Inc. 814p.
- Litter, M. 1973. The population and community structure fo Hawaiian fringing-reef crustose corallineae (Rhodophyta, Cryptonemiales). *Journal of Experimental Marine Biology and Ecology* 11:103-120
- Litter, M.M. and Litter, D.S. 1984. Models of tropical reef biogenesis: The contribution of algae. Round, E.F., and Chapman, D.J. eds. In: Progress in Phycological Research, Vol. 3. Bristol: Biopress, Ltd. pp. 323-364
- Liu, J. and Taylor, W.W. 2002. Coupling landscape ecology with natural resource management: Paradigm shifts and new approaches. In: Integrating Landscape Ecology into Natural Resource Management. Eds. Liu, J. and Taylor, W.W. New York: Cambridge University Press pp. 3-19
- Longenecker, K. and Langston, R. 2008. Life History Compendium of Exploited Hawaiian Fishes. A Report prepared for Fisheries Local Action Strategy and Division of Aquatic Resources, Honolulu, HI 61p.
- Macdonald, G.A., Abbott, A.T., and Peterson, F.L. 1990. Volcanoes in the Sea: The Geology of Hawai'i. 2nd ed. Honolulu: University of Hawai'i Press 517p.
- McCormick, M. 1994. Comparison of field methods for measuring surface topography and their associations with a tropical reef fish assemblage. *Marine Ecology Progress Series* 112: 87-96
- McManus, J. 1988. Grain size determination and interpretation. In: *Techniques in Sedimentology* Ed. Tucker, M. Oxford: Blackwell Scientific Publications, pp. 63-85

Minitab 15 Statistical Software. 2007. State College, PA: Minitab, Inc.
www.minitab.com

Moberg, F. and Folke, C. 1999. Ecological goods and services of coral reef ecosystems.
Ecological Economics 29: 215-233

Moran, P.A.P. 1950. Notes on continuous stochastic phenomena. *Biometrika* 37(1/2):
17-23.

Morse, D.E., Hooker, N., Morse, A.N.C., and Jensen, R.A. 1988. Control of larval
metamorphosis and recruitment in sympatric agariciid corals. *Journal of
Experimental Marine Biology and Ecology* 116: 193-217

Mumby, P.J., Green, E.P., Edwards, A.J., and Clark, C.D. 1997. Coral reef habitat-
mapping: how much detail can remote sensing provide? *Marine Biology* 130(2):
193-202

Mumby, P.J., Skirving, W., Strong, A.E., Hardy, J.T., LeDrew, E.F., Hochberg, E.J.,
Stumpf, R.P., and David, L.T. 2004a. Remote sensing of coral reefs and their
physical environment. *Marine Pollution Bulletin* 48: 219-228

Mumby, P.J., Hedley, J.D., Skirving, W., Strong, A.E., Hardy, J.T., LeDrew, E.F.,
Hochberg, E.J., Stumpf, R.P., and David, L.T. 2004b. The cover of living and
dead corals from airborne remote sensing. *Coral Reefs* 23(2): 171-183

Nyström, M., Folke, C., and Moberg, F. 2000. Coral reef disturbance and resilience in a
human-dominated environment. *Trends in Ecology & Evolution* 15: 413-417

O'Neill R.V., Turner S.J., Cullinan V.I., Coffin D.P., Cook T., Conley W., Brunt J.,
Thomas J.M., Conley M.R. and Gosz J. 1991. Multiple landscape scales: An
intersite comparison. *Landscape Ecology* 5: 137-144

Ong, L., and Holland, K.N. 2010. Bioerosion of coral reefs by two Hawaiian
parrotfishes: Species, size differences, and fishery implications. *Marine Biology*
157:1313-1323

Orr, J. C., Fabry, V. J., Aumont, O., Bopp, L., Doney, S. C., Feely, R. A., Gnanadesikan,
A., Gruber, N., Ishida, A., Joos, F., Key, R. M., Lindsay, K., Maier-Reimer, E.,
Matear, R., Monfray, P., Mouchet, A., Najjar, R. G., Plattner, G.K., Rodgers, K.
B., Sabine, C. L., Sarmiento, J. L., Schlitzer, R., Slater, R. D., Totterdell, I. J.,
Weirig, M.F., Yamanaka, Y. and Yool, A. 2005. Anthropogenic ocean
acidification over the twenty-first century and its impact on calcifying organisms.
Nature 437: 681-686.

- Ortiz, D. M. and Tissot, B. N. 2008. Ontogenetic patterns of habitat use by reef-fish in a marine protected area network: A multi-scaled remote sensing and *in situ* approach. *Marine Ecology Progress Series* 365: 217-232.
- Pandolfi, J. M., Bradbury, R.H., Sala, E., Hughes, T.P., Bjorndal, K.A., Cooke, R.G., McArdle, D., McClenachan, L., Newman, M.J.H., Paredes, G., Warner, R.R., Jackson, J.B.C. 2003. Global trajectories of the long-term decline of coral reef ecosystems. *Science* 301: 955-958
- Pandolfi, J. M., Jackson, J.B.C., Baron, N., Bradbury, R.H., Guzman, H.M., Hughes, T.P., Kappel, C.V., Micheli, G., Ogden, J.C., Possingham, H.P., Sala, E. 2005. Are U.S. coral reefs on the slippery slope to slime? *Science* 307: 1725-1726
- Parker, J. G. 1983. A comparison of methods used for the measurement of organic matter in marine sediment. *Chemistry and Ecology* 1: 201-210
- Peterson, F.L. 1972. Water development on tropic volcanic islands, type example: Hawai‘i. *Ground Water* 10(5): 18-23
- Petitgas, P. Geostatistics and their applications to fisheries survey data. 1996. pp. 113-142. Megrey, B.A. and Moksness, E. eds. In: Computers in Fisheries Research. New York: Chapman and Hall 224p.
- Pickett, S.T.A., and Cadenasso, M.T. 1995. Landscape ecology: Spatial heterogeneity in ecosystems. *Science* 269(5222): 331-334
- Pinheiro, J., and Bates, D. 2009. Mixed Effects Models in S and S-Plus. 2nd printing. New York: Springer 528p.
- Pittman, S.J., McAlpine, C.A., Pittman, K.M. 2004. Linking fish and prawns to their environment: A hierarchical landscape approach. *Marine Ecology Progress Series* 283: 233-254
- Pittman, S.J., Christensen, J.D., Cladow, C., Menza, C., and Monaco, M.E. 2007. Predictive mapping of fish species richness across shallow-water seascapes in the Caribbean. *Ecological Modeling* 204: 9-21
- Ramsey, M. Āhihi Kīna‘u Natural Area Reserve System. Personal communication. Kahului, HI. September 20, 2008.
- Randall, J.E. 2007. Reef and Shore Fishes of the Hawaiian Islands. Honolulu: Sea Grant College Program, University of Hawai‘i 546p.

R Development Core Team. 2011. R: A language and environment for statistical Computing (downloadable on-line software). R Foundation for Statistical Computing, Vienna, Austria. ISBN 3-900051-07-0, URL <http://www.R-project.org>.

Ribeiro Jr., P.J. and Diggle, P.J. 2001. geoR: a package for geostatistical analysis. *R-NEWS* 1(2):15-18

Richmond, R. H. 1993. Coral reefs: Present problems and future concerns resulting from anthropogenic disturbance. *American Zoologist* 33(6): 524-536

Risser, P.G., Karr, J.R., and Forman, R.T.T. 1984. Landscape Ecology: directions and approaches. Special Publication Number 2. Illinois Natural History Survey, Champaign, Illinois, U.S.A. pp. 6-16

Rodgers, K. S. 2001. A Quantitative Evaluation of Trampling Effects on Hawai‘i’s Coral Reefs. Masters Thesis. University of Hawai‘i, Department of Geography. Honolulu, Hawai‘i. 163p.

Rodgers, K.S. 2005. Evaluation of Nearshore Coral Reef Condition and Identification of Indicators in the Main Hawaiian Islands. Dissertation. Department of Geography, University of Hawai‘i Mānoa, Honolulu. 203p.

Rodgers, K.S. and Cox, E.F. 2003. The effect of trampling on Hawaiian corals along a gradient of human use. *Biological Conservation* 112: 383-389

Rodgers, K.S., Cox, E.F., and Newtonson, C. 2003. Effects of mechanical fracturing and experimental trampling on Hawaiian corals. *Environmental Management* 31(3): 377-384

Rodgers, K.S. and Jokiel, P.L. 2008. Evaluation of the Āhihi Kīna‘u Natural Area Reserve Marine Resources: Human Impact Evaluation on Nearshore Environments. Hawai‘i Coral Reef Monitoring Program Report (CRAMP) for Hawai‘i Natural Area Reserve System (NARS), Department of Land and Natural Resources, Honolulu, Hawai‘i. April 2, 2008. 24p.

Rodgers, K.S., Jokiel, P.L., Naughton, E.N., Morgan, T. and Farrell, A. 2008. Marine Resources of the Āhihi-Kīna‘u Natural Area Reserve: Compilation of Existing Information on the Marine Environment. Hawai‘I Coral Reef Monitoring Program Report (CRAMP) for Hawai‘i Natural Area Reserve System (NARS), Department of Land and Natural Resources, Honolulu, Hawai‘i. June 1, 2008. 124p.

Rodgers, K.S., Jokiel, P.L., Franklin, E.C., Uchino, K and Ross, L. 2009. Biological Assessment of ‘Āhihi-Kīna‘u Natural Area Reserve, Maui, Hawai‘i. Hawai‘i Coral Reef Monitoring Program Report (CRAMP) for Hawai‘i Natural Area Reserve System (NARS), Department of Land and Natural Resources, Honolulu, Hawai‘i. January 25, 2009. 59p.

Rogers, C.S. 1990. Responses of coral reefs and reef organisms to sedimentation. *Marine Ecology Progress Series* 62: 185-202

Rosenberg, E. and Ben-Haim, Y. 2002. Microbial diseases of corals and global warming. *Environmental Microbiology* 4(6): 318-326

Ross, M. University of Hawai‘i Mānoa, Department of Zoology. Personal communication. Honolulu, HI. January 08, 2010.

Sales, M.H., Souza, C.M. Jr., Kyriakidis, P.C., Roberts, D.A., Vidal, E.D. 2007. Improving spatial distribution estimation of forest biomass with geostatistics: A case study for Rondônia, Brazil. *Ecological Modeling* 205: 221-230

SAS Institute Inc. 1999. The VARIOGRAM Procedure, SAS/STAT User’s Guide, Version 8. NC: SAS Institute Inc. web. Accessed July, 2011.
<http://v8doc.sas.com/sashelp/>

Sequir, C. University of Hawai‘i Mānoa, Department of Botany. Personal communication. Honolulu, HI. May 6, 2010.

Sherrod, D.R., Sinton, J.M., Watkins, S.E., and Brunt, K.M. 2007. Geologic map of the state of Hawai‘i, Sheet 7, Island of Maui. web. Accessed September, 2010.
<http://pubs.usgs.gov/of/2007/1089/>

Smith, J.S., Smith, C.S., and Hunter, C.L. 2001. An experimental analysis of the effects of herbivory and nutrient enrichment on benthic community dynamics on a Hawaiian reef. *Coral Reefs* 19(4): 332-342

Smith, J.S., Hunter, C.L., and Smith, C.S. 2010. The effects of top-down versus bottom-up control on benthic coral reef community structure. *Oecologia* 163(2): 497-507Stearns, H.T. 1985. Geology of the State of Hawaii. 2nd ed. Palo Alto, CA: Pacific Books 335p.

Storlazzi, C.D., Field, M.E., Dykes, J.D., Jokiel, P.L., and Brown, E. 2002. Wave control on reef morphology and coral distribution: Moloka‘i, Hawai‘i. pp. 784-793 WAVES 2001 Conference Proceedings, American Society of Civil Engineers, San Francisco, California, Vol. 1

- Storlazzi, C.D., Ogston, A.S., Bothner, M.H., Field, M.E., and Presto, M.K. 2004. Wave- and tidally-driven flow and sediment flux across a fringing coral reef: Southern Moloka‘i, Hawai‘i. *Continental Shelf Research* 24: 1397-1419
- Storlazzi, C.D., Field, M.E., Bothner, M.H., Presto, M.K., and Draut, A.E. 2009. Sedimentation processes in a coral reef embayment: Hanalei Bay, Kauai. *Marine Geology* 246: 140-151
- Sutherland, R.A. 1998. Loss-on-ignition estimates of organic matter and relationships to organic carbon in fluvial bed sediments. *Hydrobiologia* 389: 153-167
- Sutherland, R.A., Bussen, J.O., Plondke, D.L., Evans, M.B., and Ziegler, A.D. 2001. Hydrophysical degradation associated with hiking-trail use: a case study of Hawai‘iloa Ridge Trail, O‘ahu, Hawai‘i. *Land Degradation & Development* 12: 71-86
- Te, F.T. 2001. Response of Hawaiian Scleractinian Corals to Different Levels of Terrestrial and Carbonate Sediment. Dissertation. Department of Zoology, University of Hawai‘i Mānoa, Honolulu. 286p.
- Thompson, M. J. and Schmidt, T.W. 1977. Validation of the species/time random count technique sampling fish assemblages. Pp. 283-288. Taylor, D.L. ed. In: Proceedings of Third International Coral Reef Symposium, Rosenstiel School of Marine and Atmospheric Science, University of Miami, Florida. Vol. 1.
- Turner, M.G. 1989. Landscape ecology: the effect of pattern on process. *Annual Review of Ecology and Systematics* 20:171-197
- Turner, M.G. 2005. Landscape ecology in North America: Past, present, and future. *Ecology* 86(8): 1967-1974
- Turner, M.G., Gardner R.H., O’neill, R.V. 2001. Landscape Ecology in Theory and Practice: Pattern and Process. New York: Springer 405p.
- Turner M.G., Crow, T.R., Liu, J., Rabe, D., Rabeni, C.F., Soranno, P.A., Taylor, W.W., Vogt, K.A., and Wiens, J.A. 2002. Bridging the gap between landscape ecology and natural resource management. In: Integrating Landscape Ecology into Natural Resource Management. Eds. Liu, J. and Taylor, W.W. New York: Cambridge University Press pp. 433-460
- Vann, C., Edwards, J., and Bernard H. 2006. Human Usage Patterns at Keone‘ō‘io, South Maui Car Census and Technical Surveys. Progress Report 7 Hawai‘i Tourism Authority Contract with DLNR No. BT-04-64 for Hawai‘i Wildlife Fund. June 26, 2006. 15p.

- Vargas-Ángel, B., Asher, J., Godwin, L.S., and Brainard, R.E. 2008. Invasive didemnid tunicate spreading across coral reefs at remote Swains Island, American Sāmoa. *Coral Reefs* 28:53
- Verger, R.P. 2008. Hawai‘i’s Vanishing Streamflows: A Case Study on the Impact of Groundwater Pumping, Rainfall, and Vegetation Changes on a Streamflow in Hawai‘i. M. Sc. Thesis. Department of Water Engineering and Management, University of Twente. 73p.
- Walsh, W.J., Cotton, S.S.P., Dierking, J., and Williams, I.D. 2004. The commercial marine aquarium fishery in Hawai‘i 1976-2003. In: Status of Hawai‘i’s Coastal Fisheries in the New Millennium, Proceedings of the 2001 Fisheries Symposium, American Fisheries Society, Hawai‘i Chapter. Friedlander, A. ed. 2004. pp. 129-156
- Weber, M., Lott, C., and Fabricius, K.E. 2006. Sedimentation stress in a scleractinian coral exposed to terrestrial and marine sediments with contrasting physical, organic, and geochemical properties. *Journal of Experimental Marine Biology and Ecology* 336: 18-32
- Webster, R. and Oliver, M.A. 2007. Geostatistics for Environmental Scientists. 2nd ed. West Sussex, England: John Wiley & Sons 315p.
- West, B.T., Welch, K.B., and Gałecki, A.T. 2007. Linear Mixed Models: a practical guide using statistical software. Boca Raton, FL: Chapman & Hall/CRC 353p.
- Wiens, J.A. 1989. Spatial scaling in ecology. *Functional Ecology* 3: 385-397
- Wiens, J.A. and Milne, B.T. 1989. Scaling of ‘landscapes’ in landscape ecology, or landscape ecology from a beetle’s perspective. *Landscape Ecology* 3: 87-96
- Wilkinson, C. R. 1999. Global and local threats to coral reef functioning and existence: Review and predictions. *Marine and Freshwater Research* 50: 867-878
- Wilkinson, C. R (Ed). 2008. Status of Coral Reefs of the World: 2008. Townsville, Australia: Global Coral Reef Monitoring Network and Australian Institute of Marine Science 296p.
- Williams, G.J., Aeby, G.S., Cowie, R.O.M., and Davy, S.K. 2010. Predictive modeling of coral disease distribution within a reef system. PLoS ONE 5(2): e9264.doi: 10.1371/journal.pone.0009264.

Williams, I.D., Sparks, R., and Smith, C. 2007. Status of Maui's Coral Reefs. Technical Report TR070404, State of Hawai'i, Department of Aquatic Resources, Honolulu. Available for download at:
<http://hawaii.gov/dlnr/dar/pubs/MauiReefDeclines.pdf>

Williams, I.D., Walsh, W.J., Claisse, J.T., Tissot, B.N., and Stamoulis, K.A. 2009. Impacts of a Hawaiian marine protected area network on the abundance and fishery sustainability of the yellow tang, *Zebrasoma flavescens*. *Biological Conservation* 142: 1066-1073

Wu, J. 2006. Cross-disciplinary, landscape ecology, and sustainability science. *Landscape Ecology* 21: 1-4

Yost, R., Loague, K., and Green, R. 1993. Reducing variance in soil organic carbon estimates: soil classification and geostatistical approaches. *Geoderma* 57: 247-262

Zakai, D. and Chadwick-Furman, N.E. 2002. Impacts of intensive recreational diving on reef corals at Eilat, northern Red Sea. *Biological Conservation* 105(2): 179-187